U-Th-Pb method

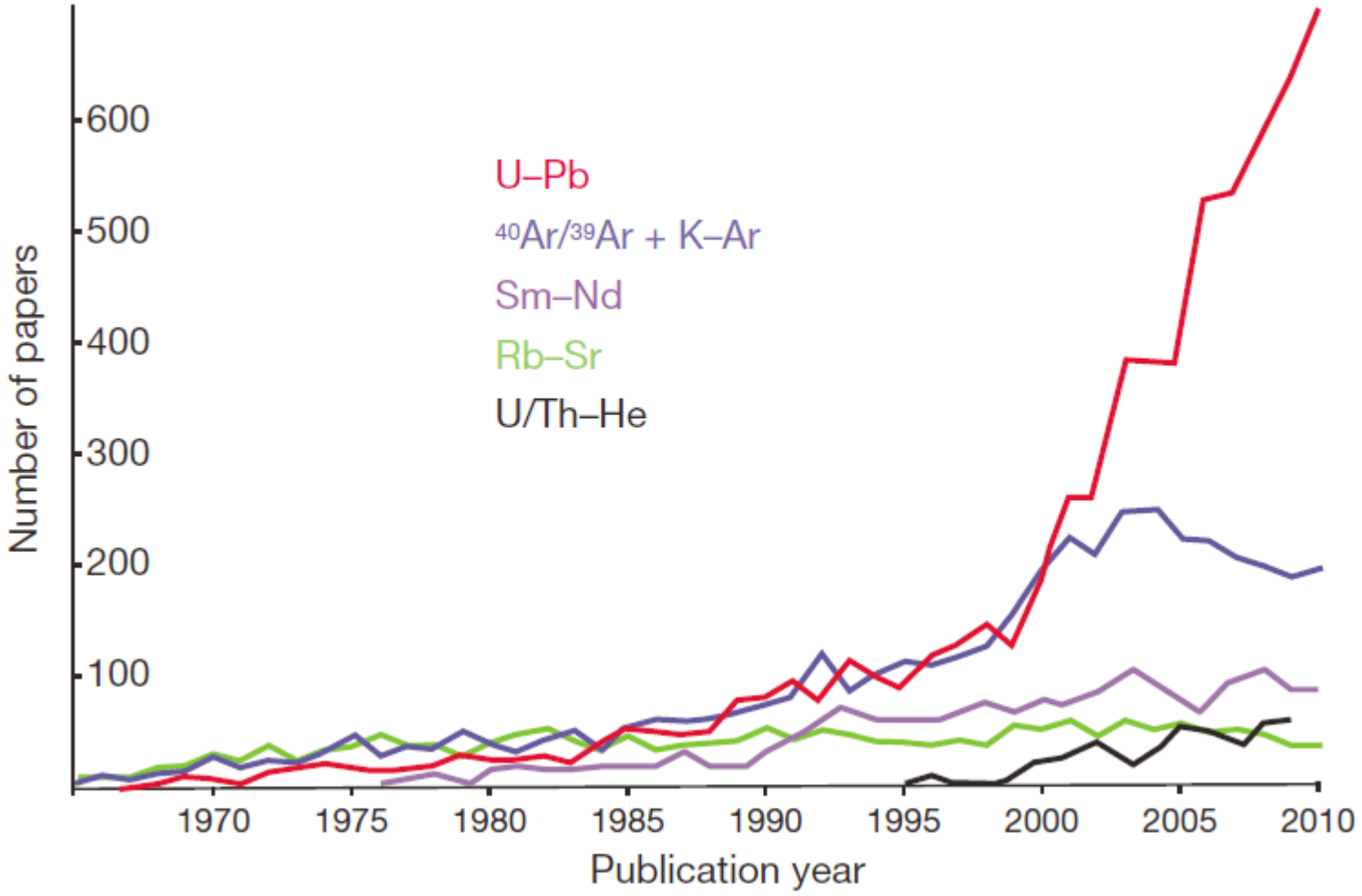

U-Th-Pb method

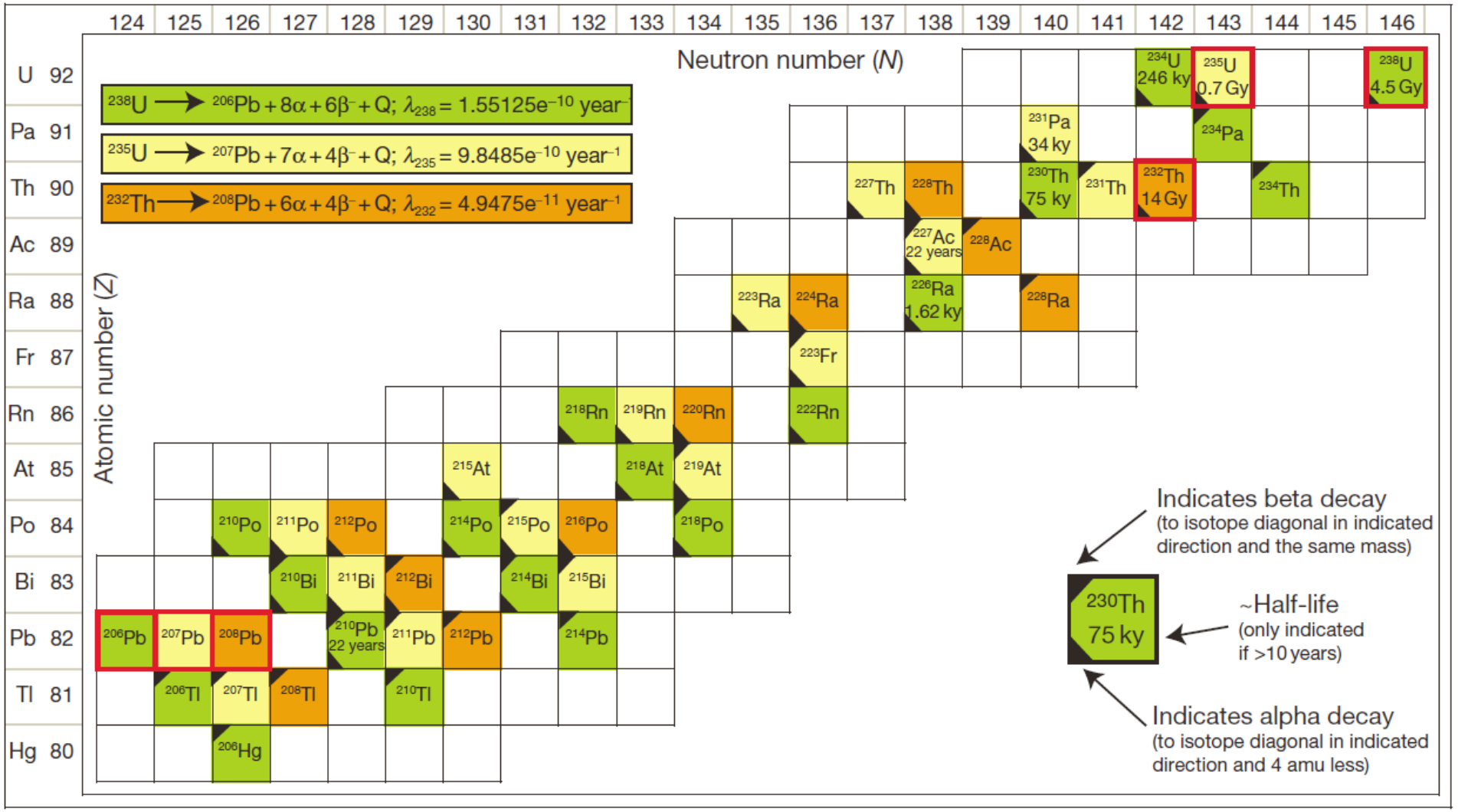

B. Schoene (2014) Treatise on Geochemistry

U-Th-Pb method

Method is based on the following three decay reactions:

$^{238}U \rightarrow {}^{206}Pb$ $T_{1/2} = 4.468$ Ga

$^{235}U \rightarrow {}^{207}Pb$ $T_{1/2} = 0.704$ Ga

$^{232}Th \rightarrow {}^{208}Pb$ $T_{1/2} = 14.01$ Ga

^{204}Pb is a non–radiogenic, stable isotope. We can therefore write:

$$\frac{^{206}Pb}{^{204}Pb} = \left(\frac{^{206}Pb}{^{204}Pb}\right)_0 + \frac{^{238}U}{^{204}Pb}(e^{\lambda_1 t} - 1)$$

$$\frac{^{207}Pb}{^{204}Pb} = \left(\frac{^{207}Pb}{^{204}Pb}\right)_0 + \frac{^{235}U}{^{204}Pb}(e^{\lambda_2 t} - 1)$$

$$\frac{^{208}Pb}{^{204}Pb} = \left(\frac{^{208}Pb}{^{204}Pb}\right)_0 + \frac{^{232}Th}{^{204}Pb}(e^{\lambda_3 t} - 1)$$

U-Th-Pb method

This equation is especially useful as the present-day $^{235}U/^{238}U$ is a constant, eliminating the need to measure U. Concentration of Pb can also be ignored. Equation can be used to calculate an age by linear fitting in $^{206}Pb/^{204}Pb$–$^{207}Pb/^{204}Pb$ space, or if initial Pb is negligible, then the measured $(^{207}Pb/^{206}Pb)^*$ can be used to directly calculate a date. In both cases, the equation must be solved iteratively; this is commonly called the Pb–Pb date.

benefit of
equation
above:

h isochron
two eqns

$$\frac{\left(\frac{^{207}\mathrm{Pb}}{^{204}\mathrm{Pb}}\right) - \left(\frac{^{207}\mathrm{Pb}}{^{204}\mathrm{Pb}}\right)_0}{\left(\frac{^{206}\mathrm{Pb}}{^{204}\mathrm{Pb}}\right) - \left(\frac{^{206}\mathrm{Pb}}{^{204}\mathrm{Pb}}\right)_0} = \left(\frac{^{235}\mathrm{U}}{^{238}\mathrm{U}}\right)\frac{\left(e^{\lambda_{235}t} - 1\right)}{\left(e^{\lambda_{238}t} - 1\right)} = \left(\frac{^{207}\mathrm{Pb}}{^{206}\mathrm{Pb}}\right)^*$$

U-Th-Pb method

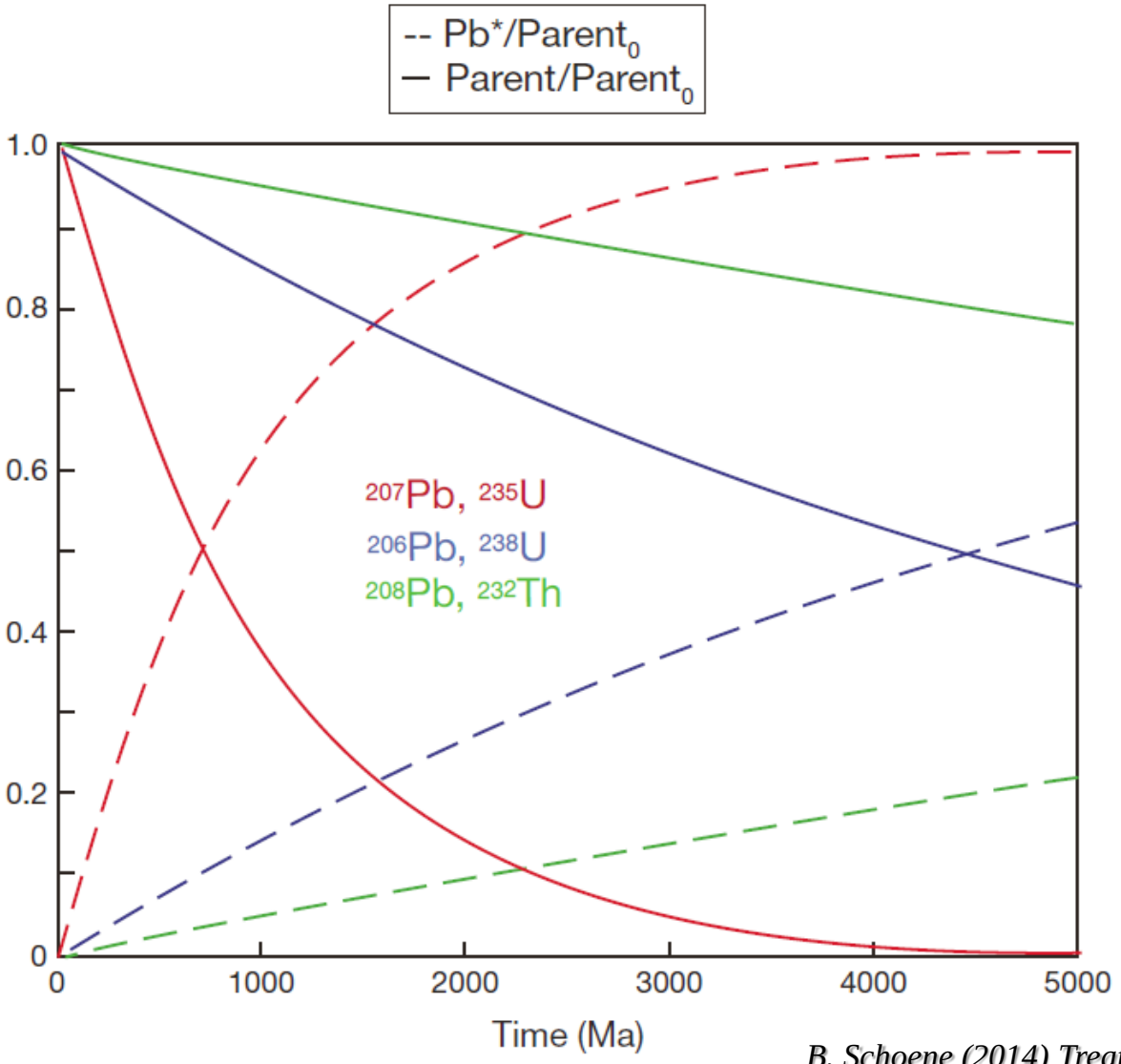

B. Schoene (2014) Treatise on Geochemistry

U-Th-Pb method

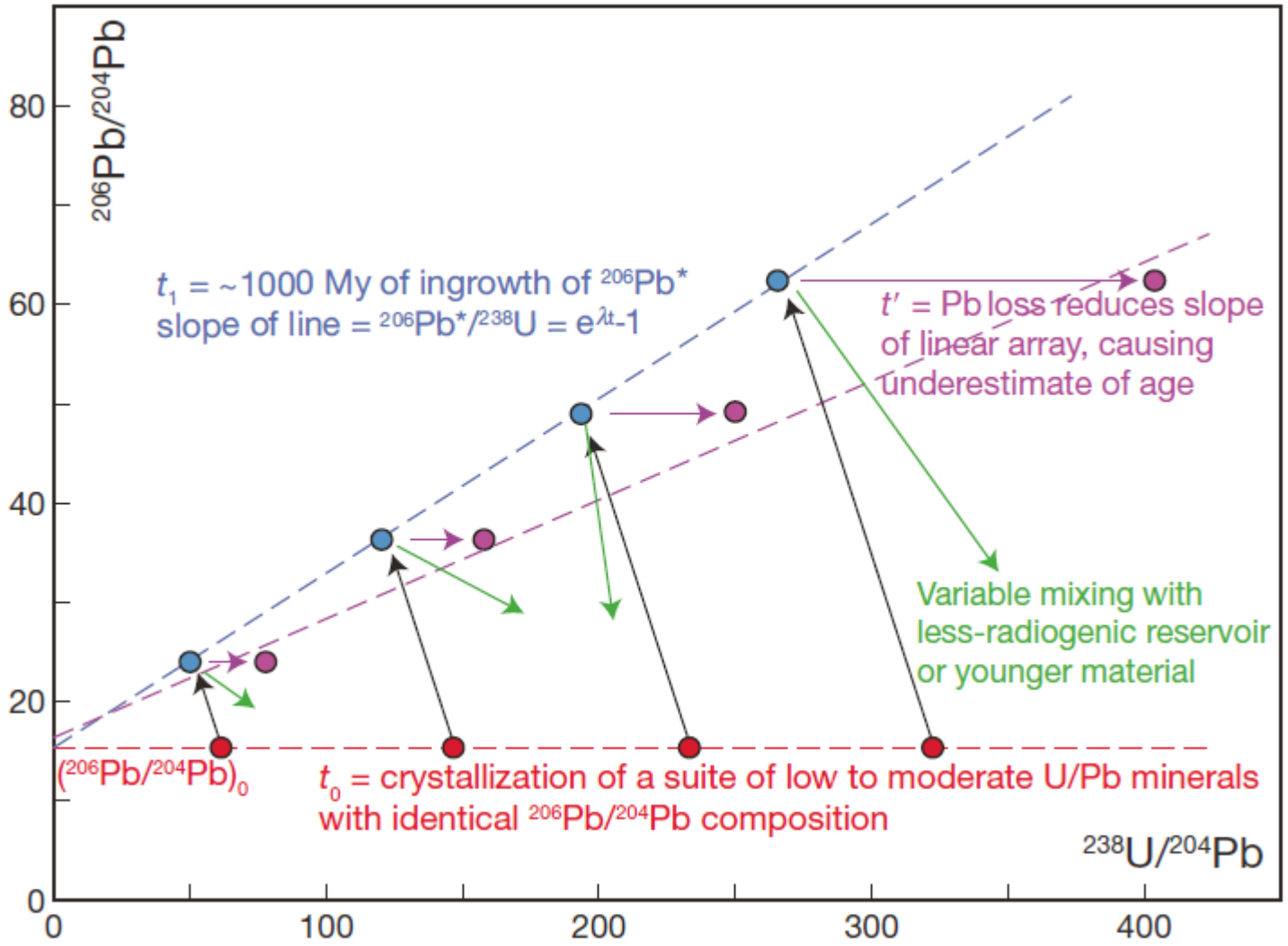

B. Schoene (2014) Treatise on Geochemistry

U-Th-Pb method

$$\left(\frac{^{206}\mathrm{Pb}^{*}}{^{238}\mathrm{U}}\right) = \left(e^{\lambda_{238}t} - 1\right)$$

$$\left(\frac{^{207}\mathrm{Pb}^{*}}{^{235}\mathrm{U}}\right) = \left(e^{\lambda_{235}t} - 1\right)$$

$$\left(\frac{^{208}\mathrm{Pb}^{*}}{^{232}\mathrm{Th}}\right) = \left(e^{\lambda_{232}t} - 1\right)$$

U-Pb Concordia diagram

$^{206}Pb^*/^{238}U = (e^{\lambda t1}-1)$, $^{207}Pb^*/^{235}U = (e^{\lambda t2}-1)$

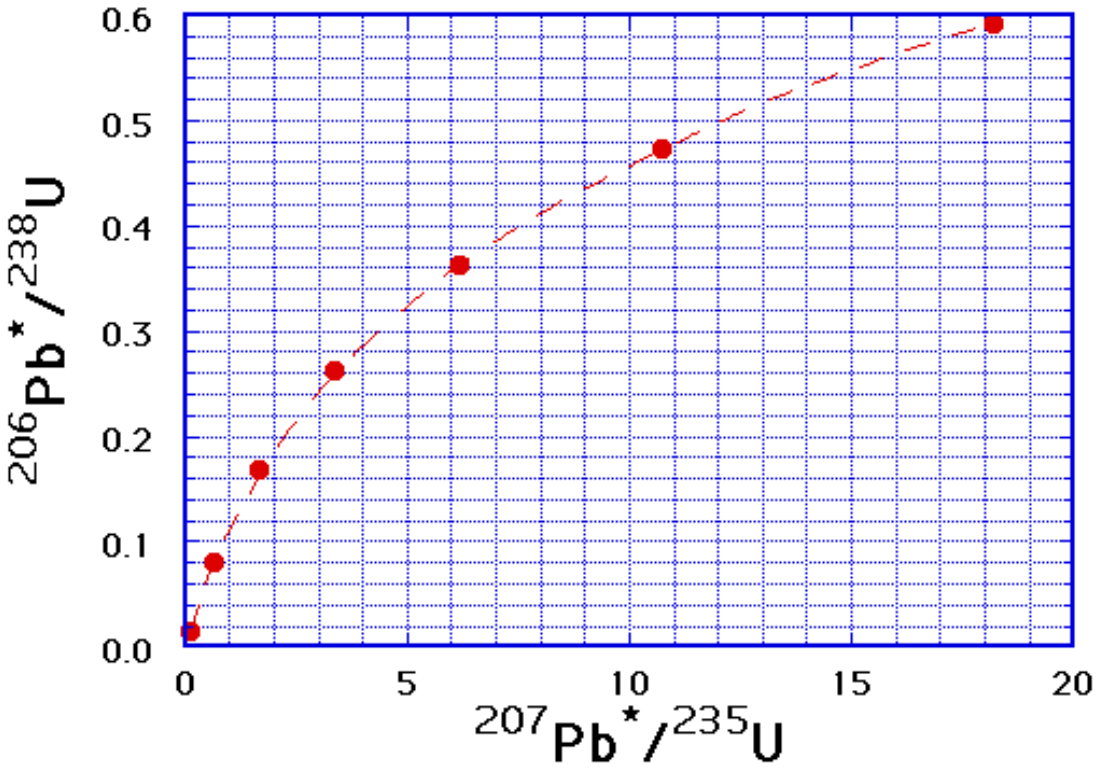

U-Pb Concordia diagram

Numerical values of $e^{\lambda 1 t} - 1$, $e^{\lambda 2 t} - 1$, and of the radiogenic $^{207}Pb/^{206}Pb$ ratio as a function of age (t)

Ga	$e^{\lambda 1 t} - 1$	$e^{\lambda 2 t} - 1$	$\left(\frac{^{207}Pb}{^{206}Pb}\right)^*$	Ga	$e^{\lambda 1 t} - 1$	$e^{\lambda 2 t} - 1$	$\left(\frac{^{207}Pb}{^{206}Pb}\right)^*$
0	0.0000	0.0000	0.04607	2.4	0.4511	9.6296	0.15492
0.2	0.0315	0.2177	0.05014	2.6	0.4968	11.9437	0.17447
0.4	0.0640	0.4828	0.05473	2.8	0.5440	14.7617	0.19693
0.6	0.0975	0.8056	0.05994	3.0	0.5926	18.1931	0.22279
0.8	0.1321	1.1987	0.06584	3.2	0.6428	22.3716	0.25257
1.0	0.1678	1.6774	0.07254	3.4	0.6946	27.4597	0.28690
1.2	0.2046	2.2603	0.08017	3.6	0.7480	33.6556	0.32653
1.4	0.2426	2.9701	0.08886	3.8	0.8030	41.2004	0.37232
1.6	0.2817	3.8344	0.09877	4.0	0.8599	50.3878	0.42525
1.8	0.3221	4.8869	0.11010	4.2	0.9185	63.5753	0.48951
2.0	0.3638	6.1685	0.12306	4.4	0.9789	75.1984	0.55746
2.2	0.4067	7.7291	0.13790	4.6	1.0413	91.7873	0.63969

U-Pb Concordia diagram

On a plot of $^{206}Pb^{*}/^{238}U$ vs. $^{207}Pb^{*}/^{235}U$, the locus of all points yielding concordant dates is called the concordia curve

Samples experiencing no Pb or U mobility move along the concordia as they age. Samples that do not plot on the concordia yield discordant dates.

The concordia curve bends over because ^{235}U decays much faster than ^{238}U; this causes ^{207}Pb to be produced faster than ^{206}Pb.

This diagram was introduced by Wetherill in 1956 and termed *Concordia diagram* (remember *Nicolaysen diagram* for Rb-Sr)

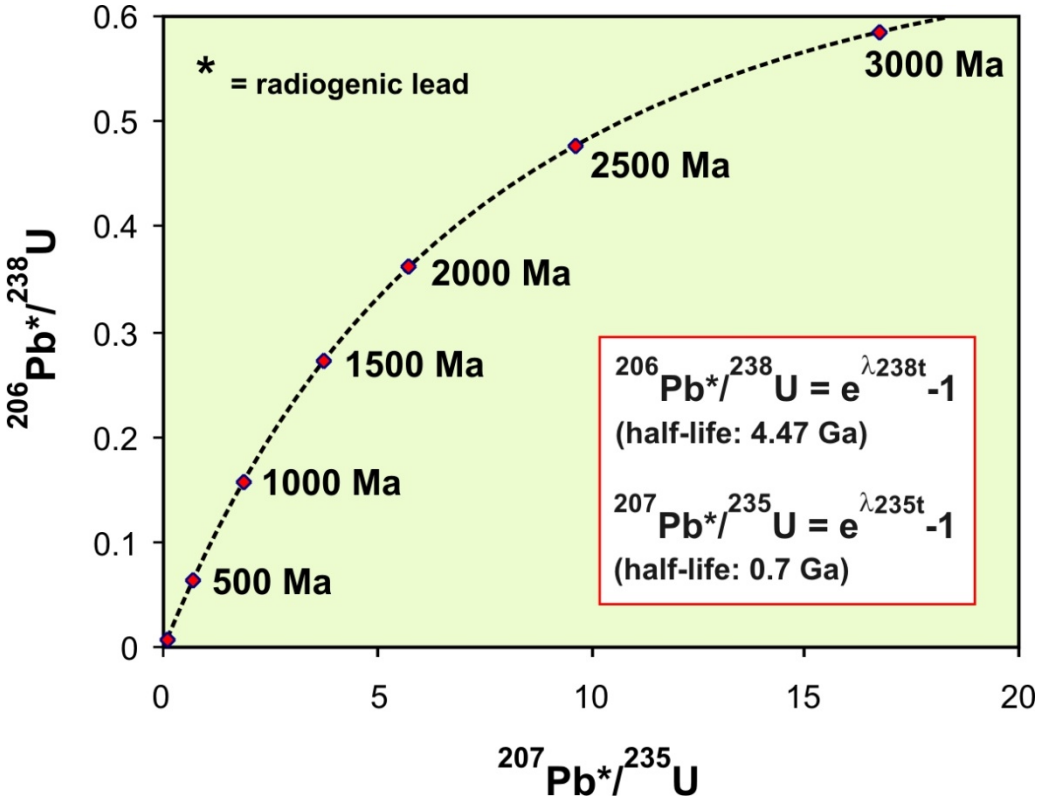

U-Th-Pb method of dating

With this geochronometer, we can get three independent age determinations of minerals or rocks containing both U and Th.

All three equations will give the same ages, provided no gain or loss of U, Th or Pb occurred during the lifetime of the system being dated. The ages are then said to be concordant.

Often, the three dates do not agree, i.e., they are discordant.

Generally, discordancy results from loss of Pb.

U-Pb Concordia method of dating

During episodic Pb loss or U gain, minerals are displaced from the concordia and move along the discordia line

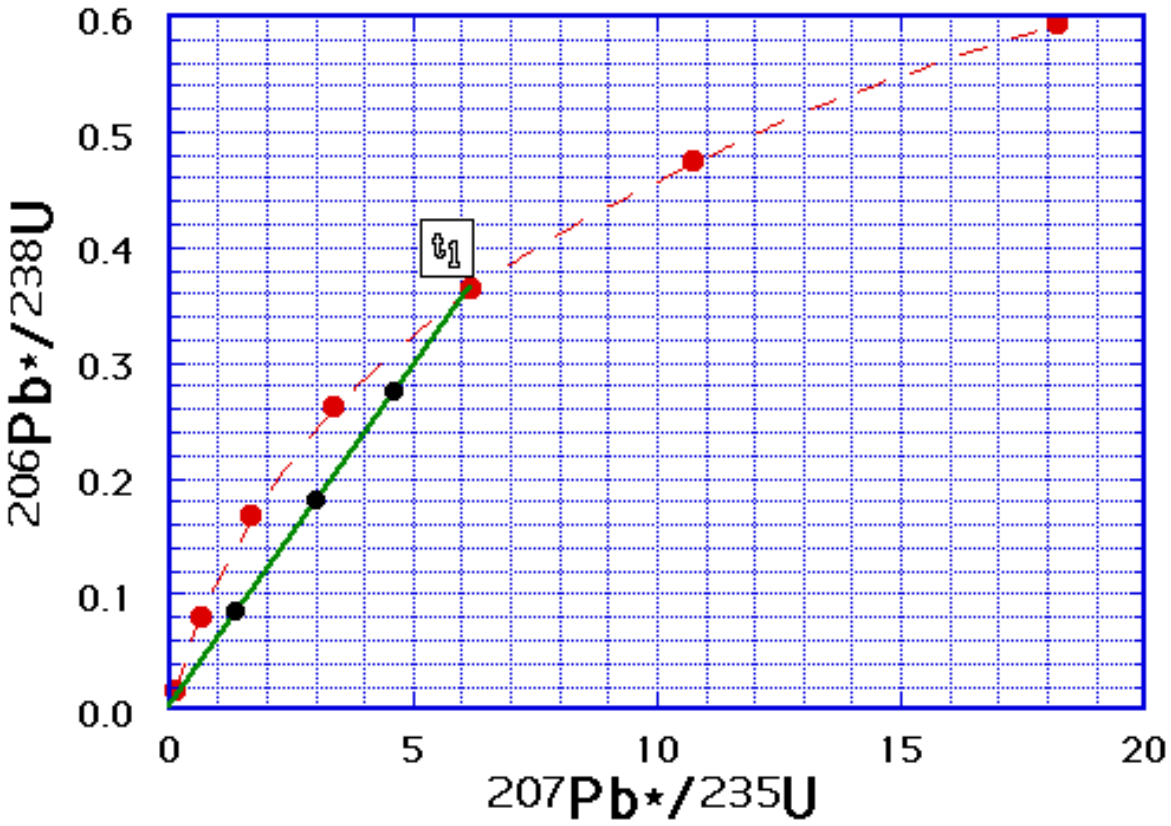

If Pb loss occurred, the rocks plot along a line below the concordia.

If U loss occurred, the rocks would plot along a line above the concordia.

The line that results from discordant samples is called discordia line. The upper discordia intercept may represent the age of formation of the rock. The lower intercept may represent the date of Pb loss, if this loss occurred in a single stage, and not continuously.

U-Pb concordia method of dating

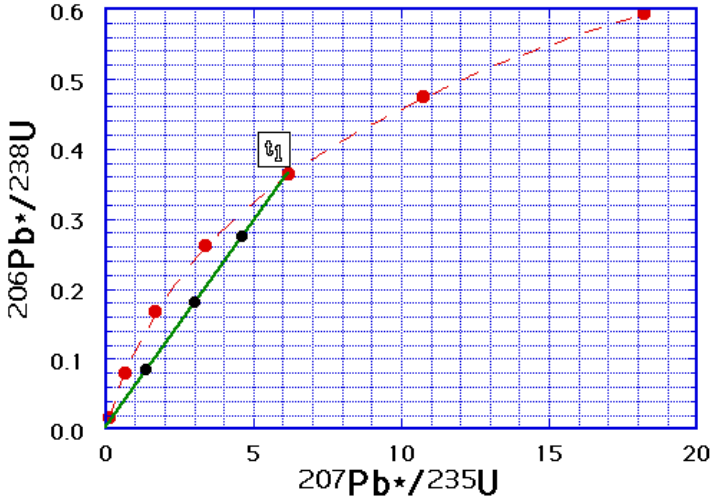

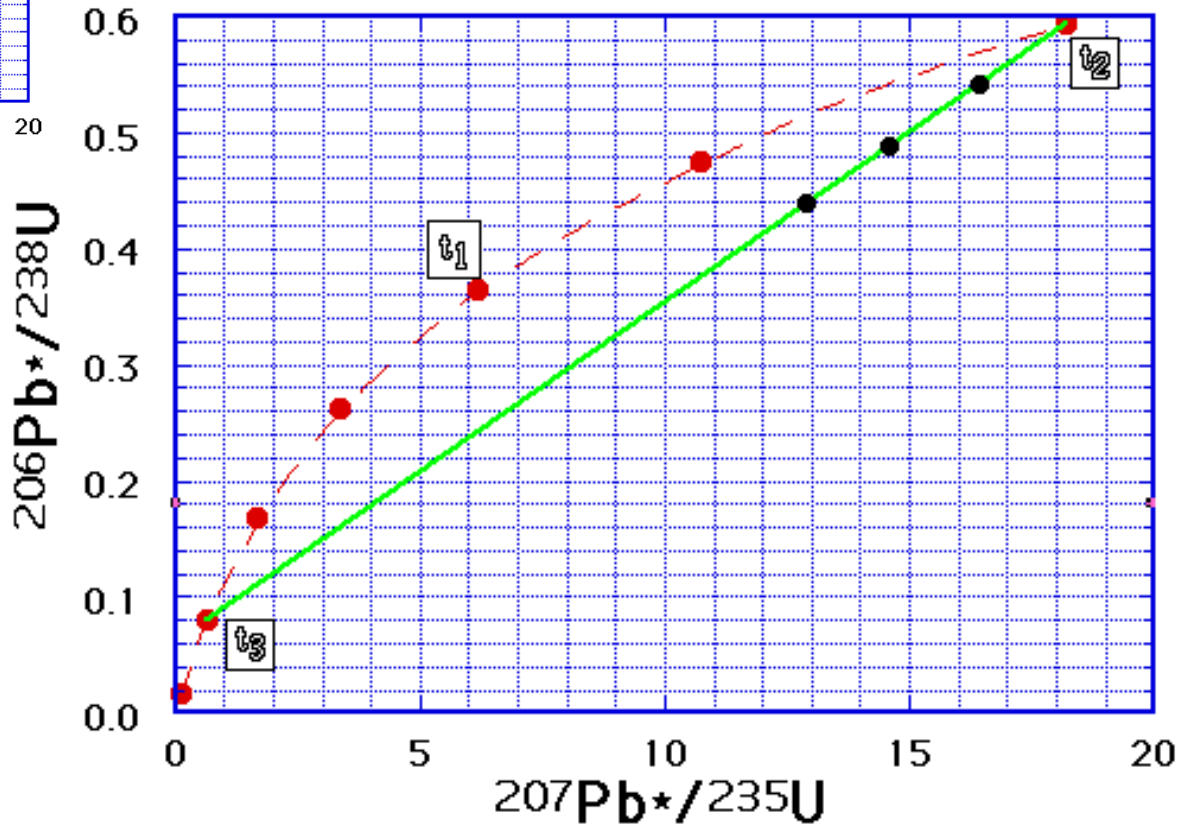

Wetherill & Tera-Wasserburg concordia

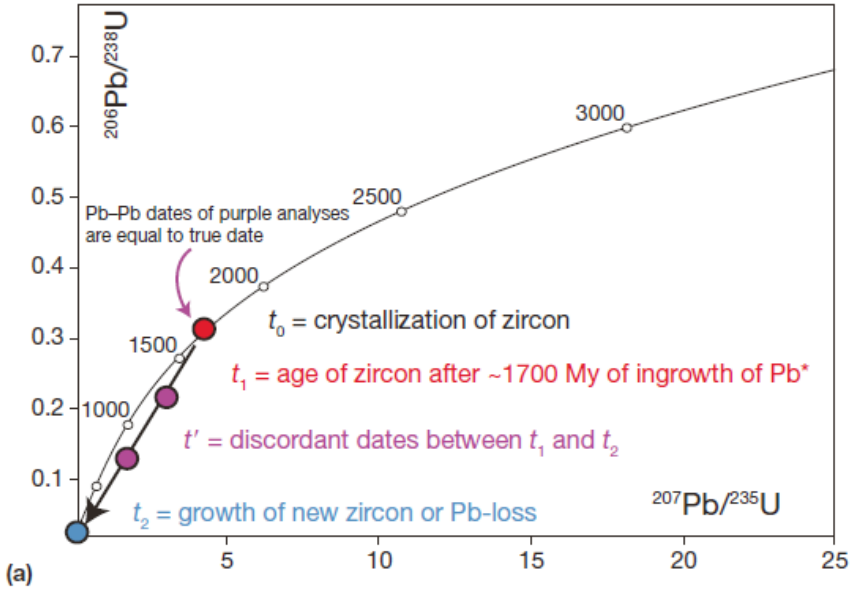

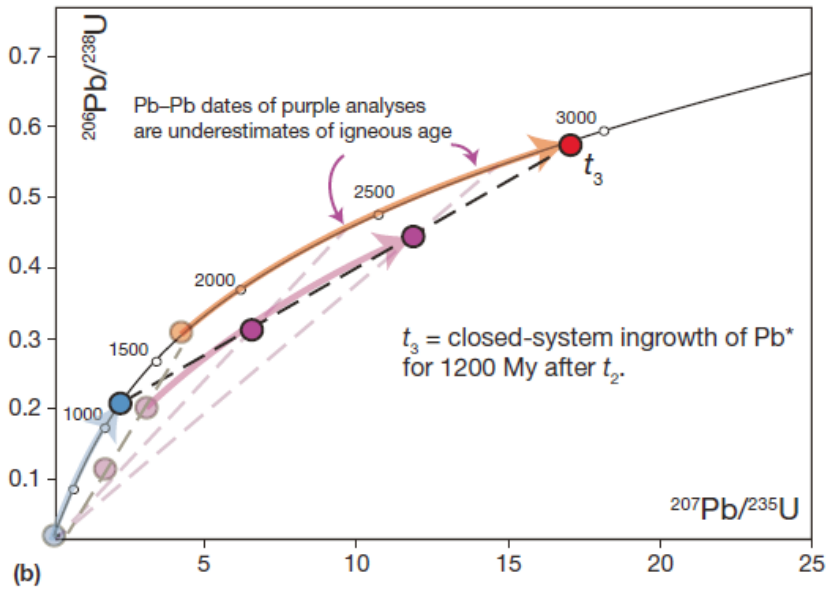

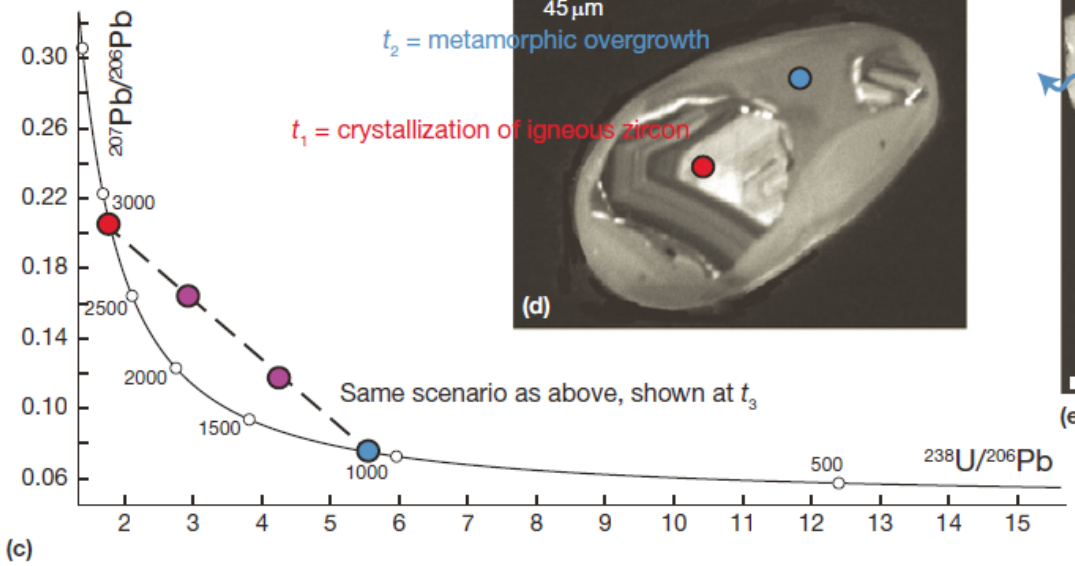

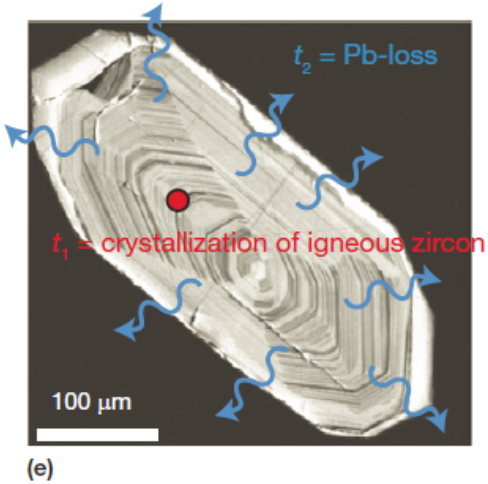

B. Schoene (2014) Treatise on Geochemistry

Tera-Wasserburg concordia

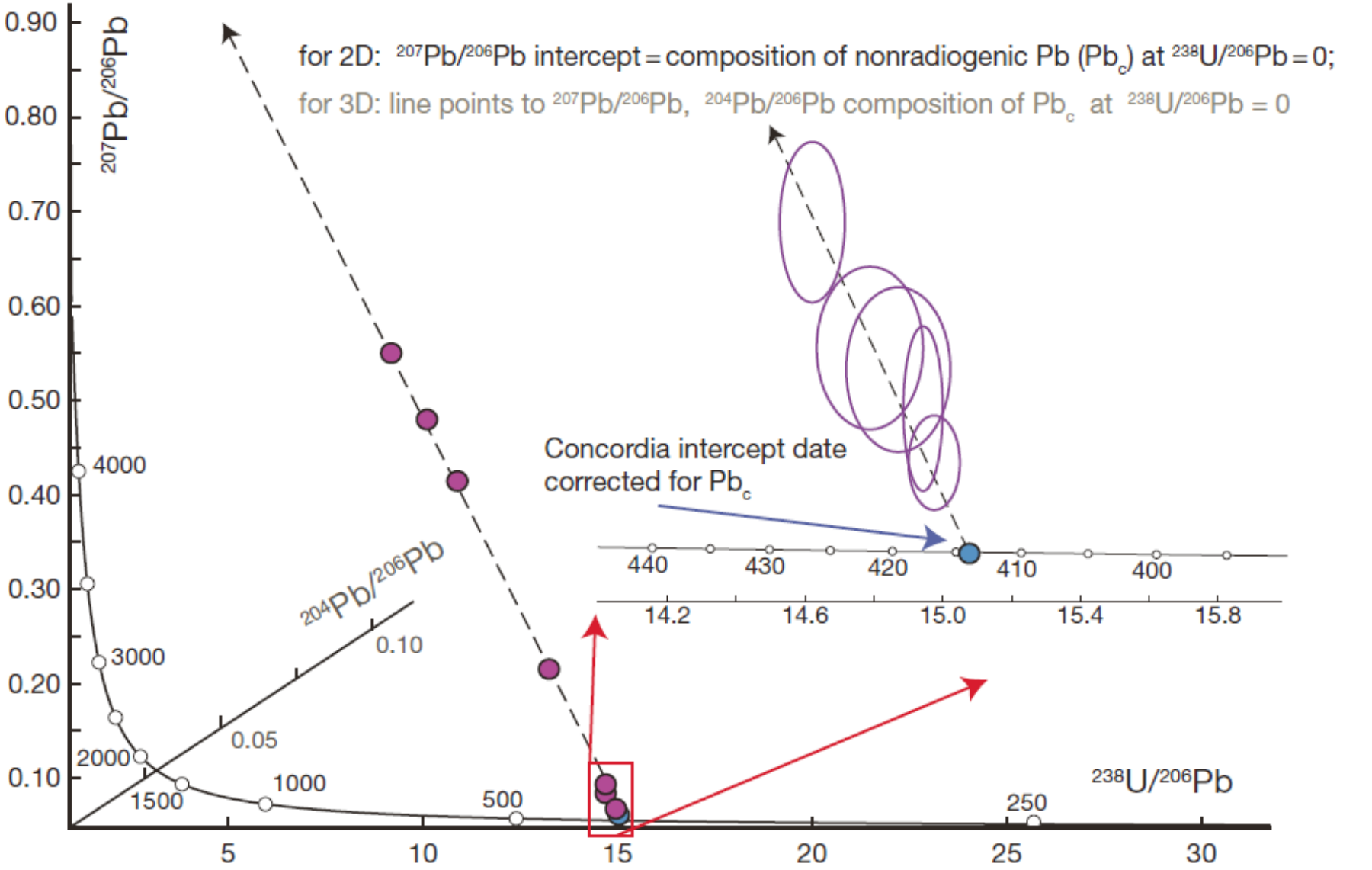

B. Schoene (2014) Treatise on Geochemistry

U-Pb Concordia method of dating

Aufschluß „Bayernexkursion“

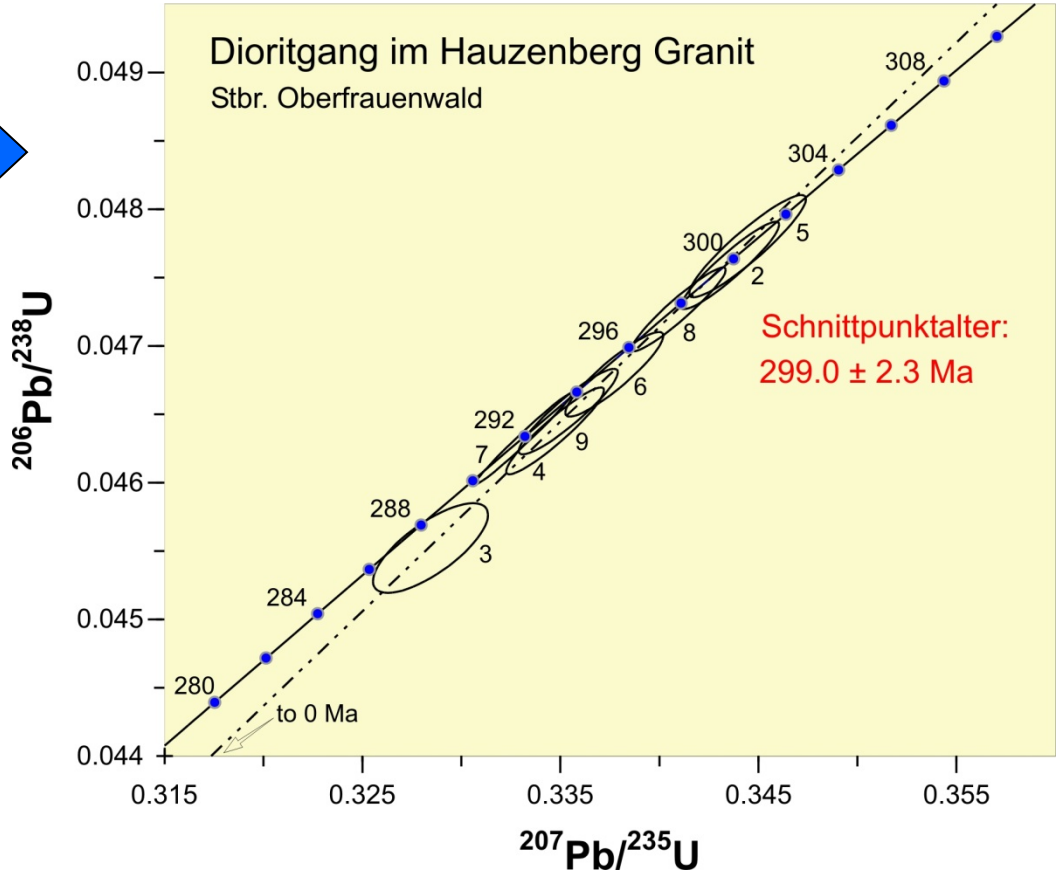

Pb loss models (for zircons)

Continuous diffusion model (Ahrens 1955, Tilton 1960)

Episodic Pb loss model – Pb loss due to thermal event(s) (Wetherill 1956)

„Dilatancy model“ – fluid driven Pb loss (Goldrich & Mudrey 1972)

Higher Pb loss in U-rich zircons (greater radiation damage) (Silver & Deutsch 1963)

Discordant Pb in filling defect and voids, concordant Pb in the lattice itself (Kober 1987)

Concordia-discordia diagram for zircon grains in granulite facies metasediments from Sri Lanka

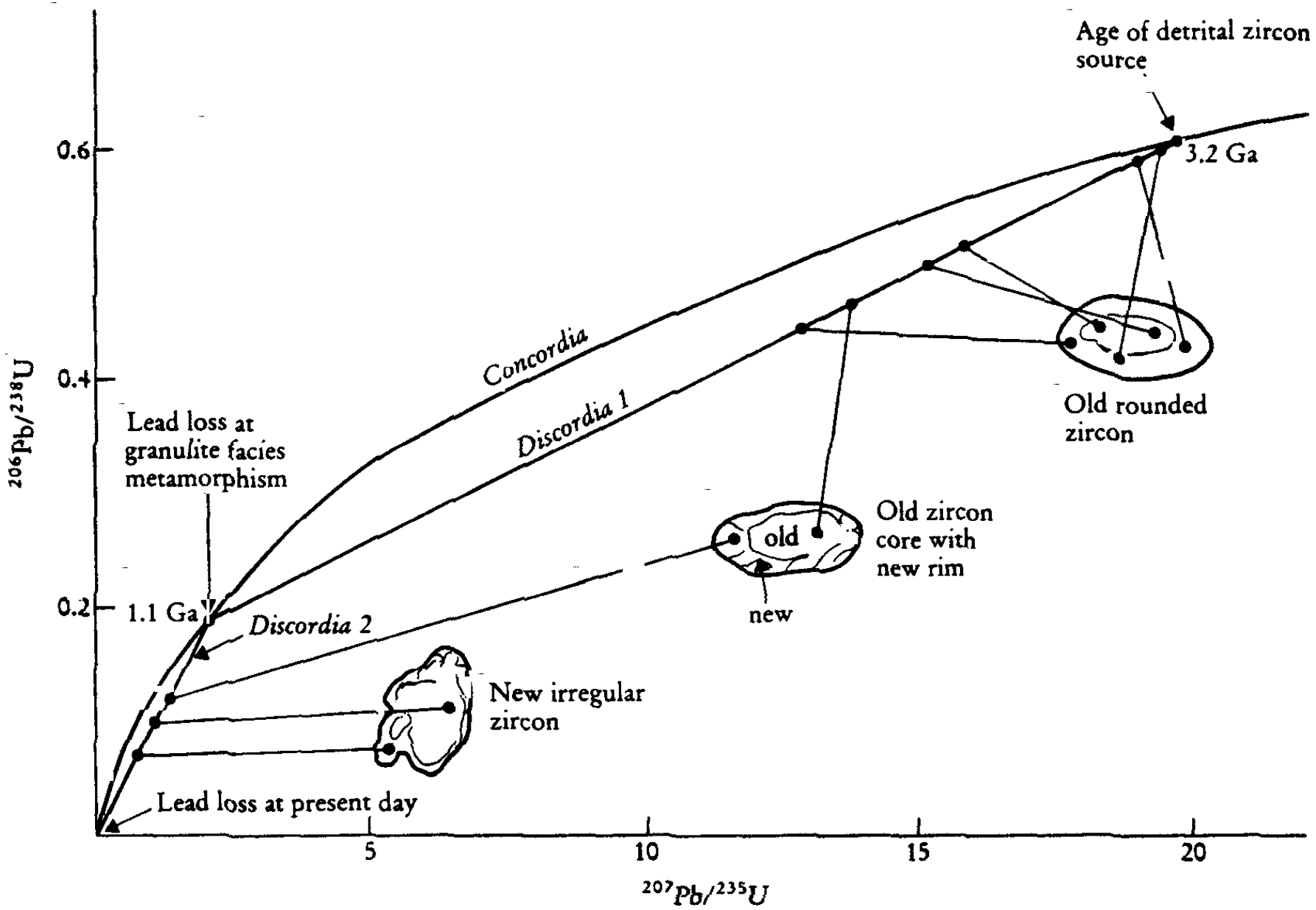

Towards more concordancy

Chemical leaching (Krogh & Davis 1975)

Air abrasion method (Krogh 1982)

Chemical abrasion/annealing method (Mattinson 2005)

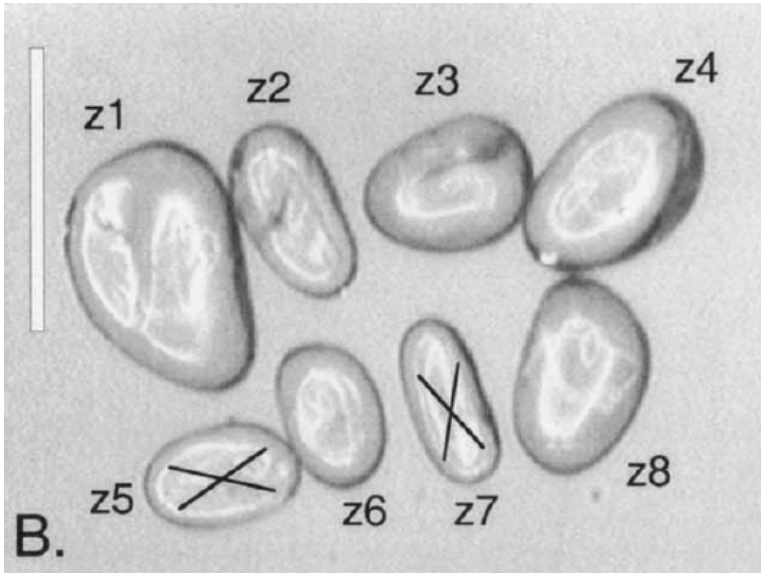

Chemical abrasion

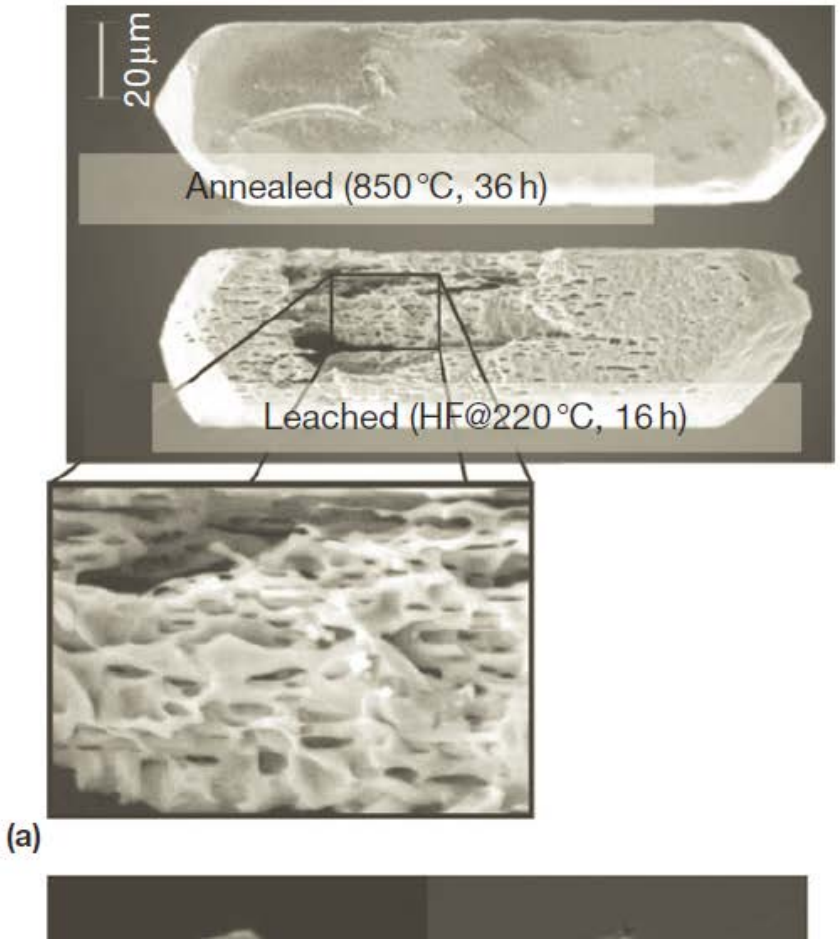

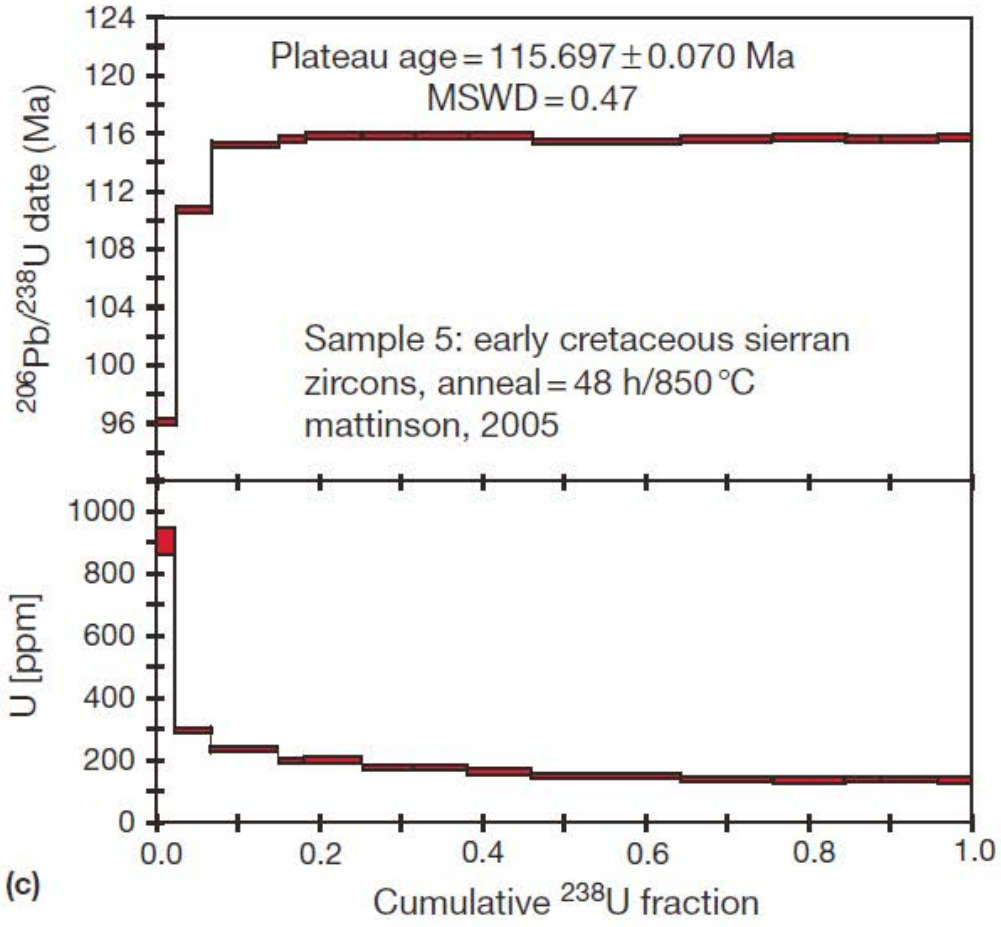

Magmatic or metamorphic zircon?

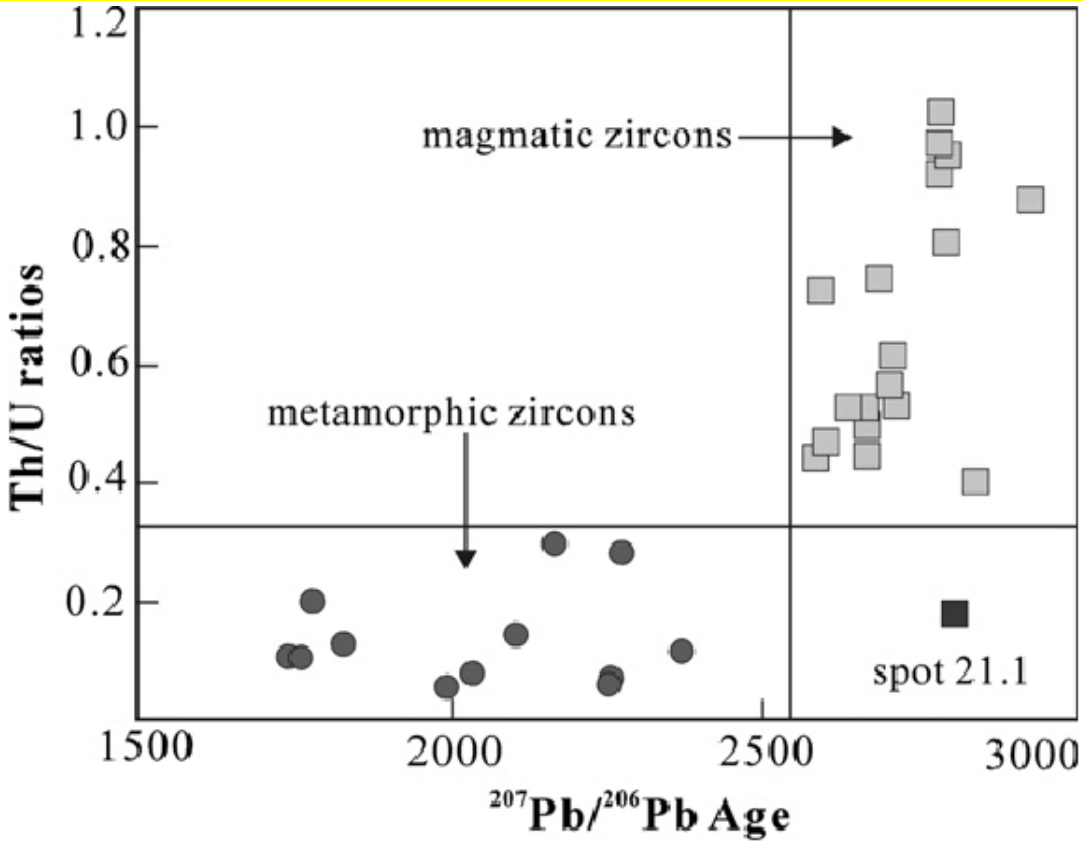

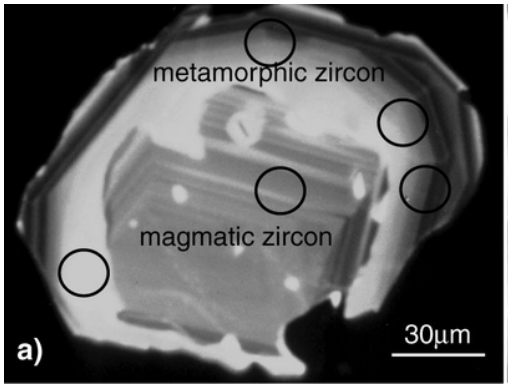

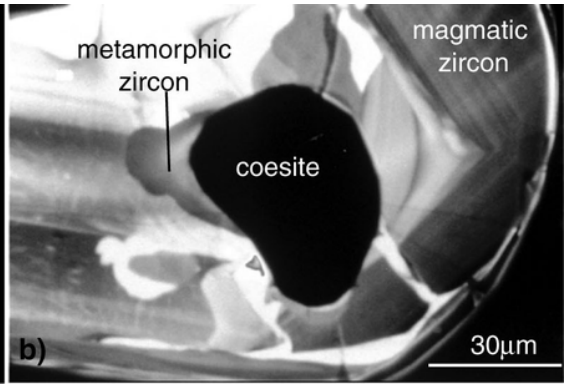

Concordia diagram vs. Tera-Wasserburg plot

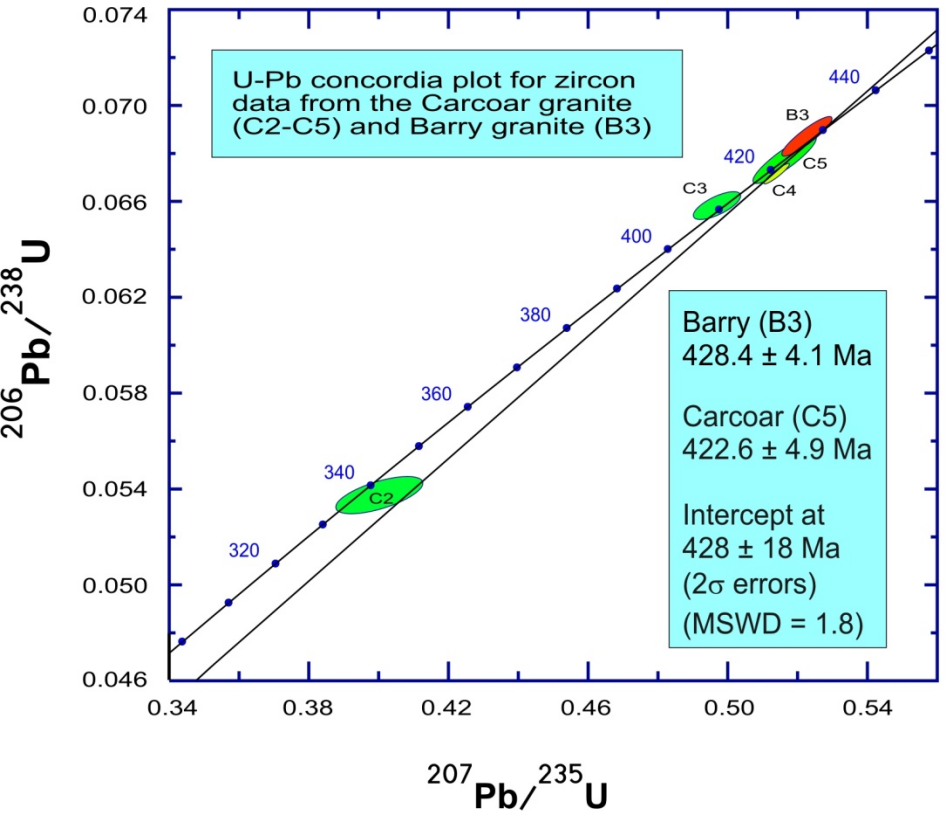

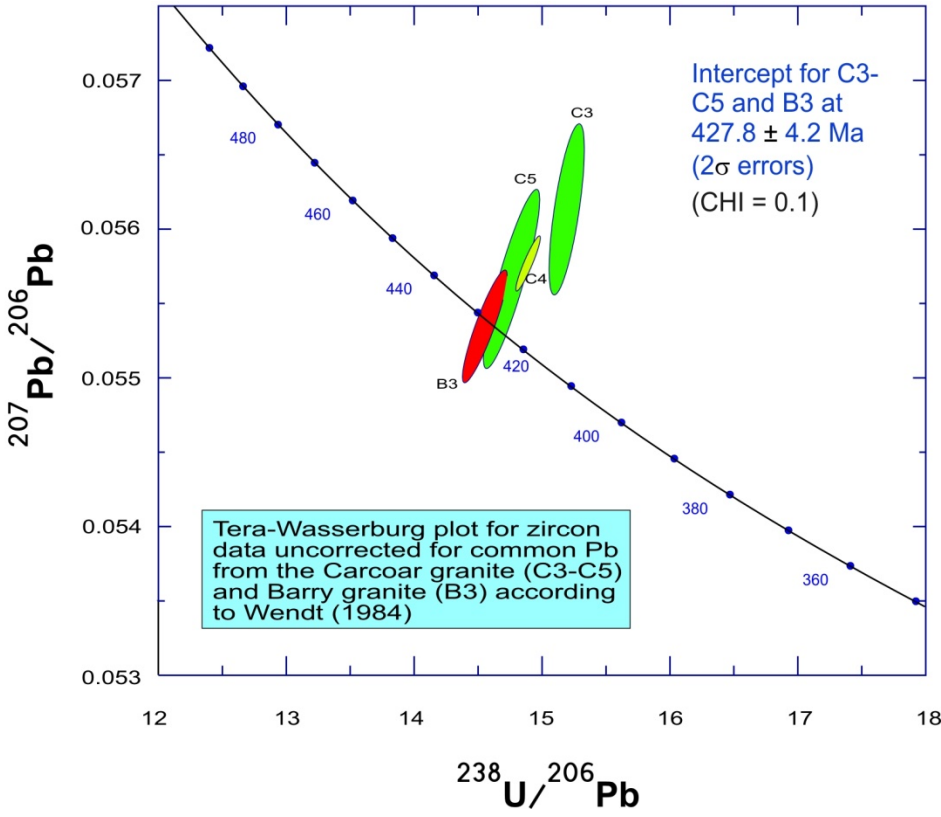

Correction for initial lead

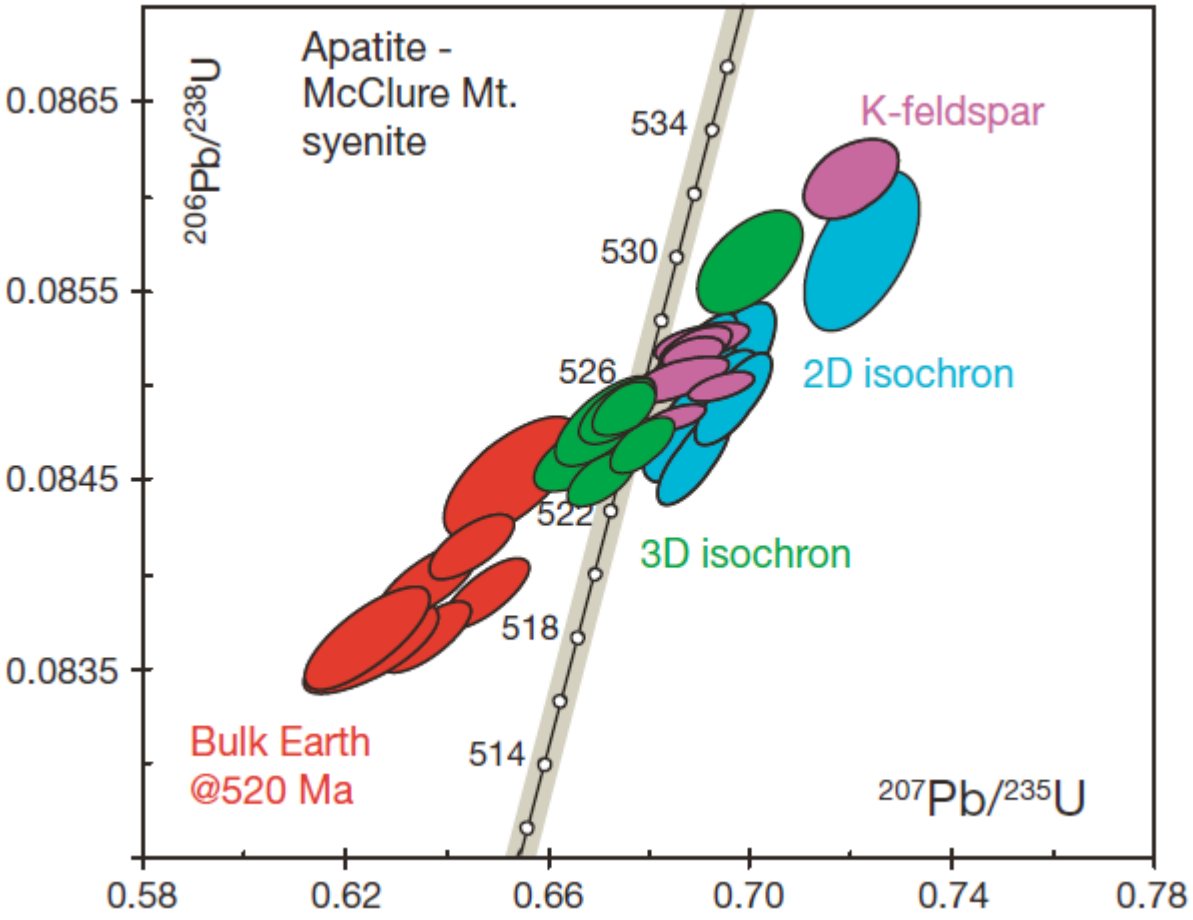

The isotope geology of Pb

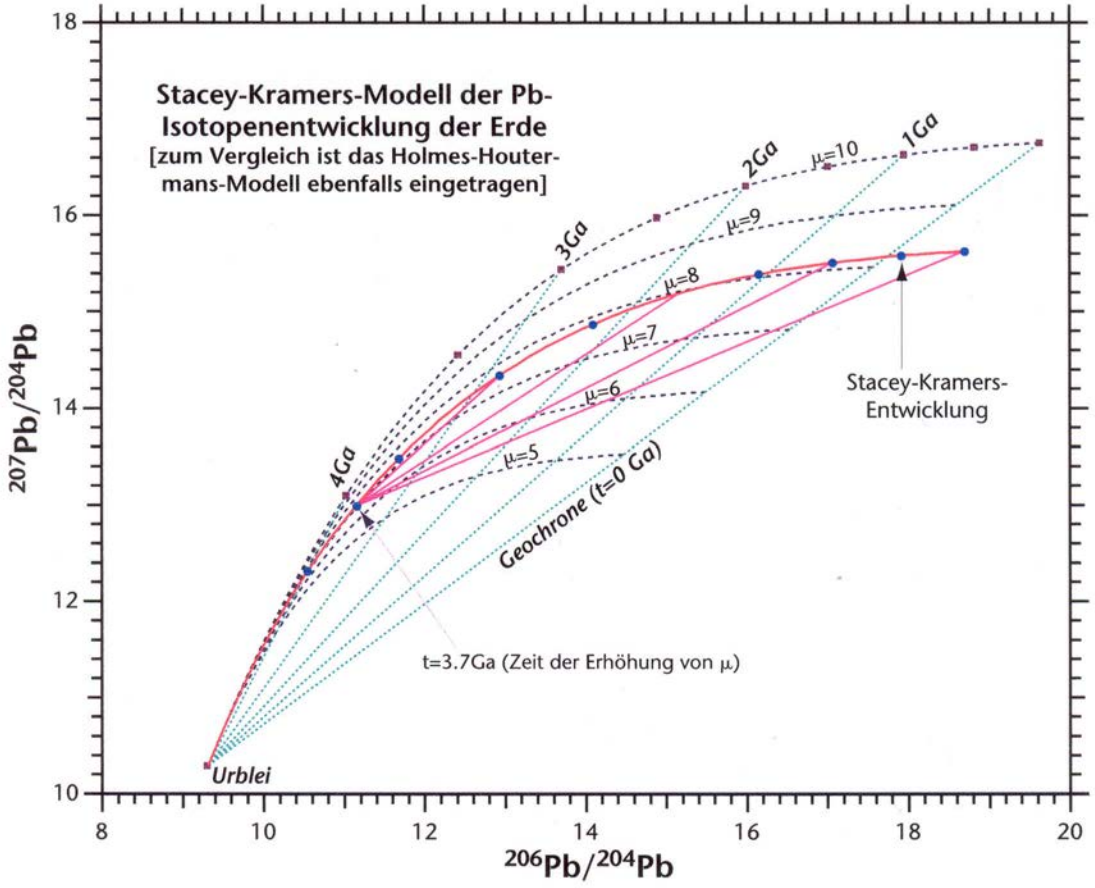

Two-stage Pb evolution model of Stacey & Kramers (1975)

In this model Pb evolves from primordial isotope ratios between 4.6 and 3.7 Ga in a reservoir with a μ-($^{238}U/^{204}Pb$) value of 7.2. At 3.7 Ga the μ-value of the reservoir was changed by geochemical differentiation to 9.7.

http://www.dmg-home.de/Ressourcen/Internet-Kurse/Isotopengeochemie.pdf

Intermediate daughter product disequilibria

$$t_{excess} = \left(\frac{1}{\lambda_{238}}\right) \ln\left[1 + (f-1)\left(\frac{\lambda_{238}}{\lambda_{230}}\right)\right]$$

$$f = \left[\frac{(Th/U)_{mineral}}{(Th/U)_{liquid}}\right]$$

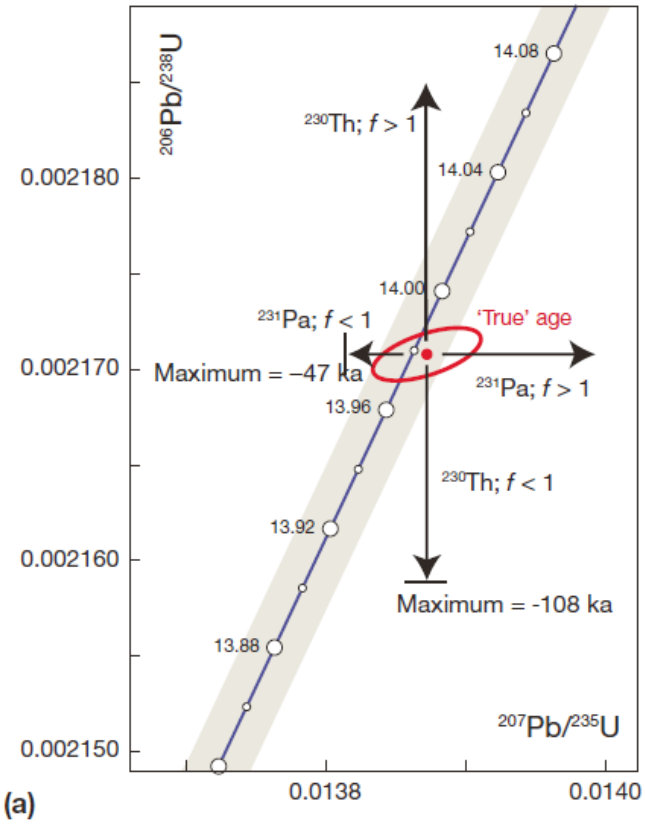

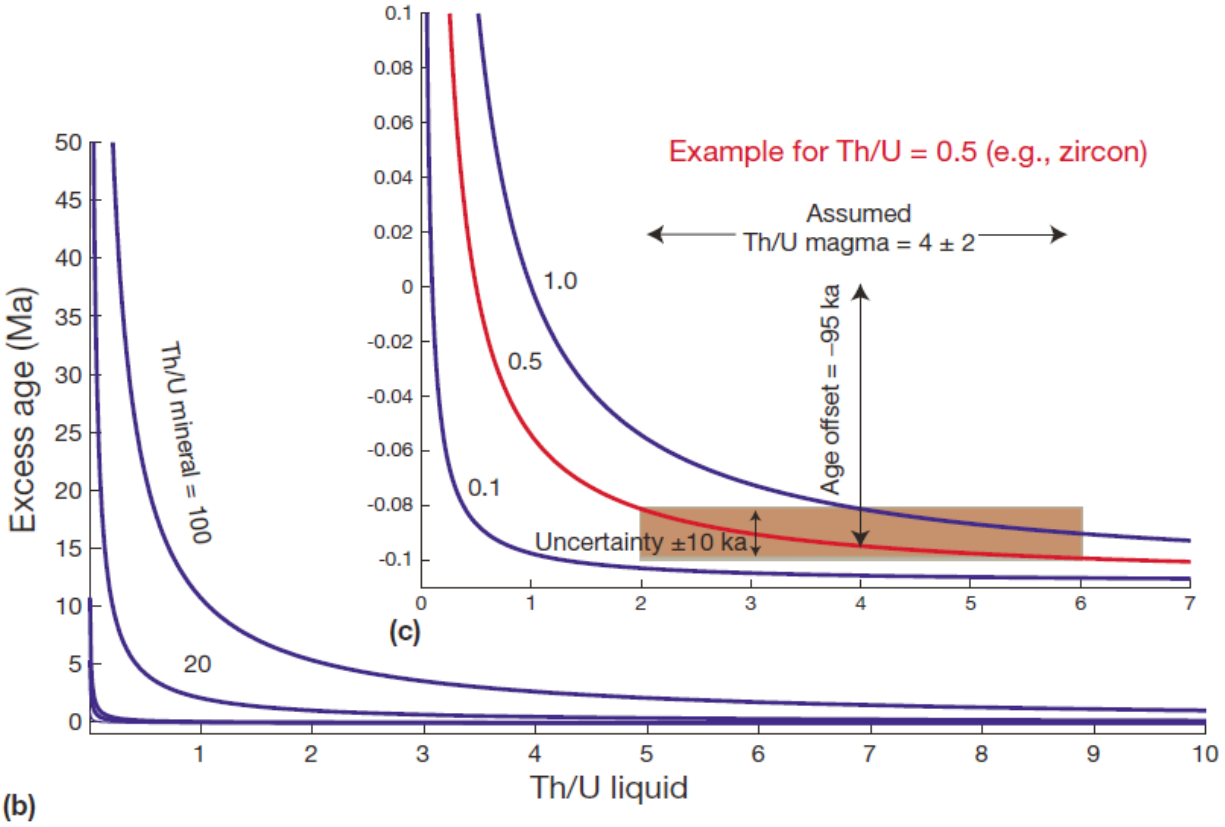

B. Schoene (2014) Treatise on Geochemistry

U-Pb monazite dating (LREE Th)PO_4

The **reverse discordant effect** in monazite is largely due to excess ^{206}Pb, which is derived from disequilibrium incorporation of ^{230}Th into the crystal lattice as an intermediate daughter product of the ^{238}U decay chain (Schärer 1984; Parrish 1990). In such case, the $^{207}Pb/^{235}U$ ages are commonly regarded as the more reliable crystallization age of monazite.

Greater Himalaya Sequence, Nyalam

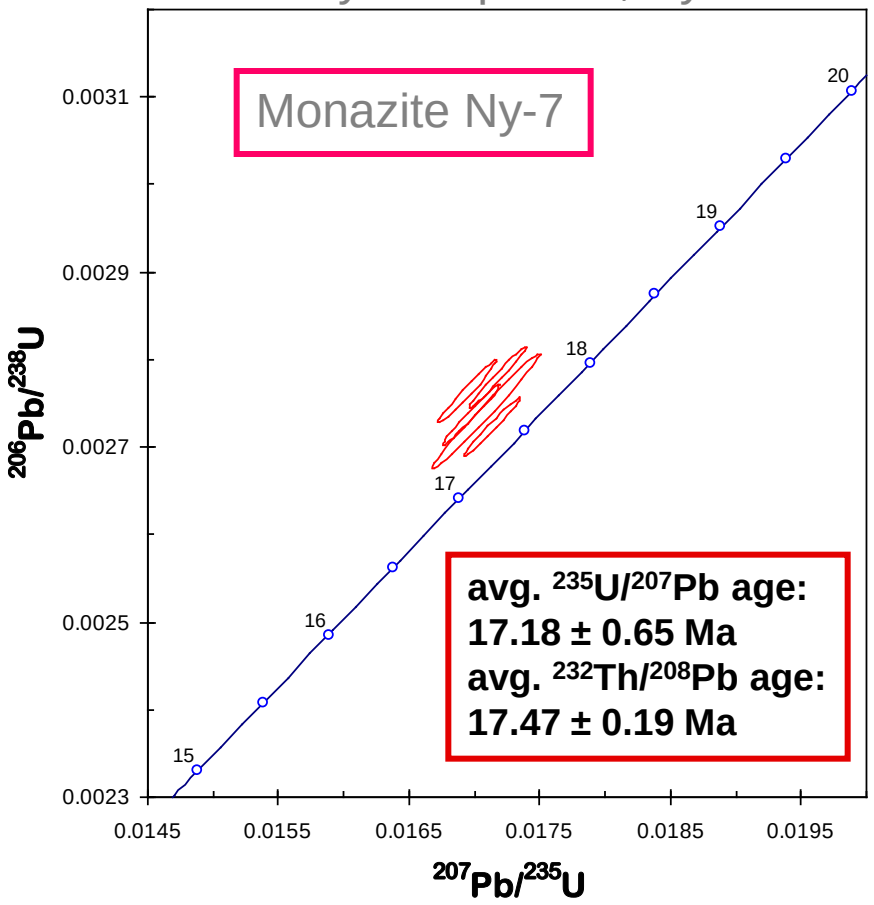

U-Pb monazite dating

$(LREE\ Th)PO_4$

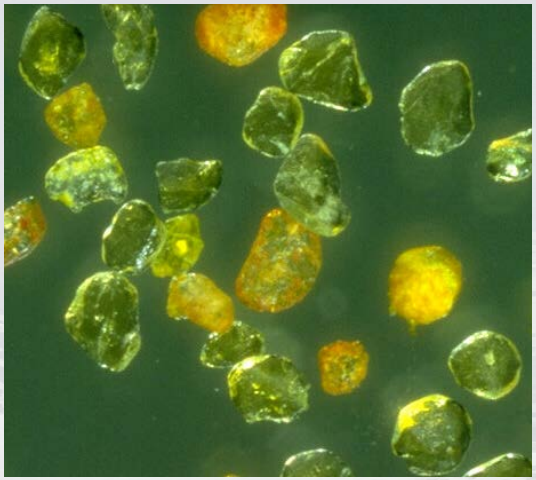

Chronological tool in metamorphic rocks

- Minimal concentrations of common Pb
- Minor risk of isotopic inheritance
- High resistance to Pb loss

apatite + allanite + muscovite + sillimanite + quartz → monazite + annite + anorthite + fluid *(Simpson et al.2000)*

Appearance in pelites:
~525°
(Smith & Barreiro 1990)

Closure Temperature:
725° +- 25°C
(Parrish 1990)

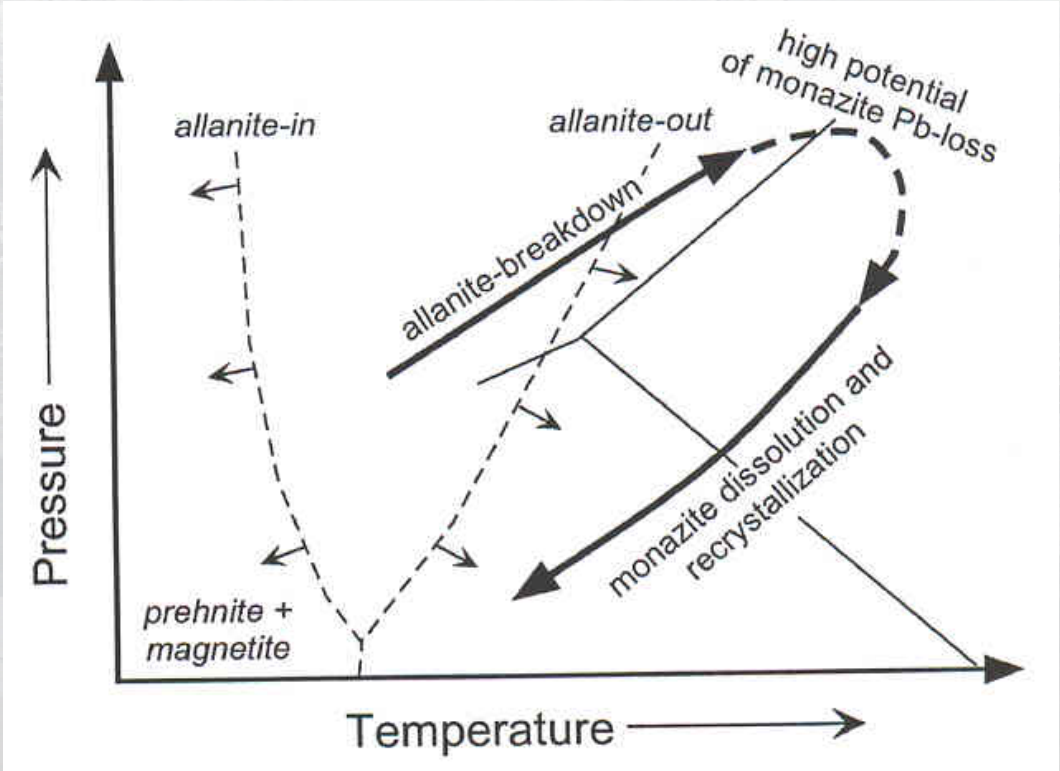

Measurement techniques

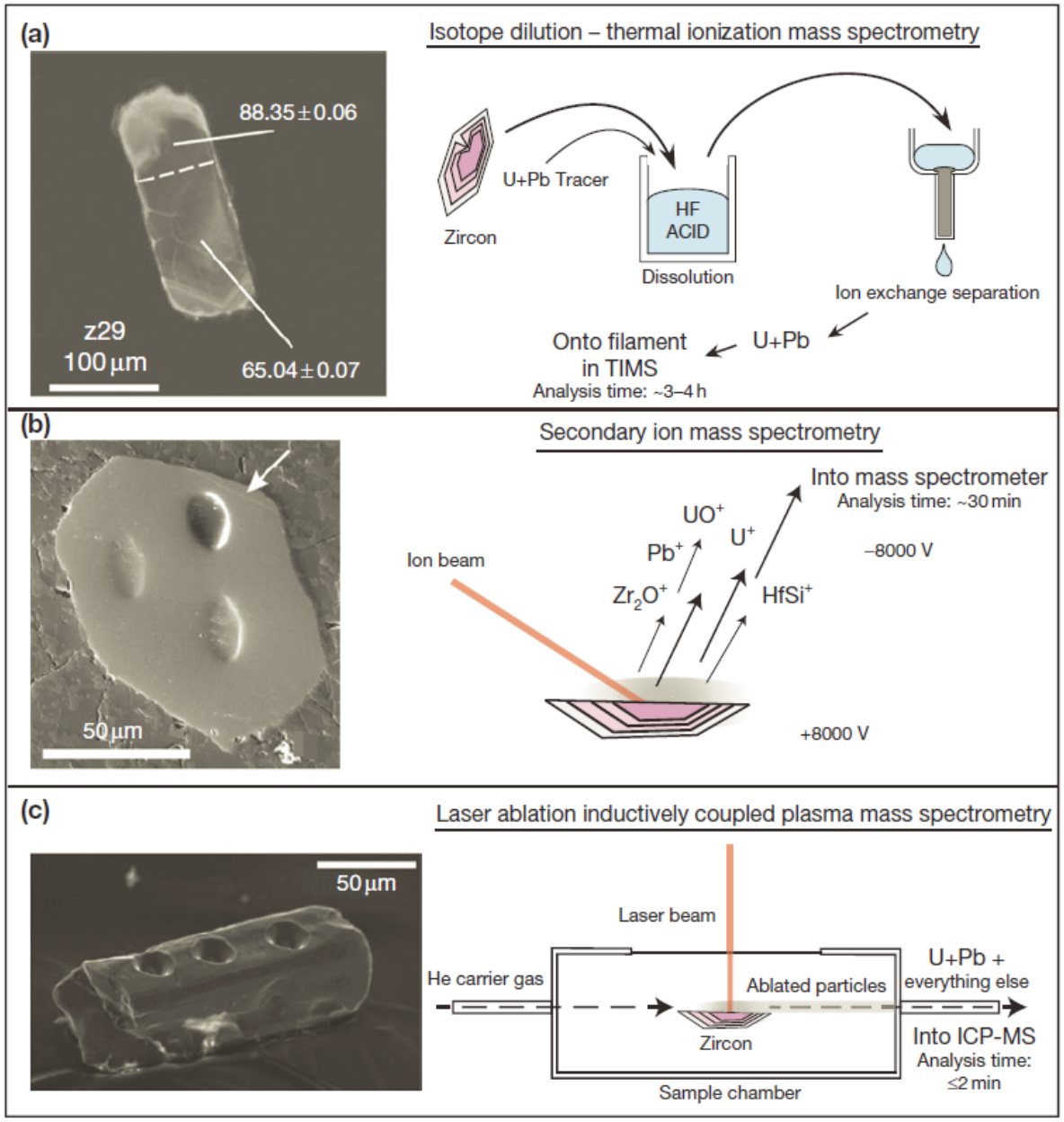

Uncertainties

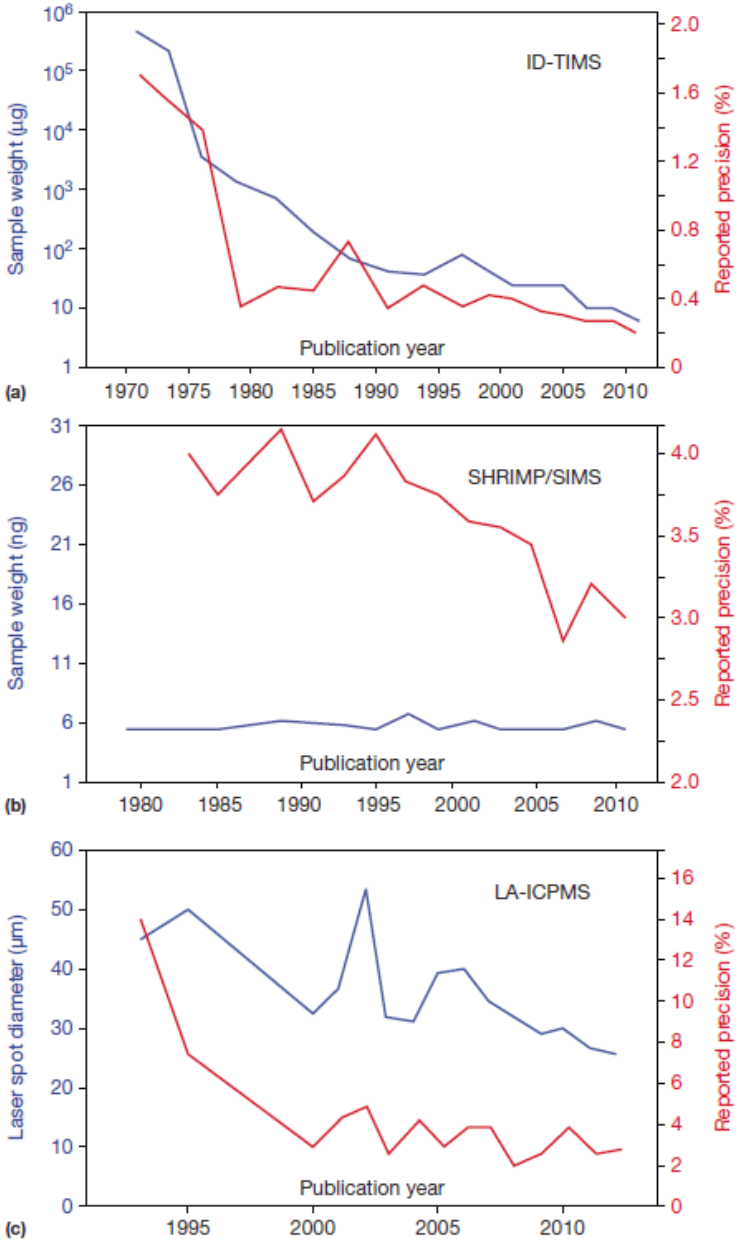

B. Schoene (2014) Treatise on Geochemistry

Zircon U-Pb geochronology

Clean room laboratory

Mass spectrometry

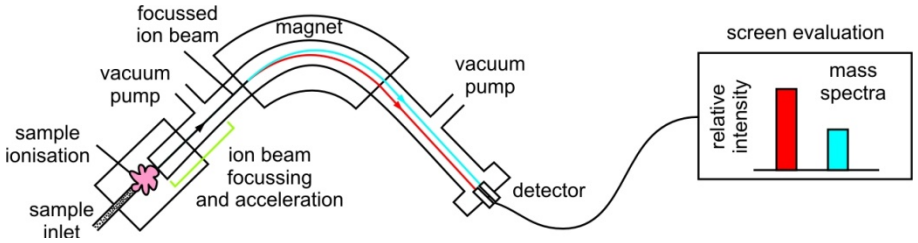

$$\left(\frac{^{206}\mathrm{Pb}}{^{205}\mathrm{Pb}}\right)_{\mathrm{measured}} = \left(\frac{^{206}\mathrm{Pb}_{\mathrm{sample}} + {}^{206}\mathrm{Pb}_{\mathrm{blank}} + {}^{206}\mathrm{Pb}_{\mathrm{tracer}}}{^{205}\mathrm{Pb}_{\mathrm{tracer}}}\right)$$

Common lead correction

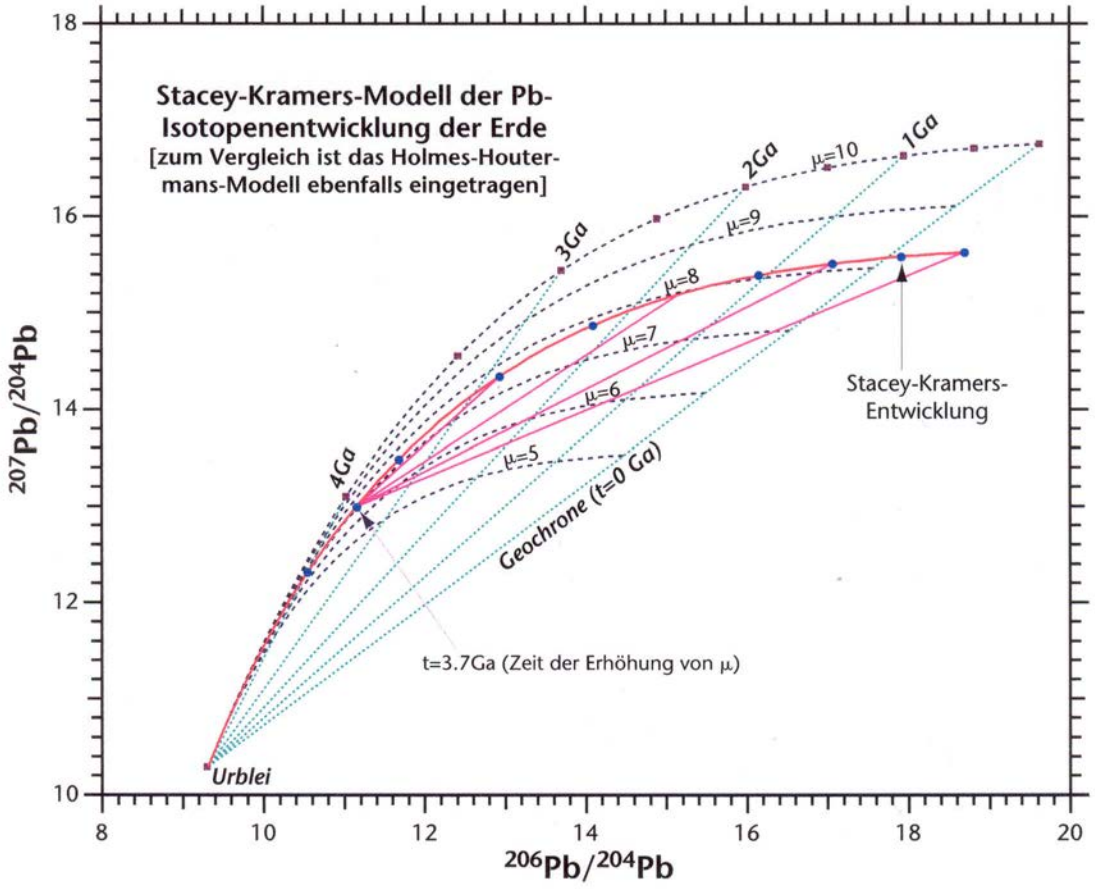

Two-stage Pb evolution model of Stacey & Kramers (1975)

In this model Pb evolves from primordial isotope ratios between 4.6 and 3.7 Ga in a reservoir with a μ-($^{238}U/^{204}Pb$) value of 7.2. At 3.7 Ga the μ-value of the reservoir was changed by geochemical differentiation to 9.7.

http://www.dmg-home.de/Ressourcen/Internet-Kurse/Isotopengeochemie.pdf

Sources of uncertainty

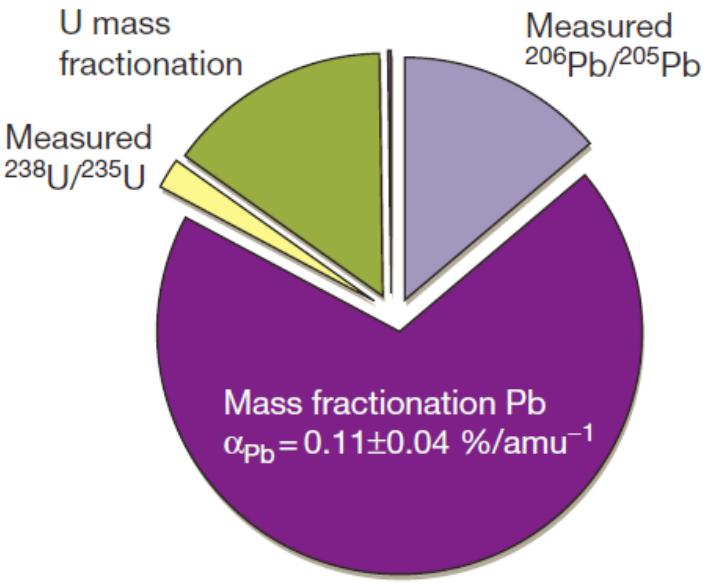

North Mt. Basalt zircon
Central Atlantic Magmatic Province

200.38 ± 0.05 Ma
$Pb^*/Pb_c = 219$
$Pb_c = 0.8$ pg

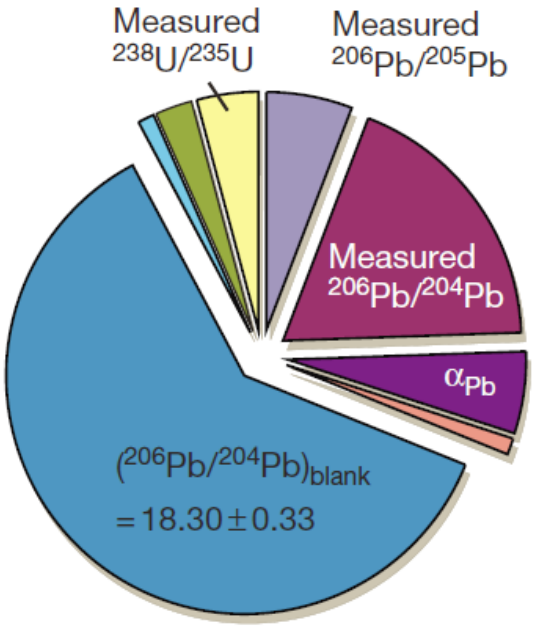

Ash bed zircon
Triassic–Jurassic boundary

200.13 ± 0.31 Ma
$Pb^*/Pb_c = 3.8$
$Pb_c = 0.5$ pg

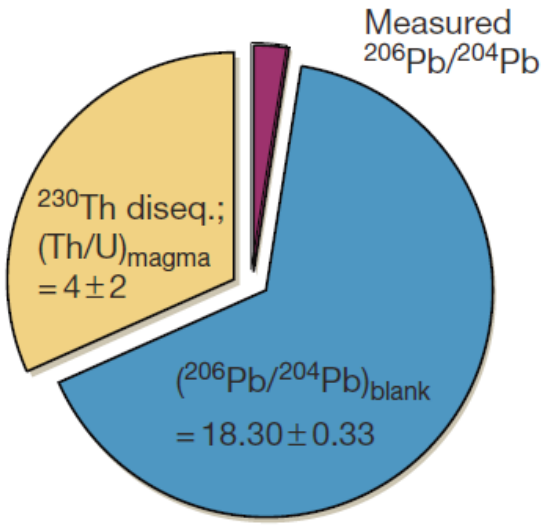

Rhyolitic tuff zircon
Kos volcanic complex

0.357 ± 0.008 Ma
$Pb^*/Pb_c = 0.5$
$Pb_c = 0.4$ pg

B. Schoene (2014) Treatise on Geochemistry

Orthoanatexite, Bayerischer Wald

Probe Wa3

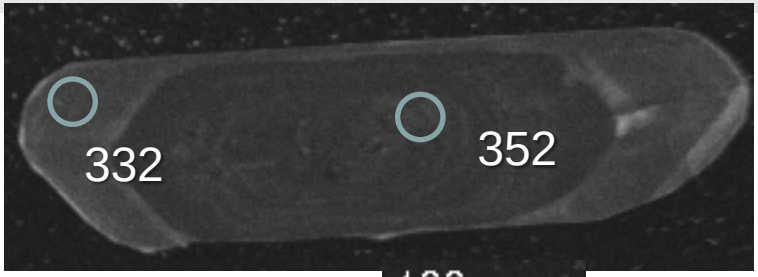

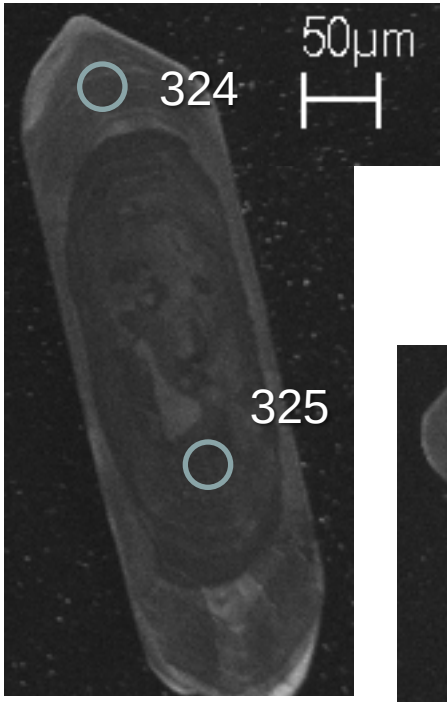

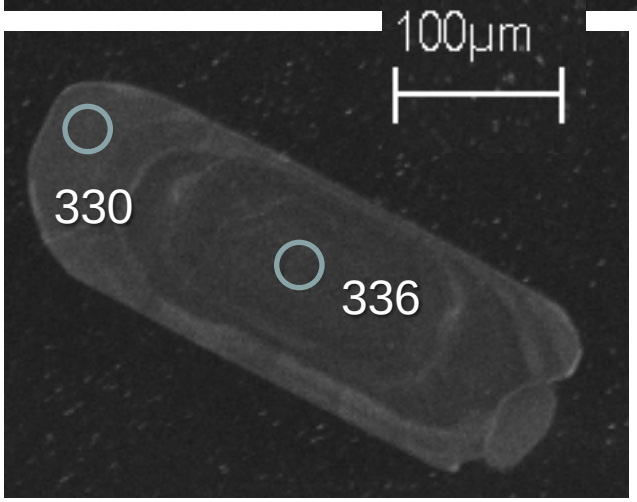

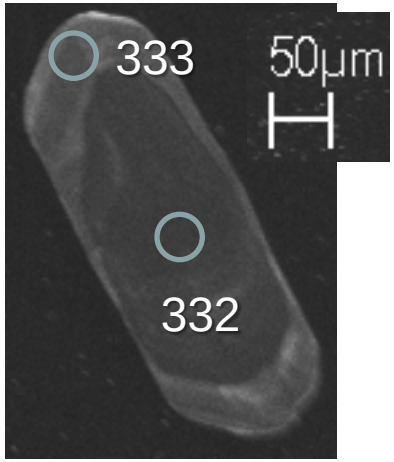

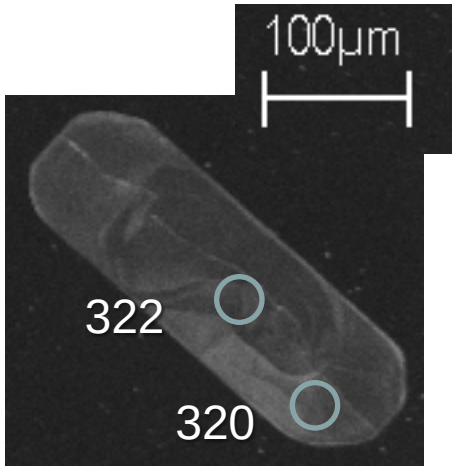

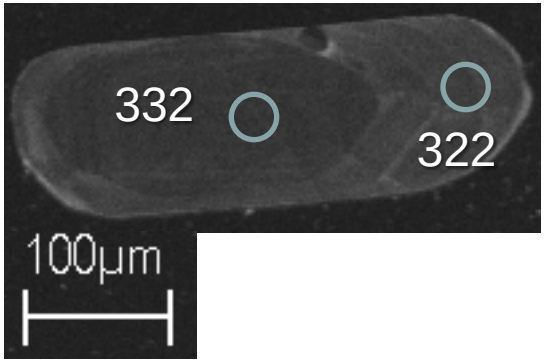

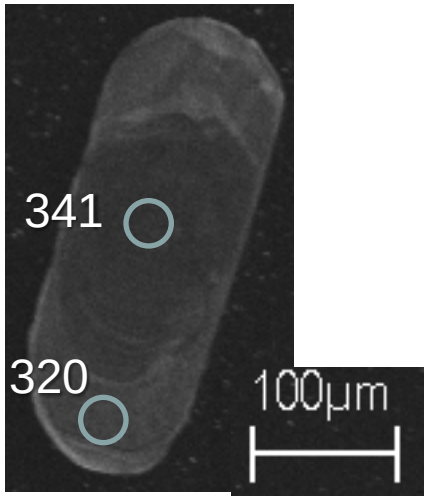

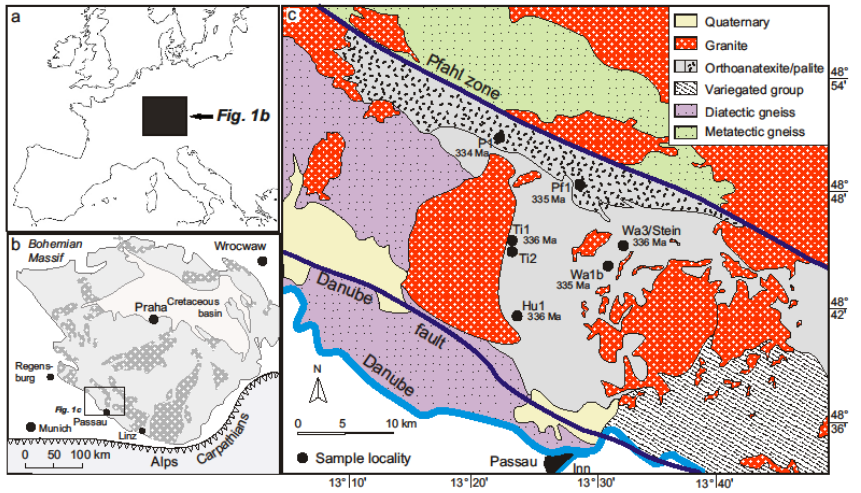

Orthoanatexite, Bayerischer Wald

Probe Wa1b

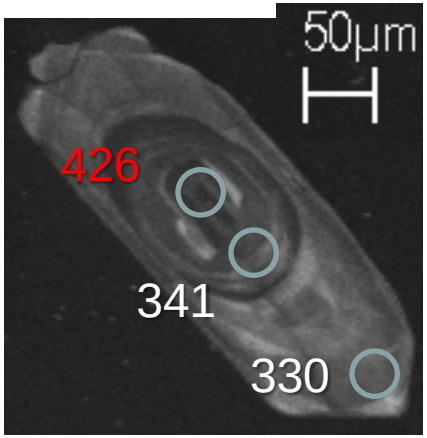

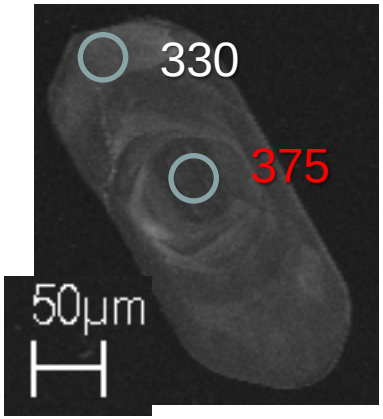

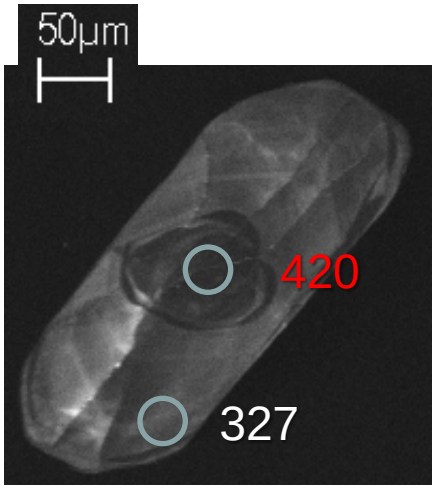

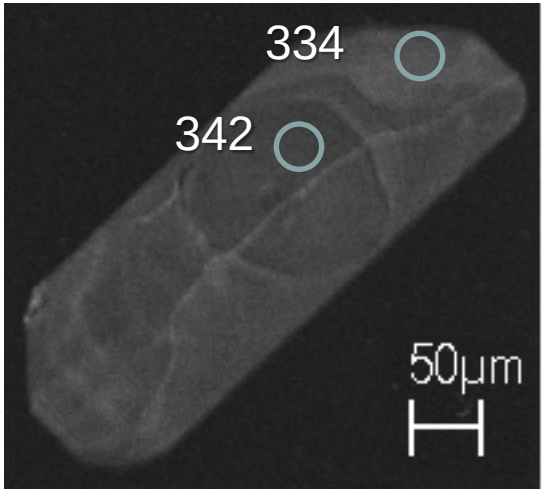

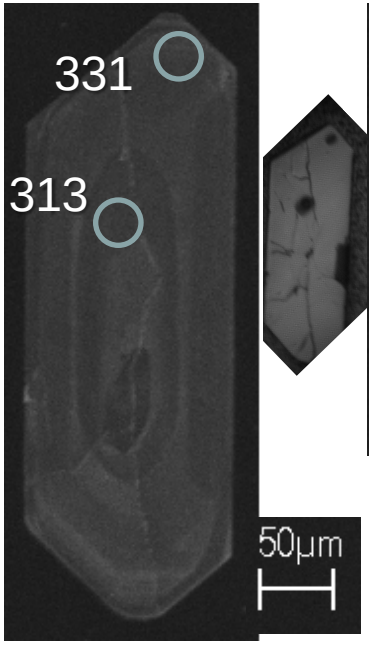

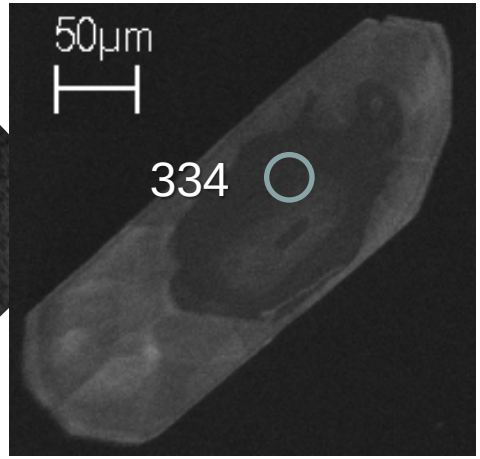

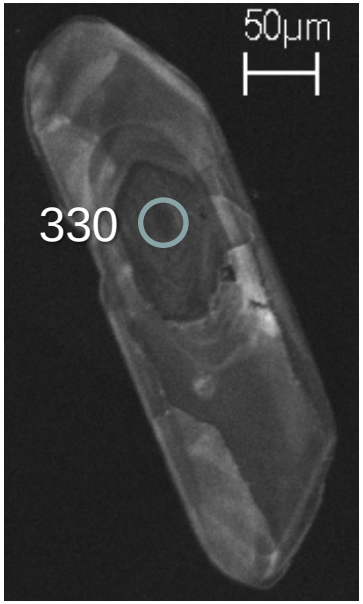

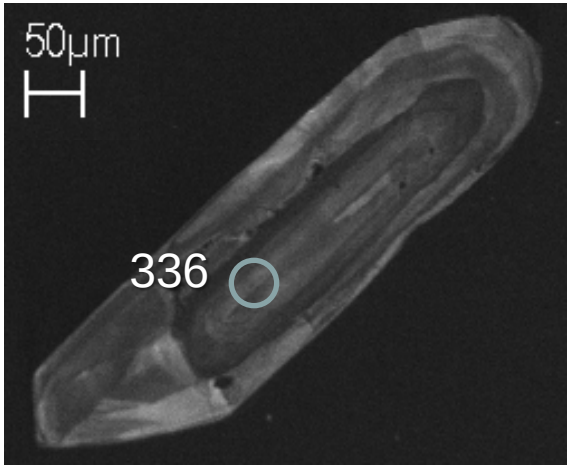

Zircon U-Pb geochronology

Mainstay in geochronology since many years

Highly radiogenic Pb can be produced in U- and Th-rich accessory minerals like zircon, titanite, monazite, uraninite

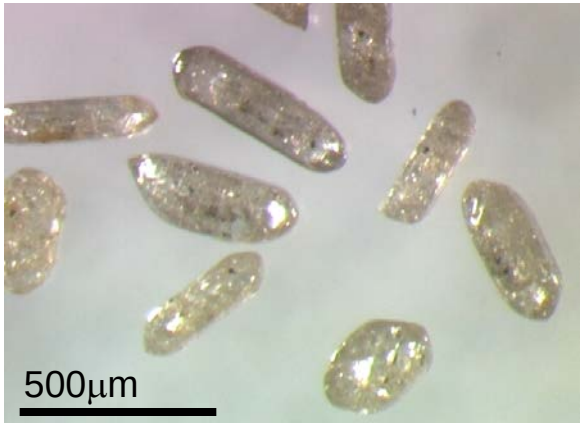

Cathodofluorescence (CL) images of polished zircon grains

Zircon ($ZrSiO_4$) - most commonly used mineral for U-Pb isotope dating and often the only method of choice in complex rocks

grain with pre-magmatic, inherited and older core

Zircon U-Pb geochronology

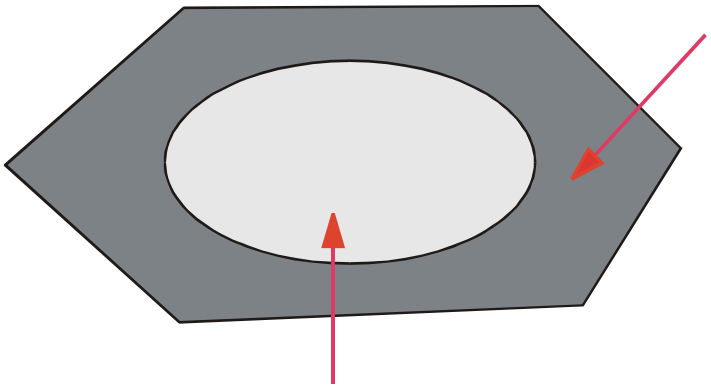

rim most likely
to lose Pb
(rims may also
be formed by
overgrowth)

core most likely
to preserve
original Pb
isotope signature

^{207}Pb-^{206}Pb zircon geochronology

Single zircon evaporation technique

$$\frac{\left(\frac{^{207}Pb}{^{204}Pb}\right) - \left(\frac{^{207}Pb}{^{204}Pb}\right)_0}{\left(\frac{^{206}Pb}{^{204}Pb}\right) - \left(\frac{^{206}Pb}{^{204}Pb}\right)_0} = \left(\frac{^{235}U}{^{238}U}\right) \frac{\left(e^{\lambda_{235}t} - 1\right)}{\left(e^{\lambda_{238}t} - 1\right)} = \left(\frac{^{207}Pb}{^{206}Pb}\right)^*$$

The ^{207}Pb-^{206}Pb age

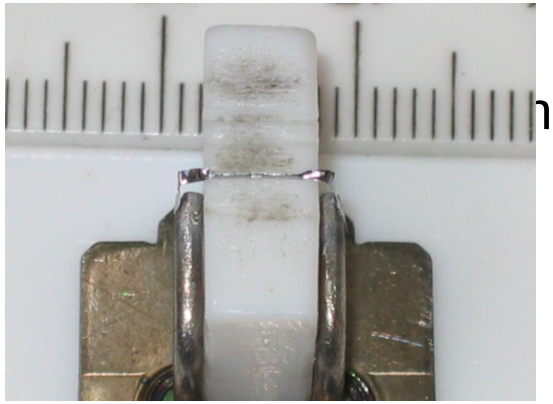

his

$$\frac{\left(\frac{^{207}Pb}{^{204}Pb}\right) - \left(\frac{^{207}Pb}{^{204}Pb}\right)_0}{\left(\frac{^{206}Pb}{^{204}Pb}\right) - \left(\frac{^{206}Pb}{^{204}Pb}\right)_0} = \frac{1}{137.88}\left(\frac{e^{\lambda_2 t} - 1}{e^{\lambda_1 t} - 1}\right)$$

$$\frac{^{207}Pb^*}{^{206}Pb^*} = \frac{\left(\frac{^{207}Pb}{^{204}Pb}\right)_t - \left(\frac{^{207}Pb}{^{204}Pb}\right)_0}{\left(\frac{^{206}Pb}{^{204}Pb}\right)_t - \left(\frac{^{206}Pb}{^{204}Pb}\right)_0}$$

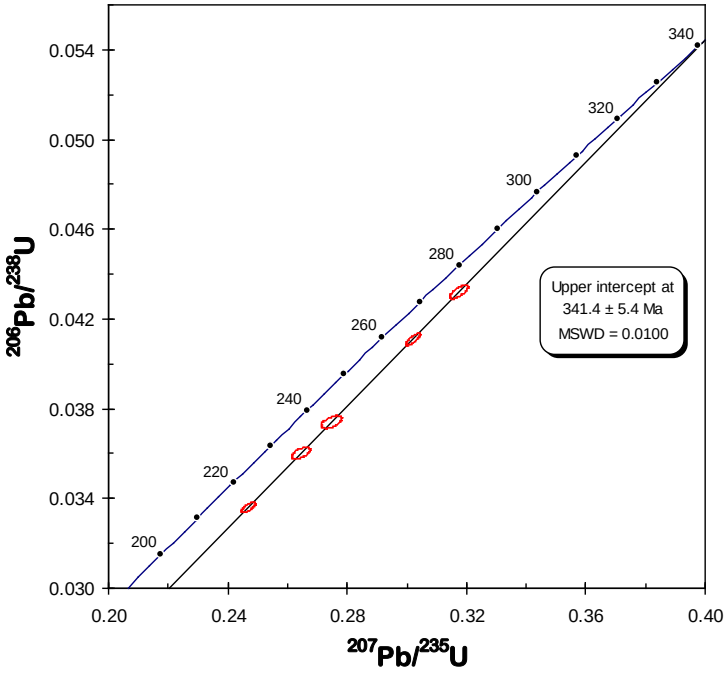

The ^{207}Pb-^{206}Pb method often yields older dates than the individual U-Pb geo-chronometers because the ratio of Pb isotopes is not as sensitive to recent Pb loss

^{207}Pb-^{206}Pb zircon geochronology

Single zircon evaporation technique

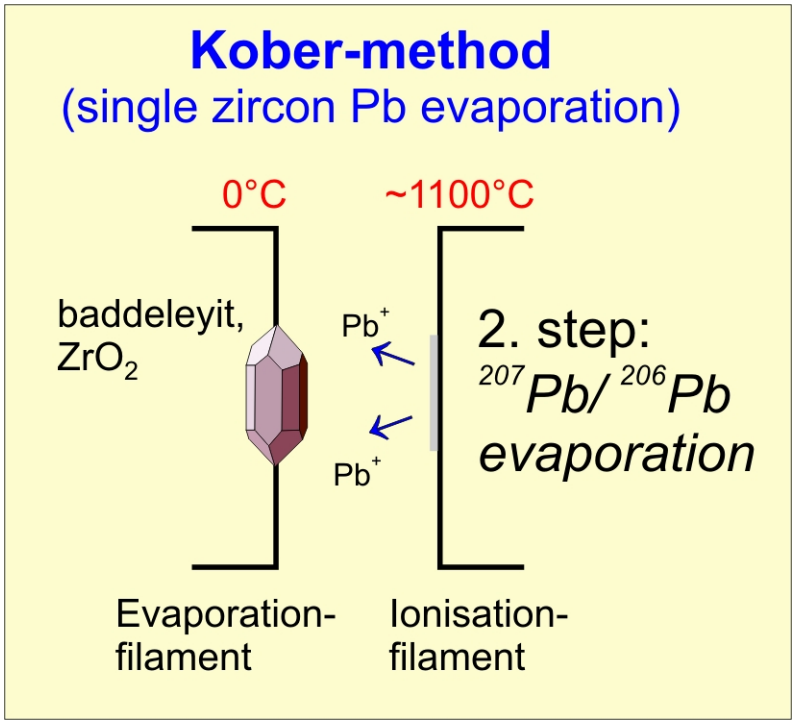

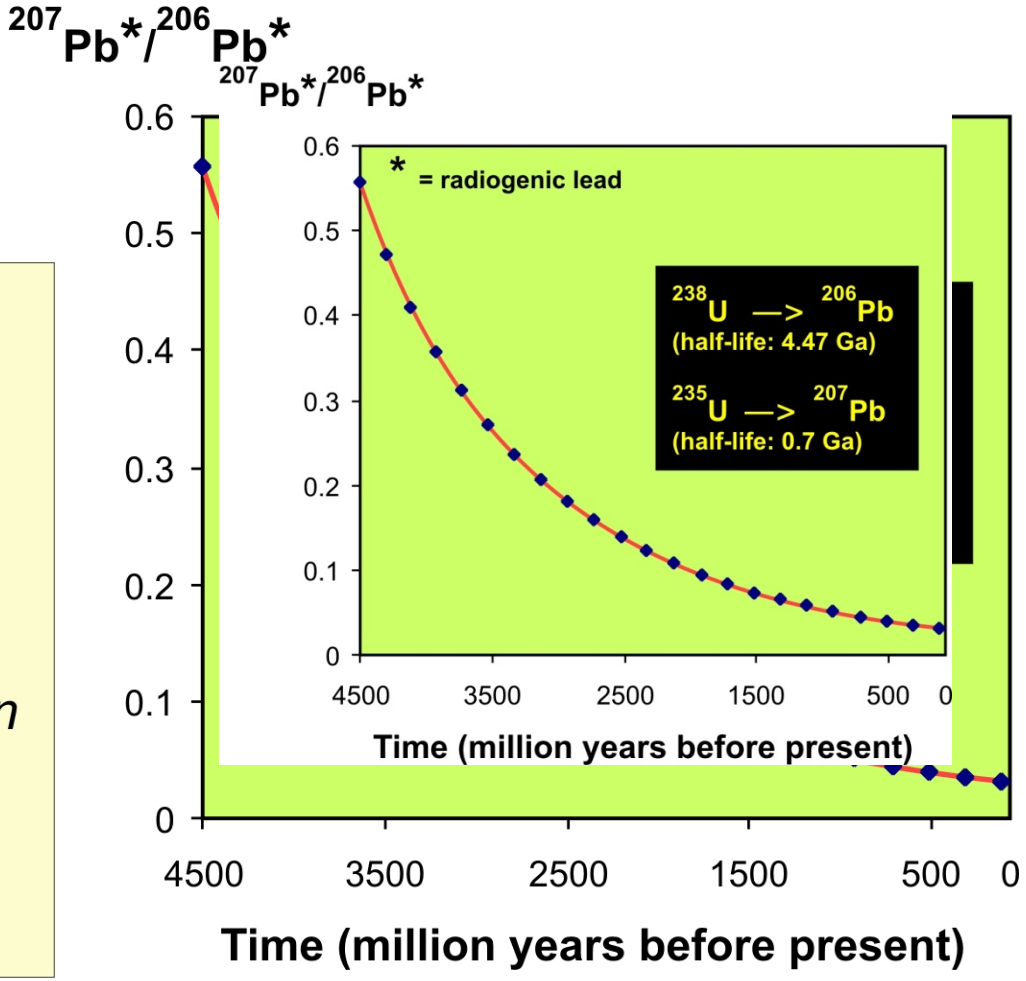

^{207}Pb-^{206}Pb zircon geochronology

Example 1:
Zircon with inherited core

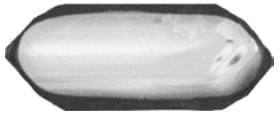

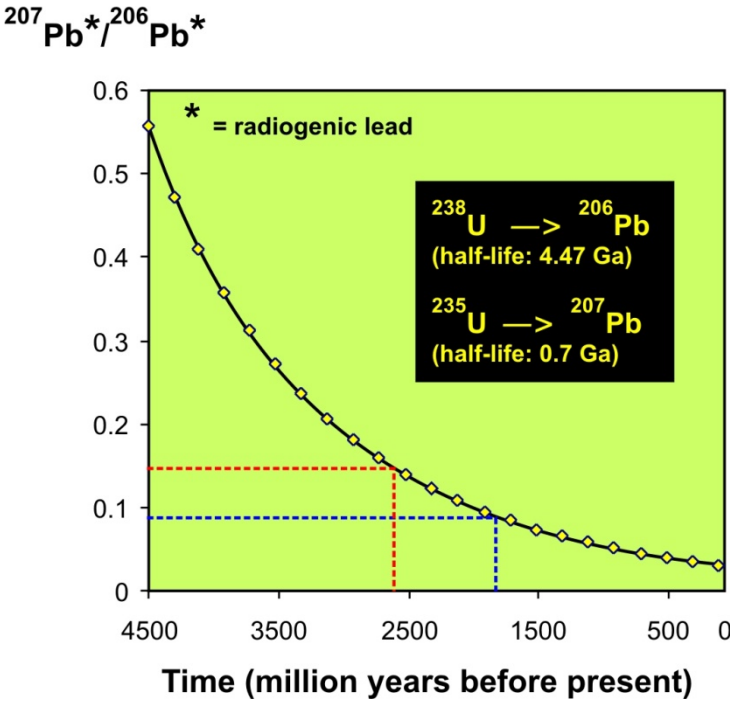

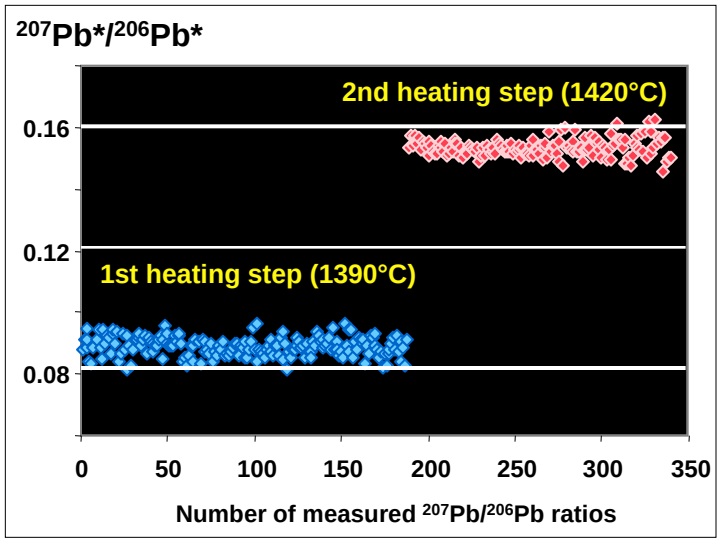

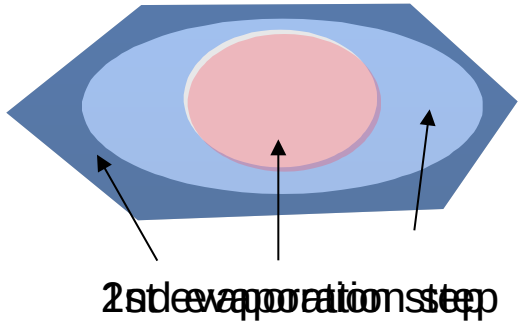

Example 2:
Zircon without core

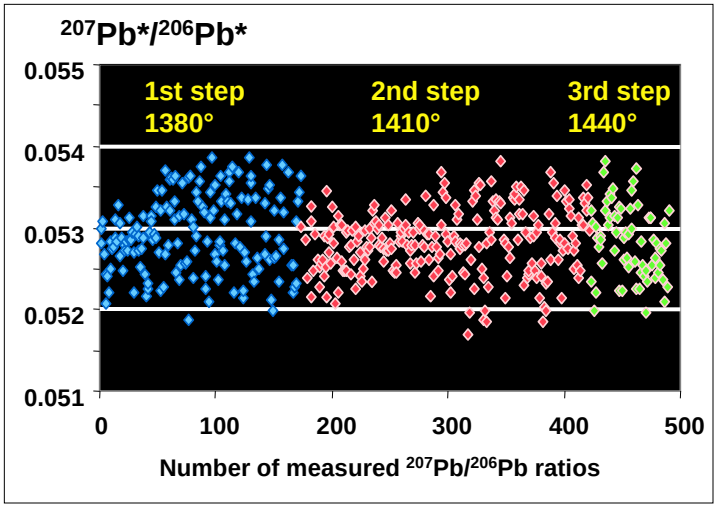

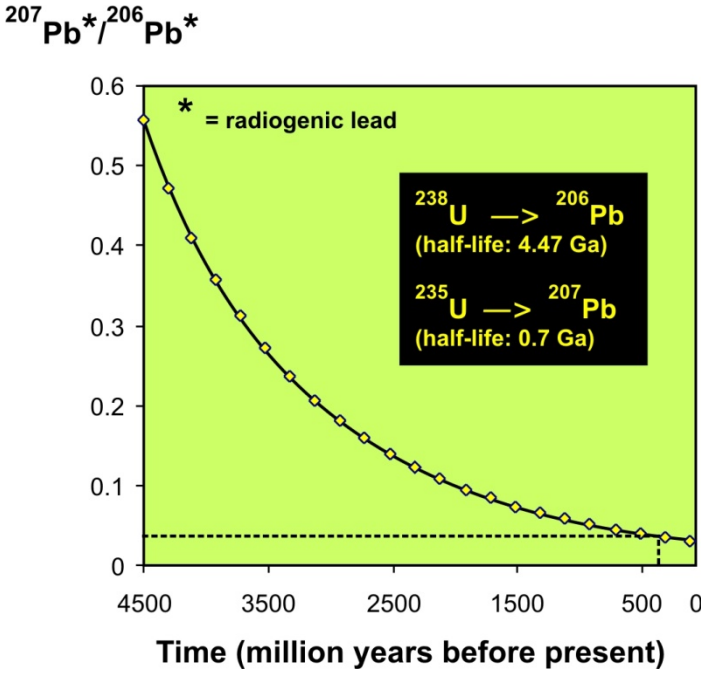

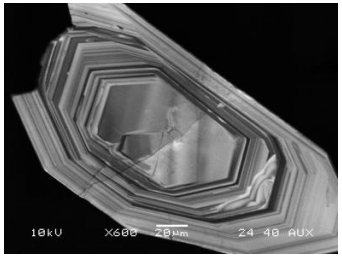

100μm

Anthropogenic Pb

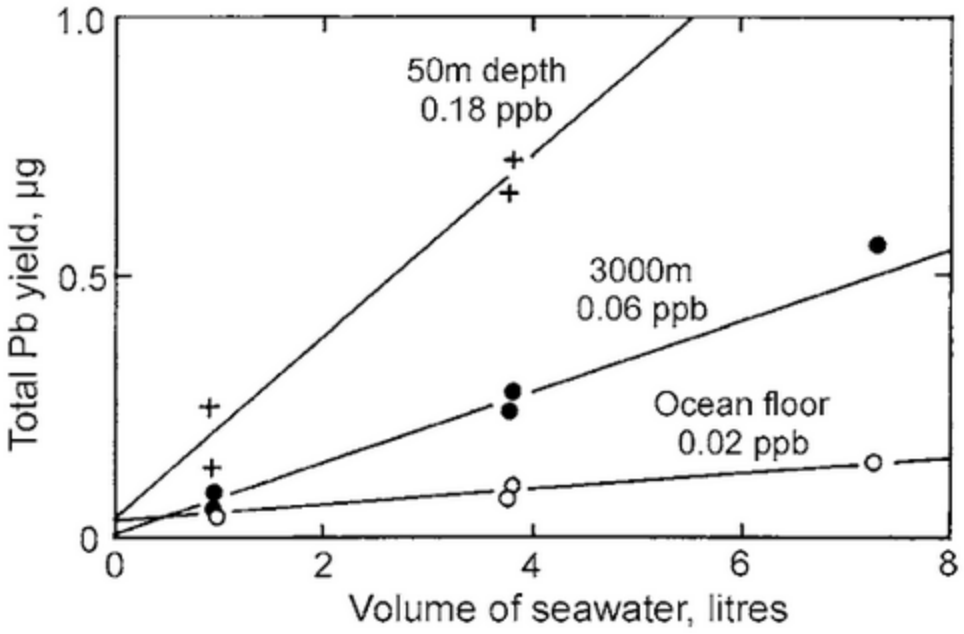

from Alan P. Dickin: http://www.onafarawayday.com/Radiogenic/

Anthropogenic Pb

Correspondence between lead ore compositions (●) and gasolines (o) from different countries on a Pb/Pb isotope plot (Chow 1970).
Strong correlation between the Pb isotope composition of gasoline Pb and local pollutant Pb.
→ gasoline additives were the principal source of pollutant lead in the environment

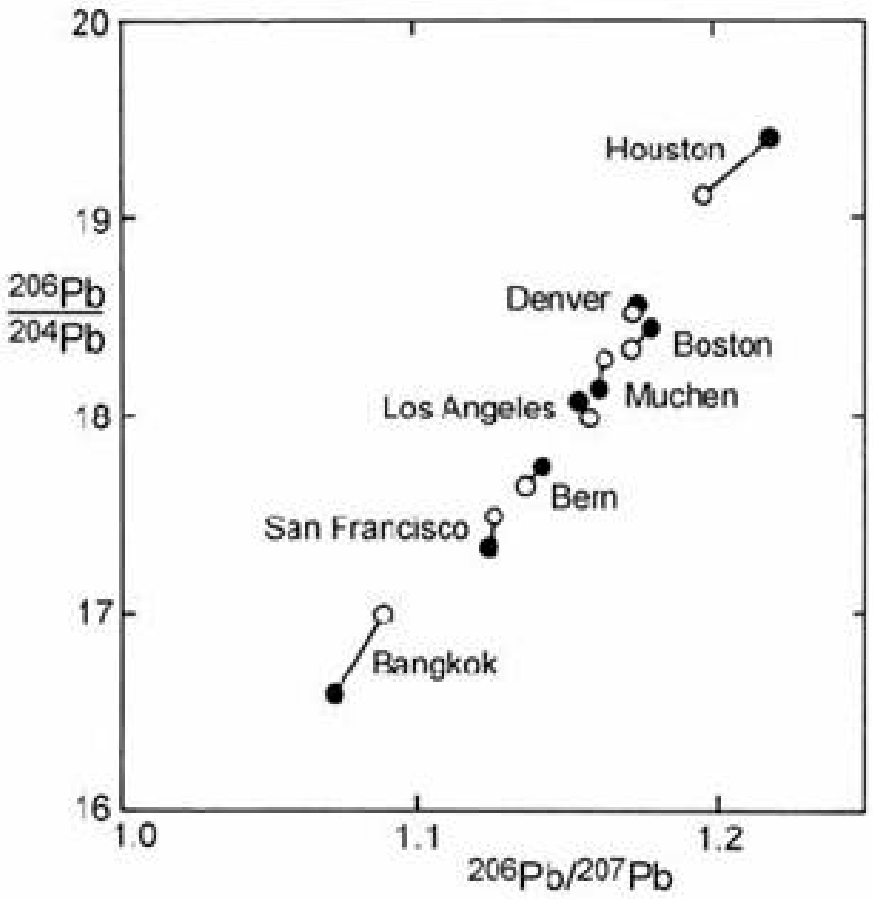

from Alan P. Dickin: http://www.onafarawayday.com/Radiogenic/

Pb composition in Shanghai

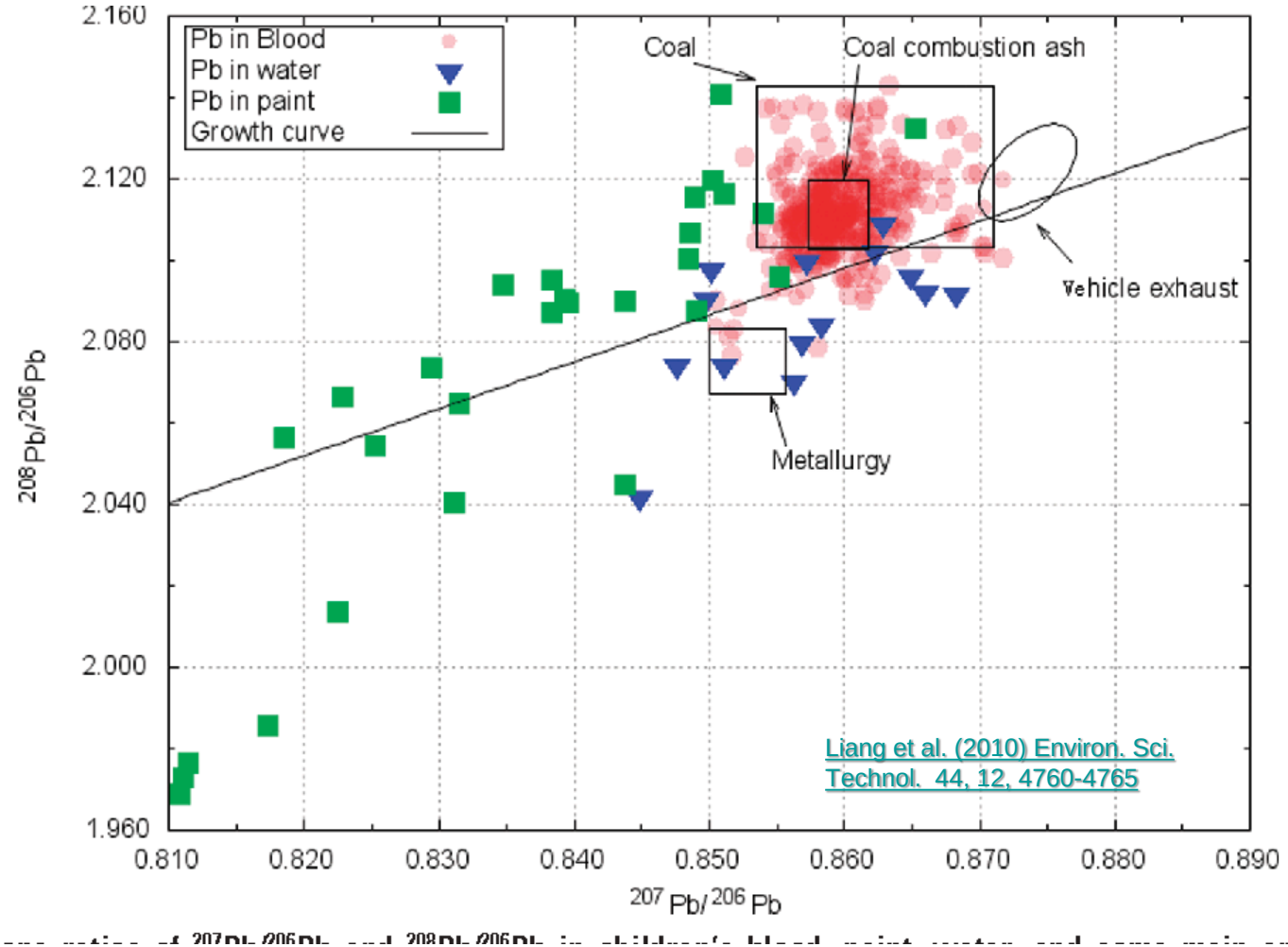

After phasing out of leaded gasoline blood lead level of children strongly correlates with the lead concentration in atmospheric particles, and the latter correlates with the coal consumption instead of leaded gasoline.

Anthropogenic Pb

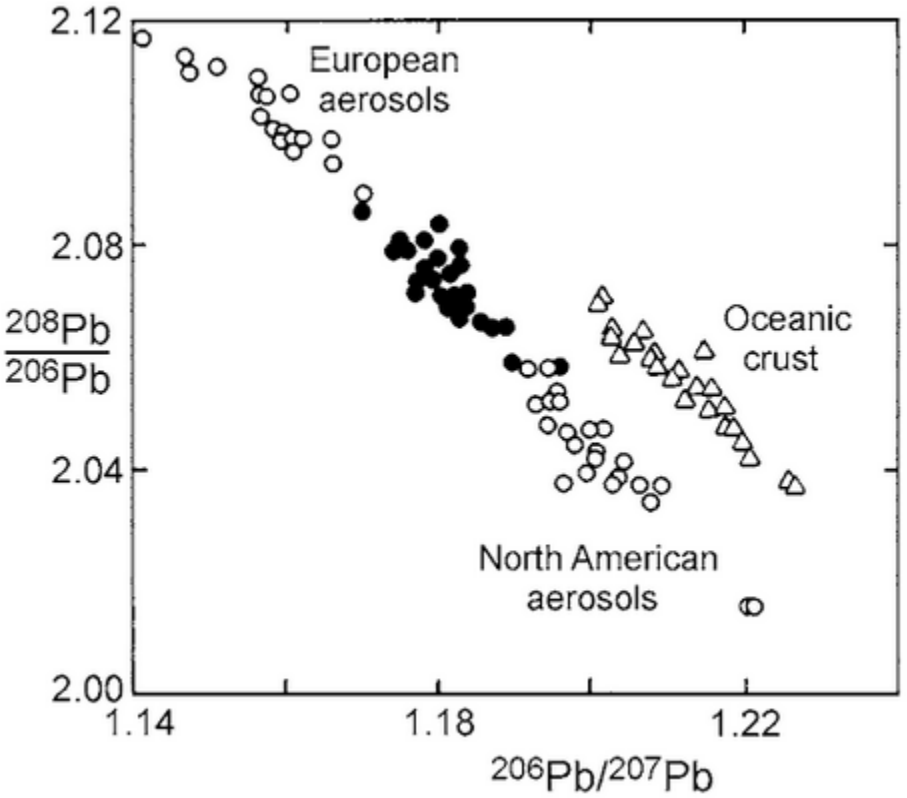

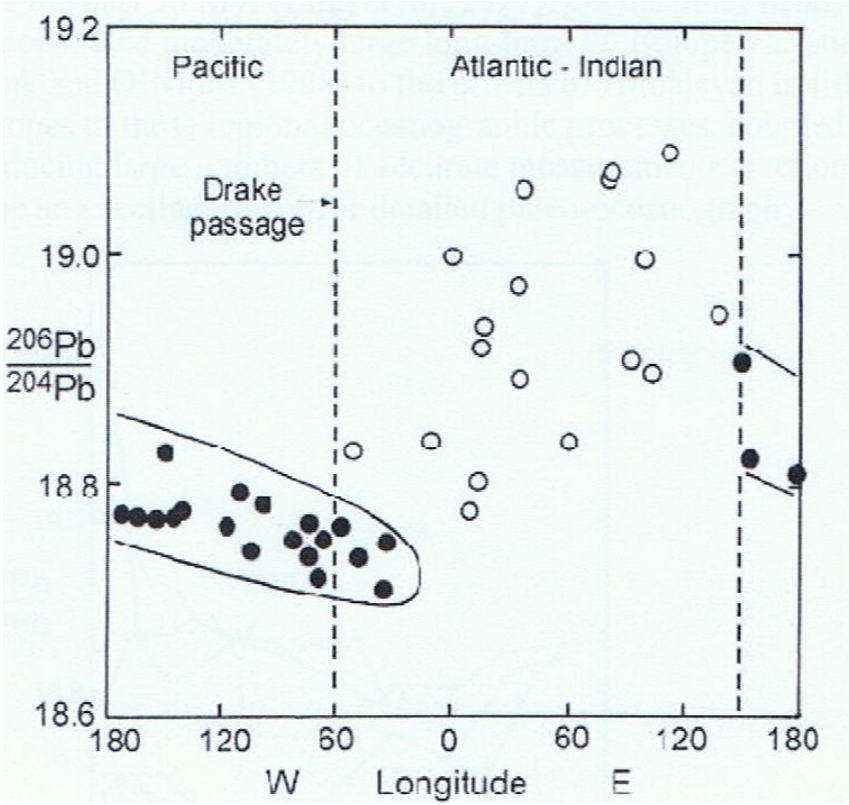

from Alan P. Dickin: http://www.onafarawayday.com/Radiogenic/

Pb isotopes in the ocean

Chow & Patterson 1959, 1962: First major Pb isotope studies on manganese nodules and pelagic sediments

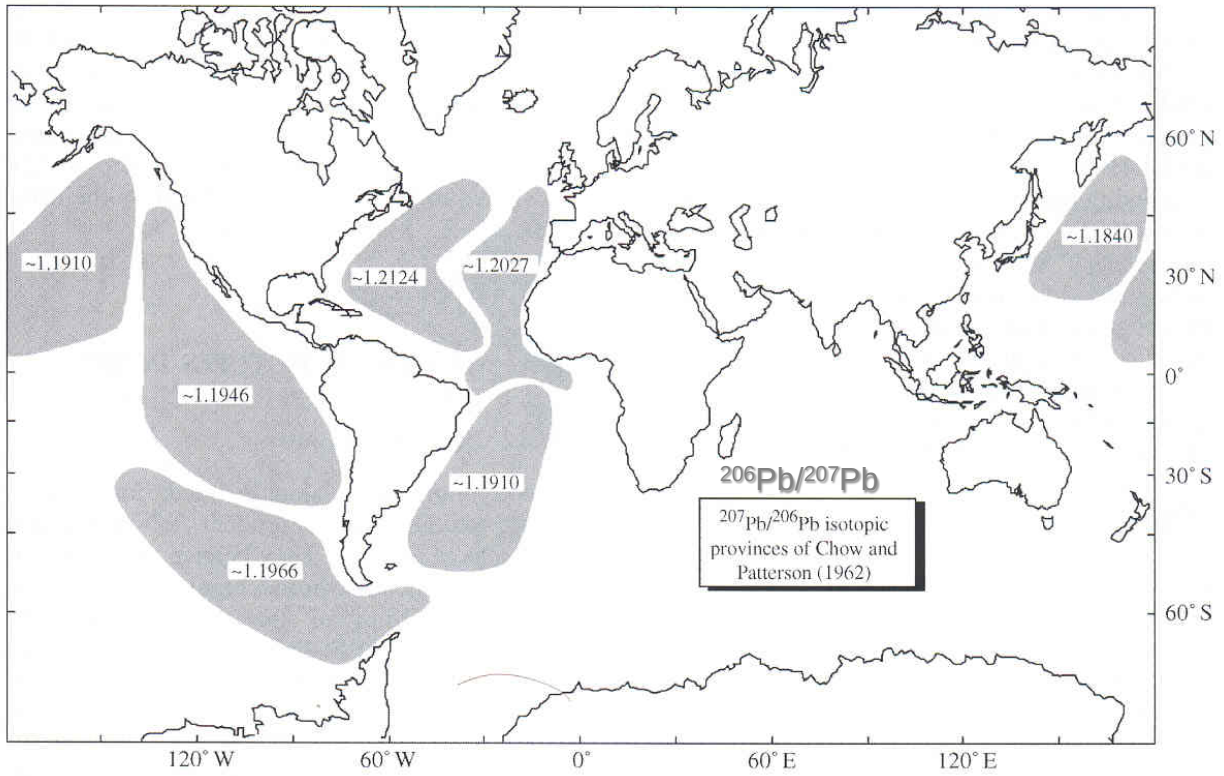

Result: General distinction between the Pb isotope signatures of Atlantic and Pacific samples. Within each ocean, manganese nodules and pelagic sediments give relatively consistent results

Conclusions: Pb has a relatively short residence time in seawater. Distinct Pacific and Atlantic Ocean signatures reflect average Pb isotope composition of the continents surrounding each ocean

from Goldstein & Hemming: Treatise on Geochemistry, Vol.6

Pb isotopes in the ocean

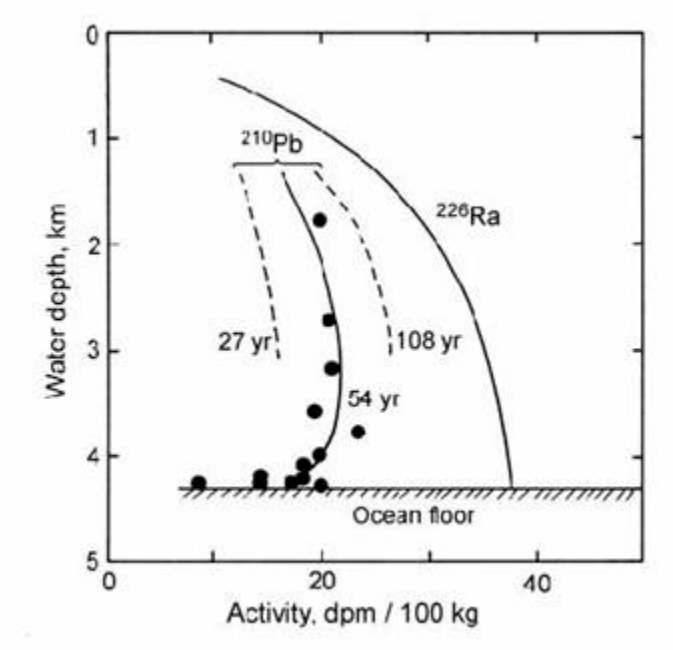

from Alan P. Dickin: http://www.onafarawayday.com/Radiogenic/

The age of the Earth

Lead isotope isochron that Clair Patterson used to determine the age of the solar system and Earth (Patterson 1956)

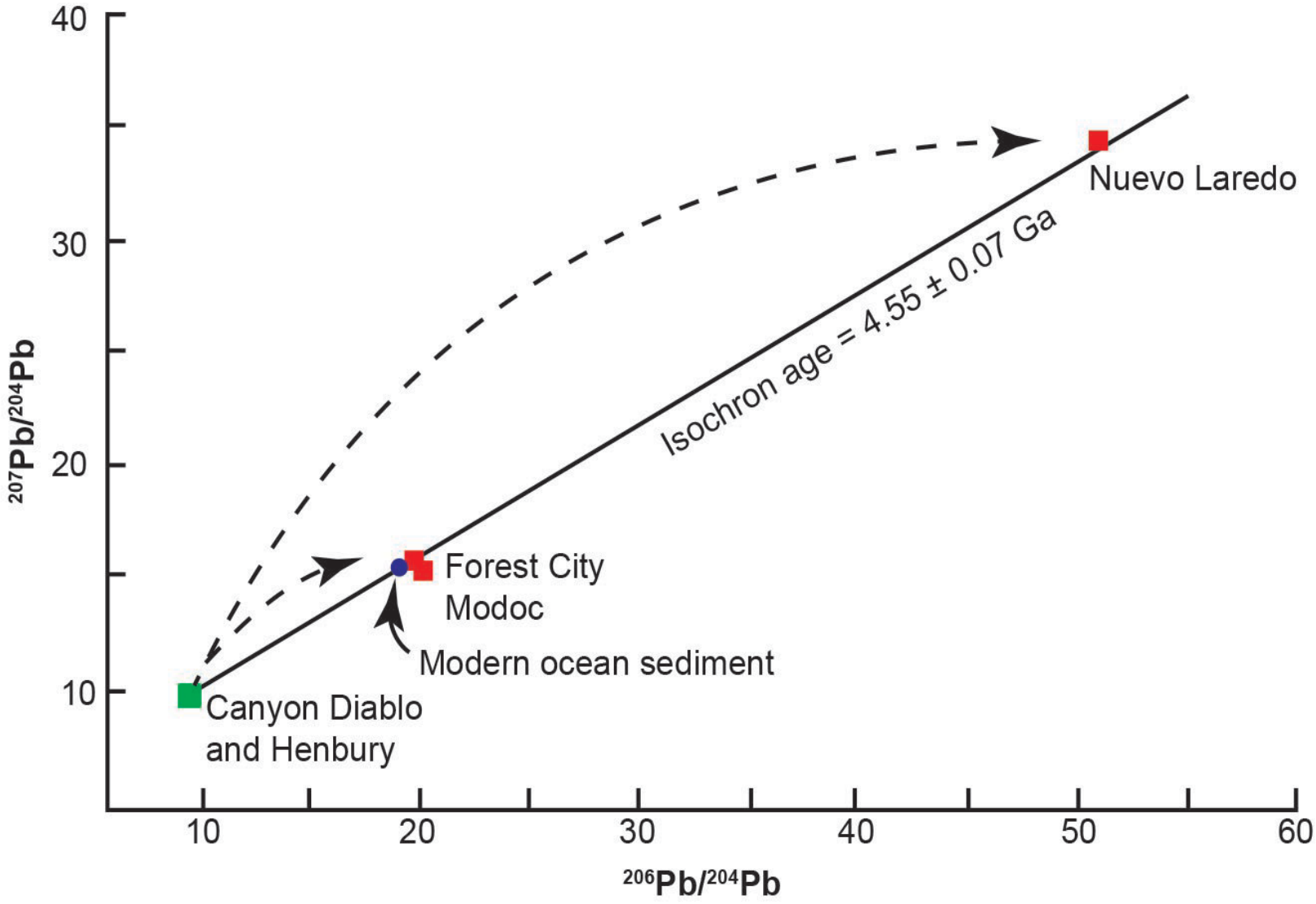

The isotope geology of Pb

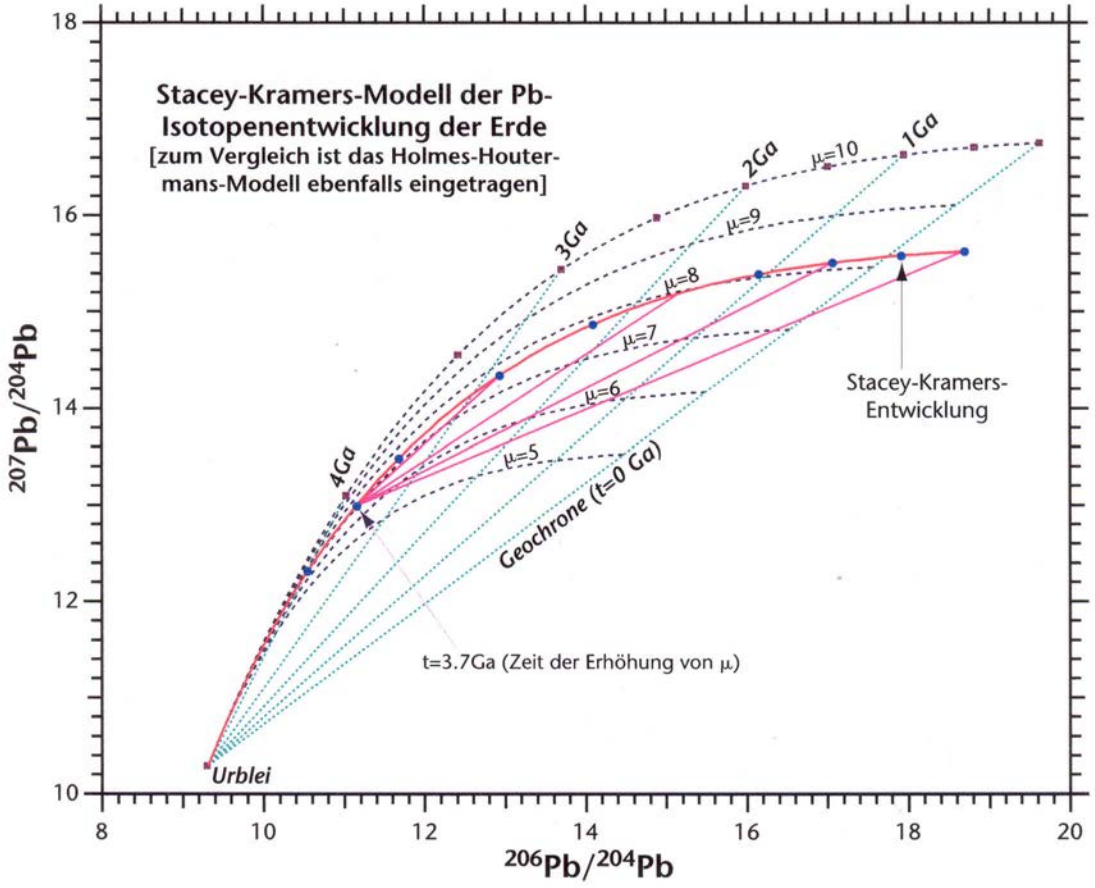

Two-stage Pb evolution model of Stacey & Kramers (1975)

In this model Pb evolves from primordial isotope ratios between 4.6 and 3.7 Ga in a reservoir with a μ-($^{238}U/^{204}Pb$) value of 7.2. At 3.7 Ga the μ-value of the reservoir was changed by geochemical differentiation to 9.7.

http://www.dmg-home.de/Ressourcen/Internet-Kurse/Isotopengeochemie.pdf

Pb-Pb dating

Combine the two U-Pb geochronometers:

$$\frac{^{207}Pb}{^{204}Pb} = \left(\frac{^{207}Pb}{^{204}Pb}\right)_0 + \frac{^{235}U}{^{204}Pb}(e^{\lambda_2 t} - 1)$$

$$\frac{^{206}Pb}{^{204}Pb} = \left(\frac{^{206}Pb}{^{204}Pb}\right)_0 + \frac{^{238}U}{^{204}Pb}(e^{\lambda_1 t} - 1)$$

$$\frac{\left(\frac{^{207}Pb}{^{204}Pb}\right) - \left(\frac{^{207}Pb}{^{204}Pb}\right)_0}{\left(\frac{^{206}Pb}{^{204}Pb}\right) - \left(\frac{^{206}Pb}{^{204}Pb}\right)_0} = \frac{^{235}U}{^{238}U}\left(\frac{e^{\lambda_2 t} - 1}{e^{\lambda_1 t} - 1}\right)$$

$$\frac{\left(\frac{^{207}Pb}{^{204}Pb}\right) - \left(\frac{^{207}Pb}{^{204}Pb}\right)_0}{\left(\frac{^{206}Pb}{^{204}Pb}\right) - \left(\frac{^{206}Pb}{^{204}Pb}\right)_0} = \frac{1}{137.88}\left(\frac{e^{\lambda_2 t} - 1}{e^{\lambda_1 t} - 1}\right)$$

The ^{207}Pb-^{206}Pb age

The left-hand side of this equation is written as:

$$\frac{\left(\frac{^{207}Pb}{^{204}Pb}\right) - \left(\frac{^{207}Pb}{^{204}Pb}\right)_0}{\left(\frac{^{206}Pb}{^{204}Pb}\right) - \left(\frac{^{206}Pb}{^{204}Pb}\right)_0} = \frac{1}{137.88}\left(\frac{e^{\lambda_2 t} - 1}{e^{\lambda_1 t} - 1}\right)$$

$$\frac{^{207}Pb^*}{^{206}Pb^*} = \frac{\left(\frac{^{207}Pb}{^{204}Pb}\right)_t - \left(\frac{^{207}Pb}{^{204}Pb}\right)_0}{\left(\frac{^{206}Pb}{^{204}Pb}\right)_t - \left(\frac{^{206}Pb}{^{204}Pb}\right)_0}$$

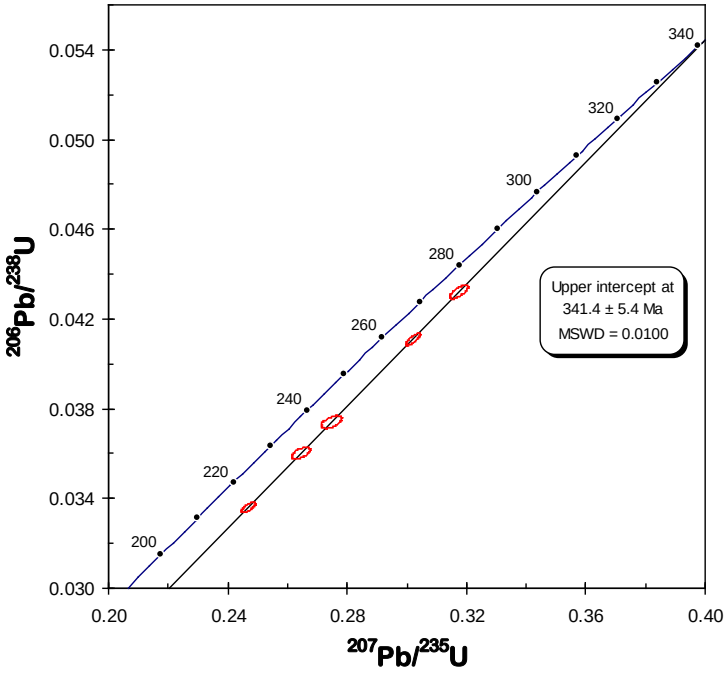

The ^{207}Pb-^{206}Pb method often yields older dates than the individual U-Pb geo-chronometers because the ratio of Pb isotopes is not as sensitive to recent Pb loss

Pb-Pb dating

A plot of $^{207}Pb/^{204}Pb$ vs. $^{206}Pb/^{204}Pb$ for rocks or minerals of the same age should yield a straight line. This line is called Pb-Pb isochron.

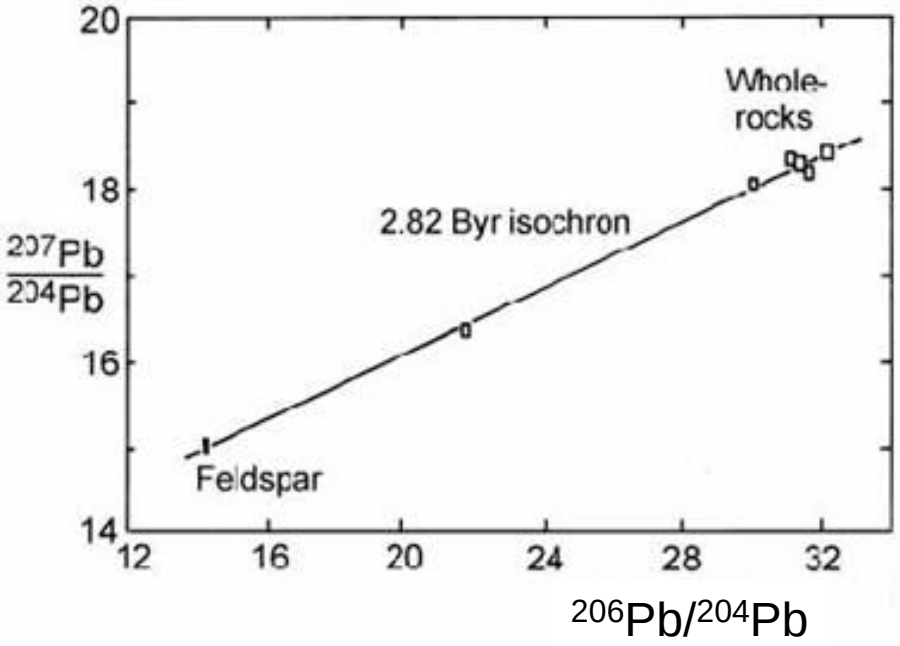

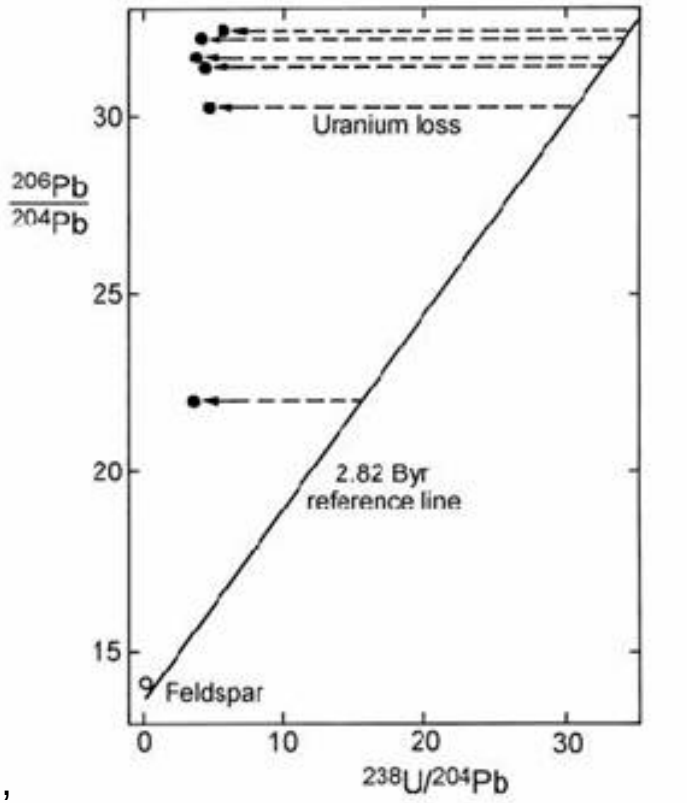

In this example uranium was lost in recent weathering processes. This invalidates the U-Pb isochron method, but since the Pb isotope ratios in the rock reflect the pre-weathering U concentrations, they are not upset by the recent alteration event.

http://www.onafarawayday.com/Radiogenic/

Pb-Pb dating

A plot of $^{207}Pb/^{204}Pb$ vs. $^{206}Pb/^{204}Pb$ for rocks or minerals of the same age should yield a straight line. This line is called Pb-Pb isochron.

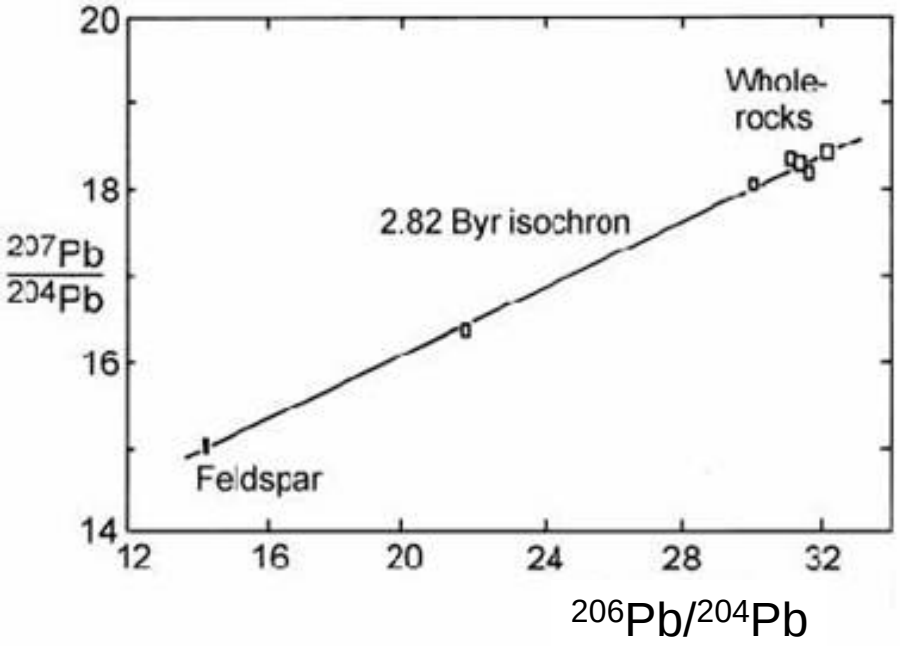

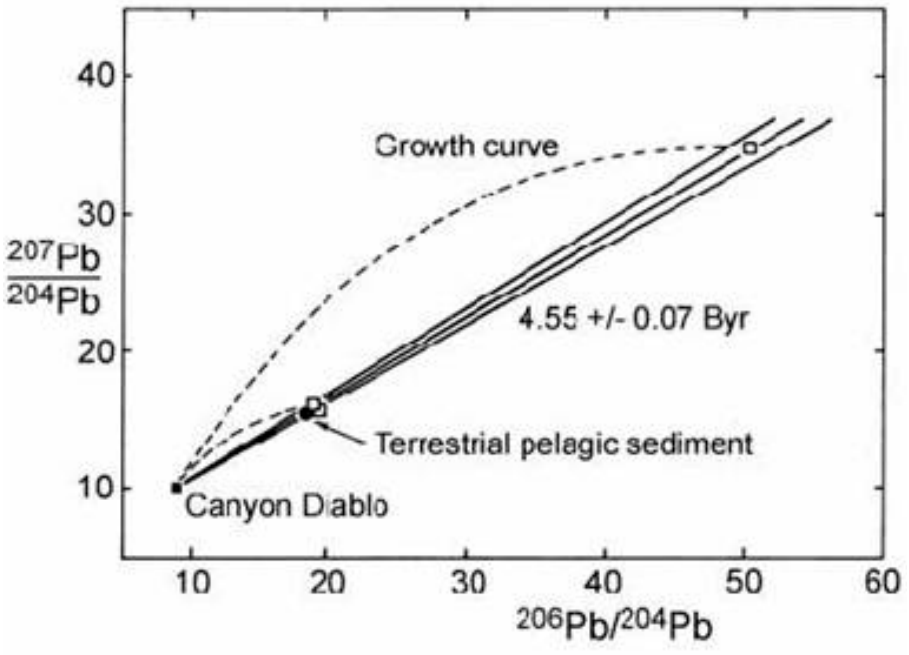

Pb-Pb isochron diagram for iron and stony meteorites (■,□) and a 'Bulk Earth' sample of oceanic sediment (●), showing that the Earth lies on the meteorite isochron, therefore also called the 'geochron'. After Patterson (1956).

http://www.onafarawayday.com/Radiogenic/

The isotope geology of Pb

$$206Pb_t = 206Pb_{0(bzw.T)} + 235U(e^{\lambda_{235}T} - e^{\lambda_{235}t})$$

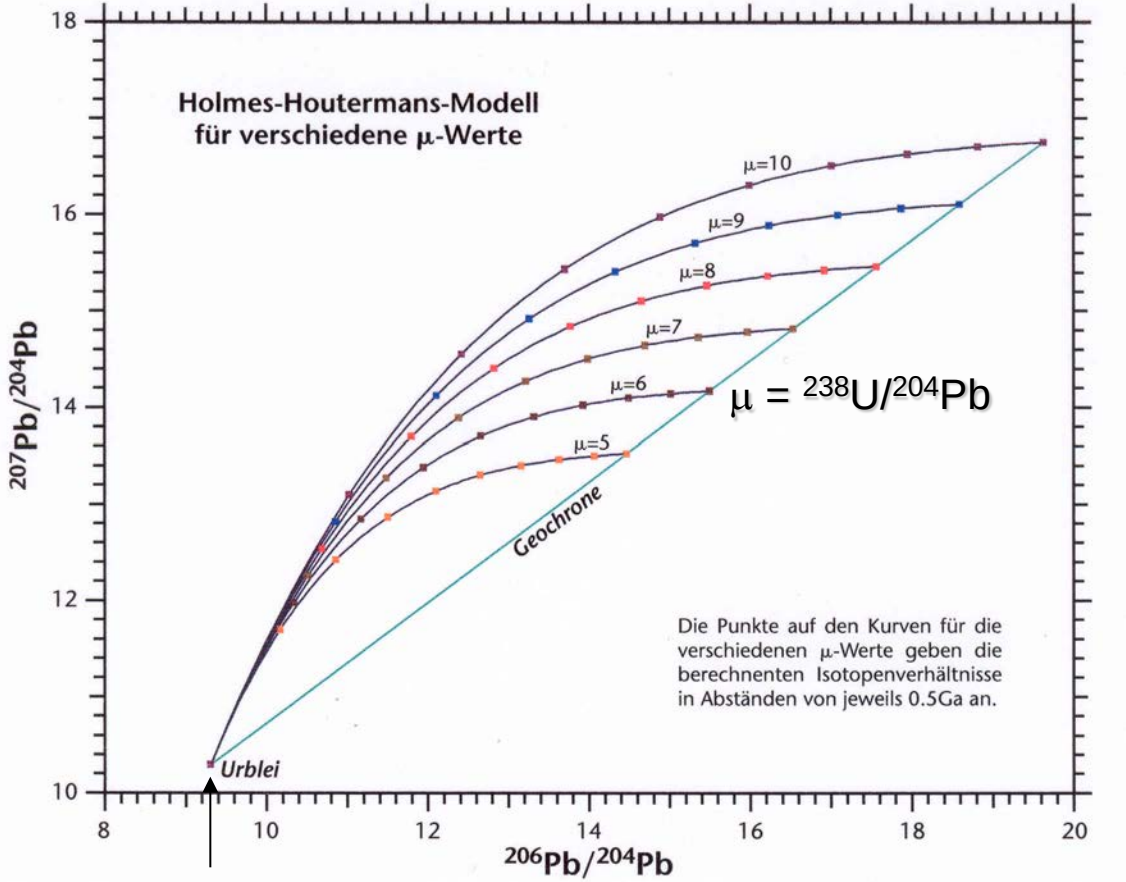

Primeval lead
(Isotope ratios of Pb in troilite of the iron meteorite Canyon Diablo)

$$\left(\frac{^{206}Pb}{^{204}Pb}\right)_t = a_0 + \mu(e^{\lambda_1 T} - e^{\lambda_1 t})$$

$$\left(\frac{^{207}Pb}{^{204}Pb}\right)_t = b_0 + \frac{\mu}{137.88}(e^{\lambda_2 T} - e^{\lambda_2 t})$$

T = Erdalter

$$\left(\frac{^{206}Pb}{^{204}Pb}\right)_i = a_0 = 9.30$$

$$\left(\frac{^{207}Pb}{^{204}Pb}\right)_i = b_0 = 10.29$$

The isotope geology of Pb

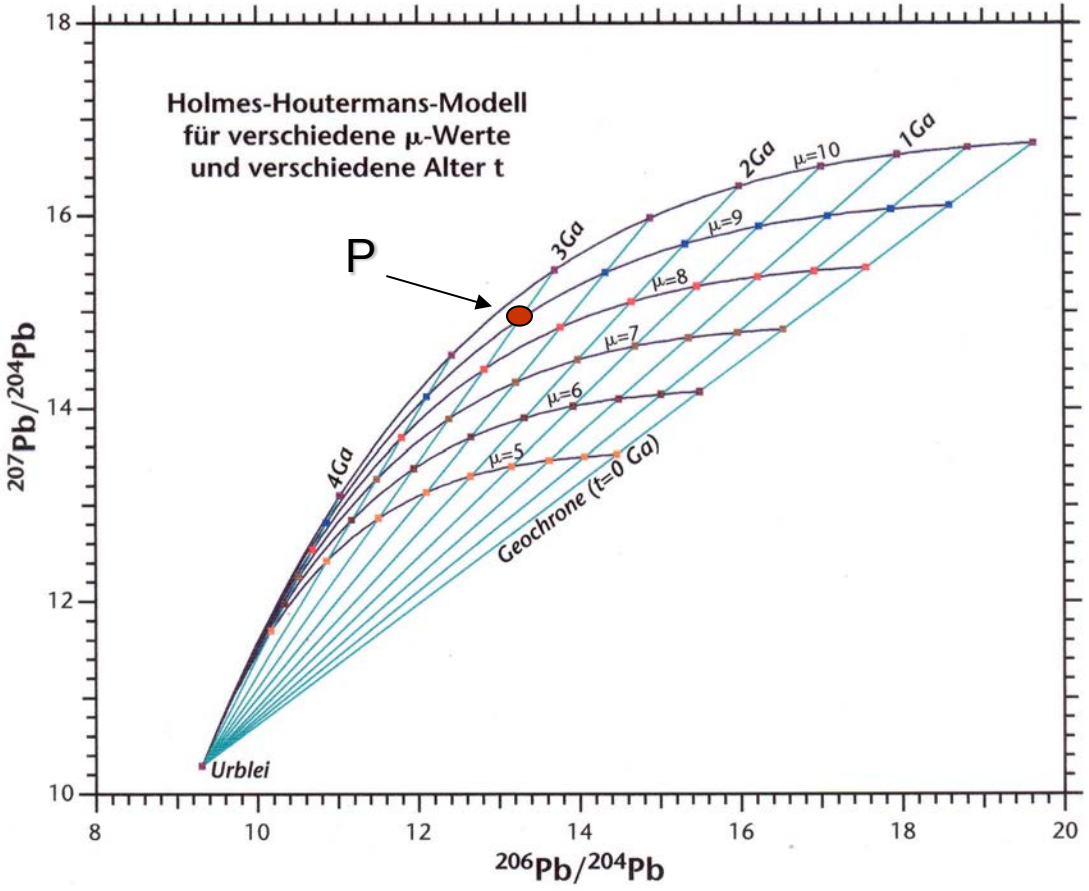

$$\left(\frac{^{206}Pb}{^{204}Pb}\right)_t = a_0 + \mu(e^{\lambda_1 T} - e^{\lambda_1 t})$$

$$\left(\frac{^{207}Pb}{^{204}Pb}\right)_t = b_0 + \frac{\mu}{137.88}(e^{\lambda_2 T} - e^{\lambda_2 t})$$

The straight lines are isochrons for selected values of t. Point P: $^{207}Pb/^{204}Pb$ and $^{206}Pb/^{204}Pb$ ratios of a lead mineral (e.g. galena that was withdrawn 3×10^9 years ago from a source region with a present μ-value of 9.

http://www.dmg-home.de/Ressourcen/Internet-Kurse/Isotopengeochemie.pdf

The isotope geology of Pb

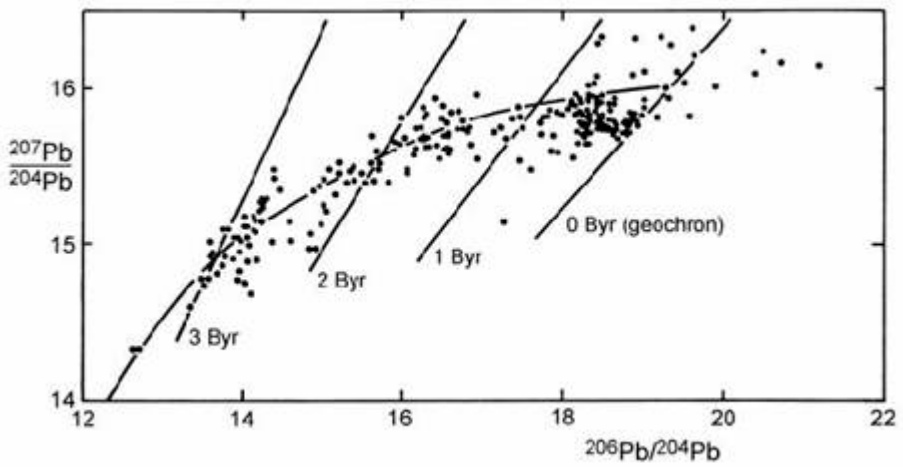

Pb-Pb isochron diagram showing a compilation of many analysed **galenas** from different environments. Stanton and Russell (1959)

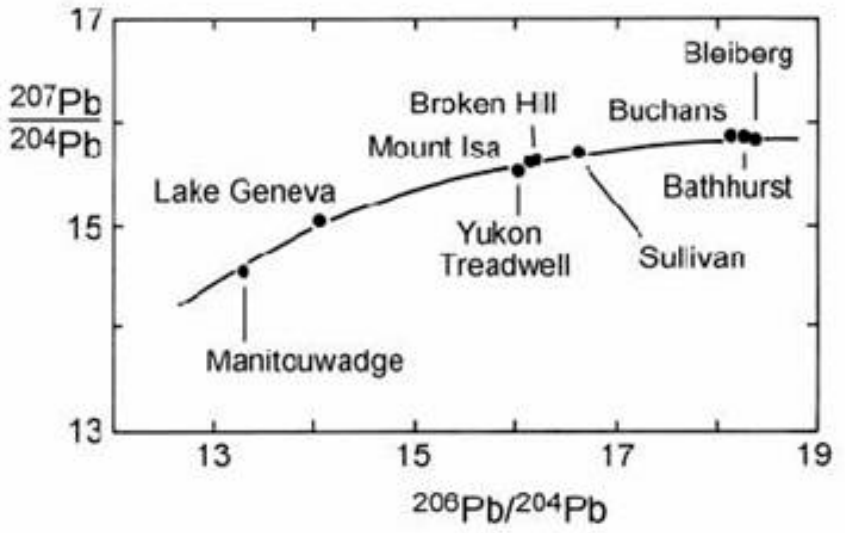

Pb-Pb isochron diagram showing galena ores that form the basis of the ‘conformable’ Pb model. Stanton and Russell (1959)

http://www.onafarawayday.com/Radiogenic/

The isotope geology of Pb

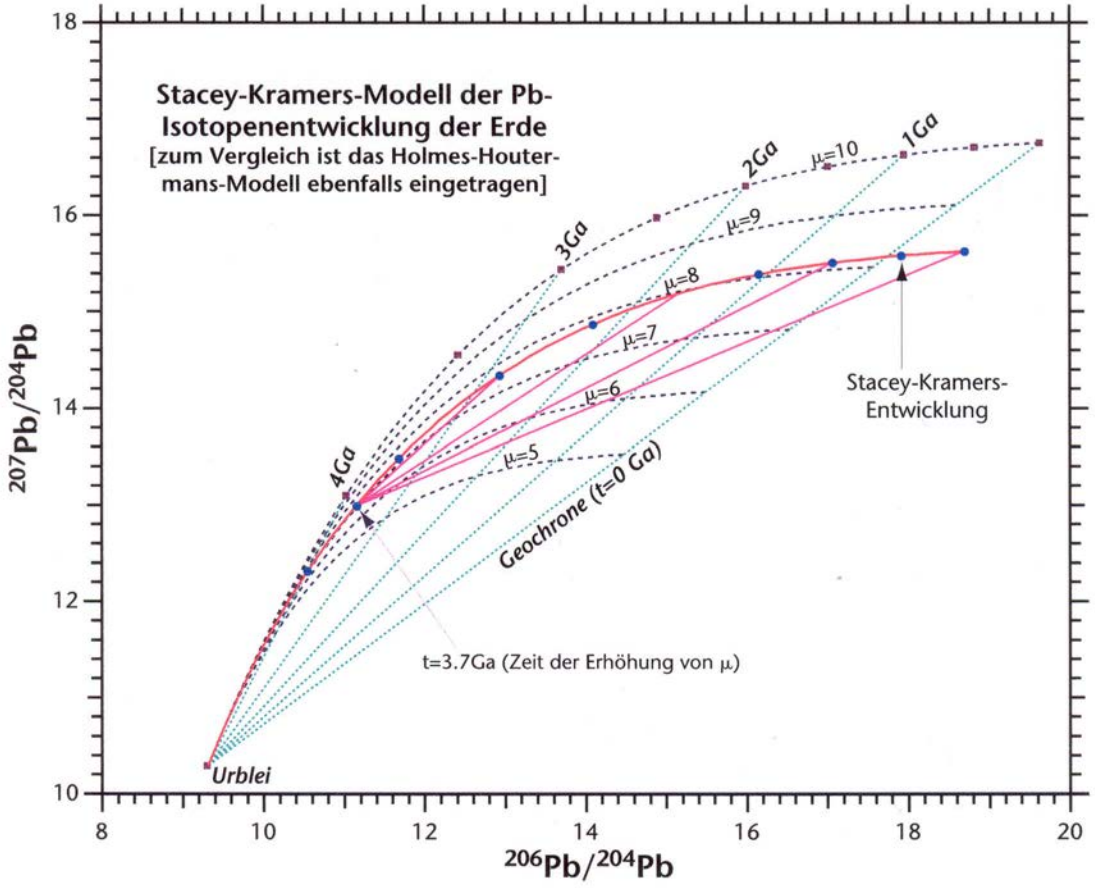

Two-stage Pb evolution model of Stacey & Kramers (1975)

In this model Pb evolves from primordial isotope ratios between 4.6 and 3.7 Ga in a reservoir with a μ-($^{238}U/^{204}Pb$) value of 7.2. At 3.7 Ga the μ-value of the reservoir was changed by geochemical differentiation to 9.7.

http://www.dmg-home.de/Ressourcen/Internet-Kurse/Isotopengeochemie.pdf

Plumbotectonics

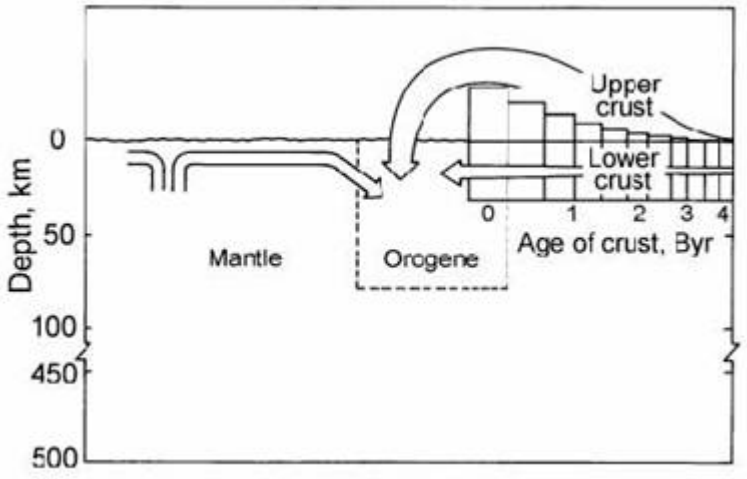

Schematic illustration of the operation of the ‘plumbotectonics’ model, showing mixing of crustal and mantle reservoirs into the orogene (galena source) reservoir. Doe & Zartman (1979)

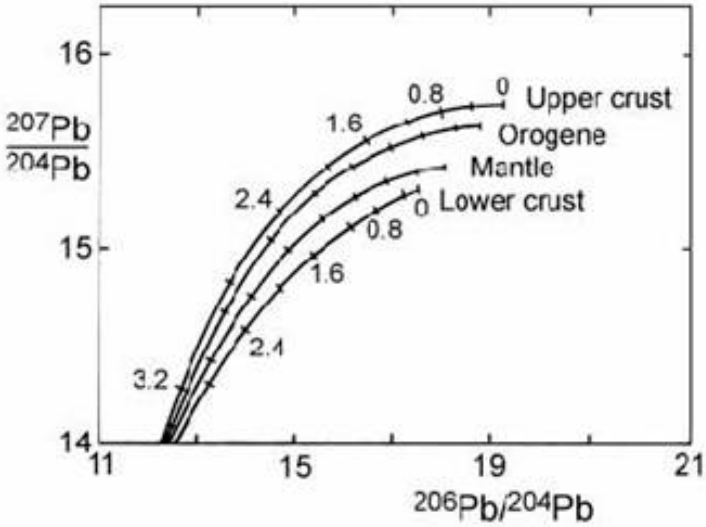

Pb-Pb isochron diagram showing isotopic evolution of the four reservoirs computed by the plumbotectonics model. Doe & Zartman (1979)

http://www.onafarawayday.com/Radiogenic/

Anthropogenic Pb

Correspondence between lead ore compositions (●) and gasolines (o) from different countries on a Pb/Pb isotope plot. After Chow (1970). The data reveal a very strong correlation between the Pb isotope composition of gasoline Pb and local pollutant Pb, conclusively demonstrating that gasoline additives were the principal source of pollutant lead in the environment.

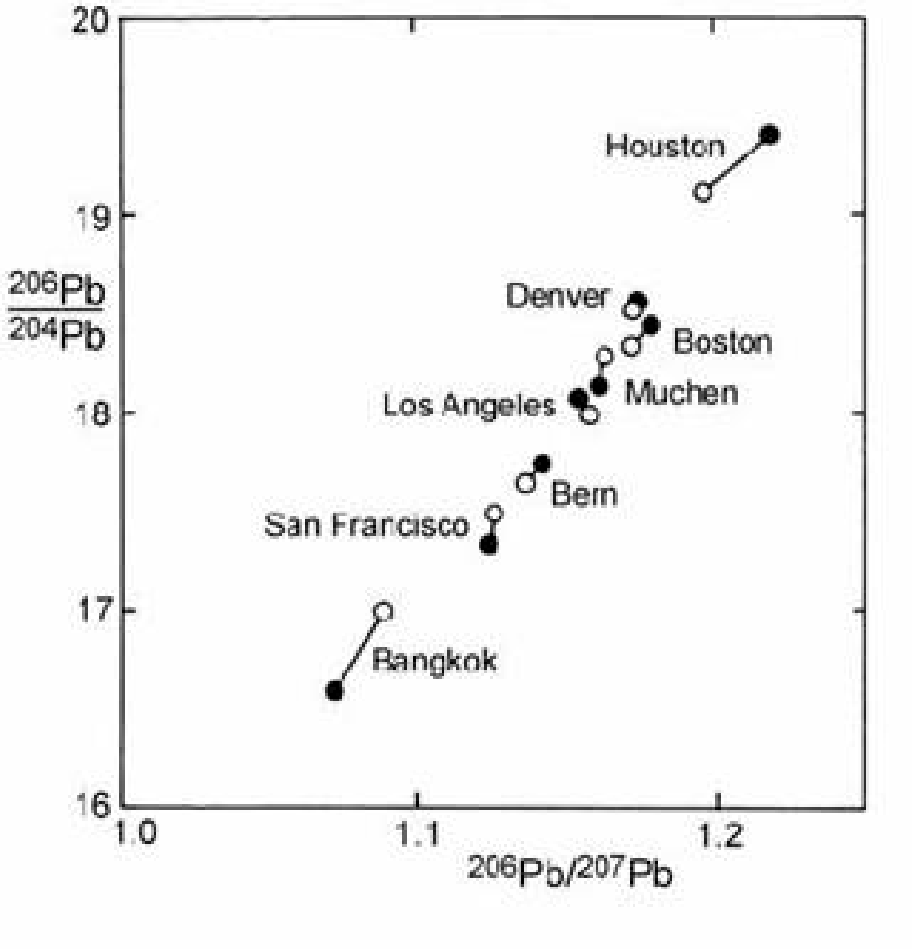

Stable Isotopes

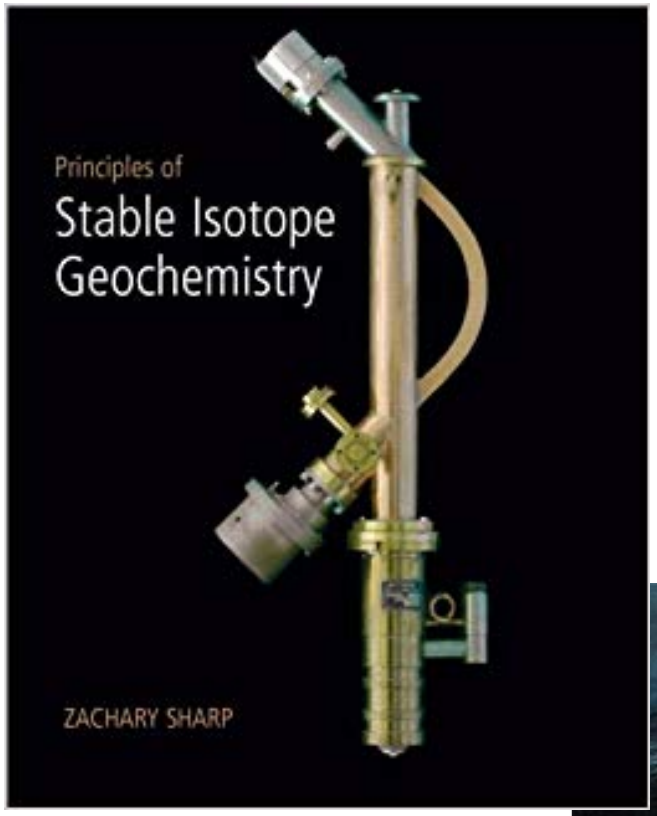

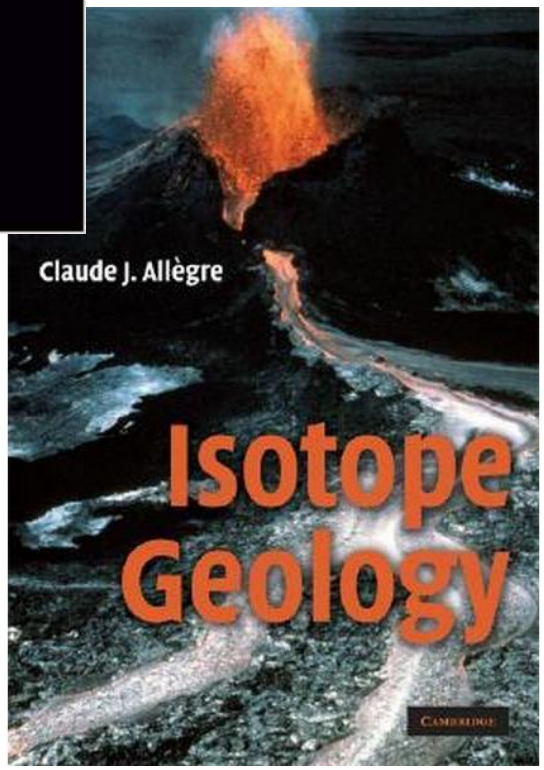

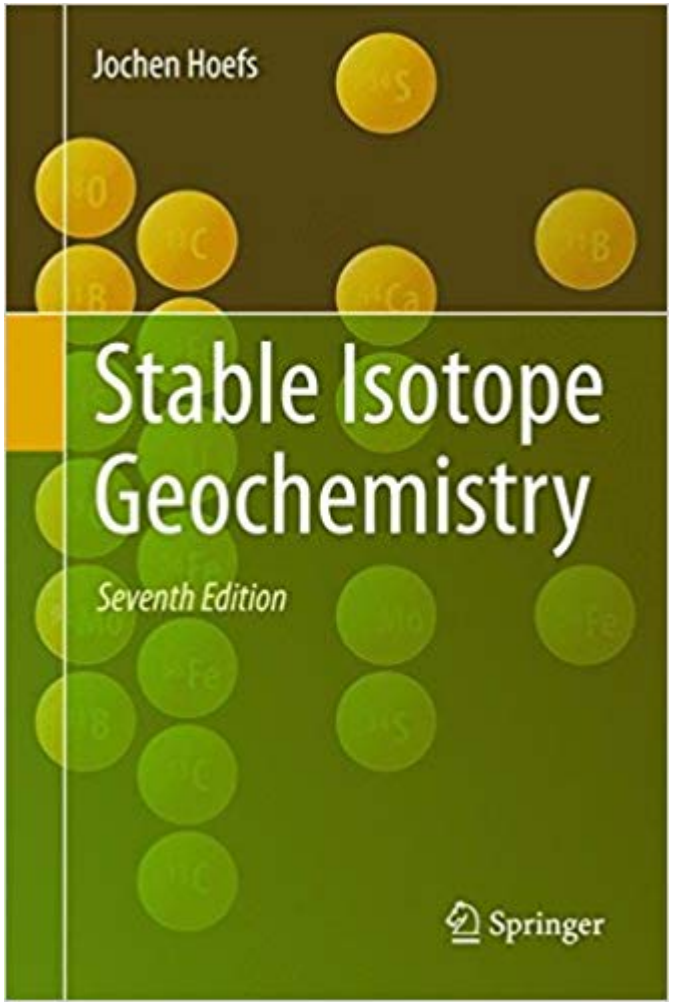

Stable Isotopes

Table 1.2 Characteristic physical properties of $H_2^{16}O$, $D_2^{16}O$, and $H_2^{18}O$

Property	$H_2^{16}O$	$D_2^{16}O$	$H_2^{18}O$
Density (20 °C, in g cm^{-3})	0.997	1.1051	1.1106
Temperature of greatest density (°C)	3.98	11.24	4.30
Melting point (760 Torr, in °C)	0.00	3.81	0.28
Boiling point (760 Torr, in °C)	100.00	101.42	100.14
Vapor pressure (at 100 °C, in Torr)	760.00	721.60	
Viscosity (at 20 °C, in centipoise)	1.002	1.247	1 .056

"isotope effects":
Differences in chemical and physical properties arising from variations in atomic mass of an element or molecule

Jochen Hoefs (Stable Isotopes)

Stable Isotopes

Evaporation/precipitation

The lighter isotopes evaporate more easily

Heavyer isotopes enriched in remaining liquid phase

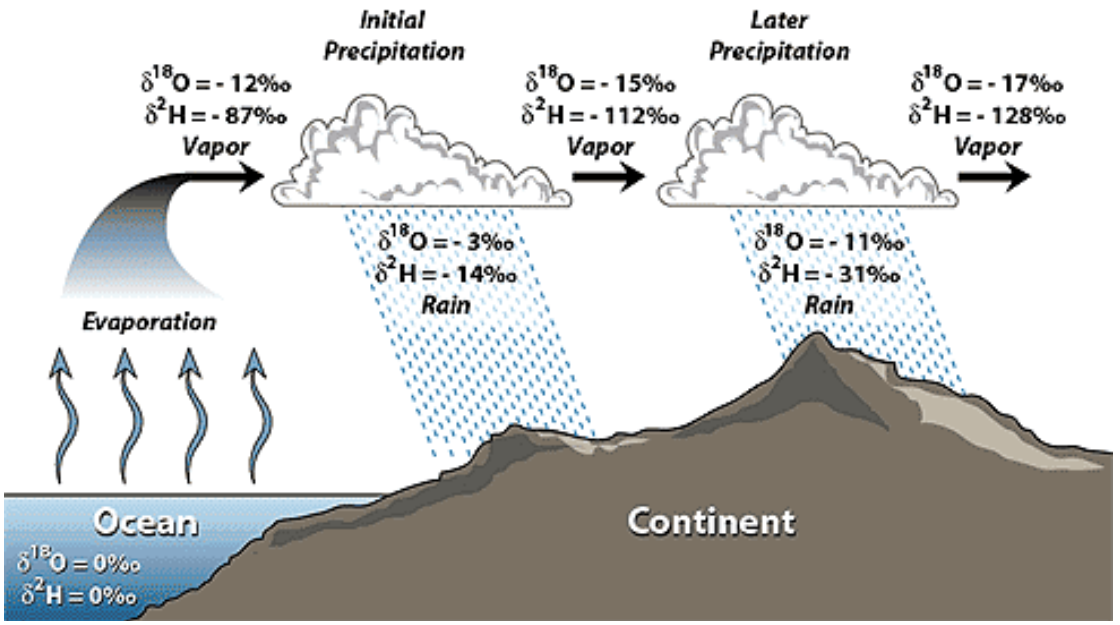

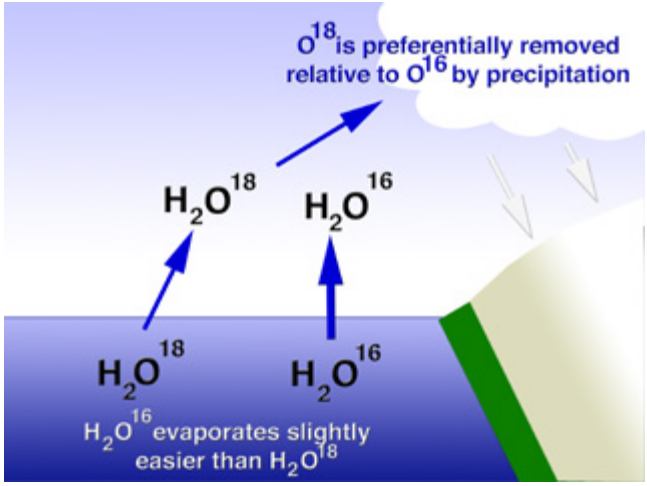

Property	H_2O	D_2O	$H_2{}^{18}O$
Density at 20°C [g cm^{-3}]	0.9982	1.1051	1.1106
Melting point [°C]	0	3.81	0.28
Boiling point [°C]	100	101.42	100.14

Stable Isotopes

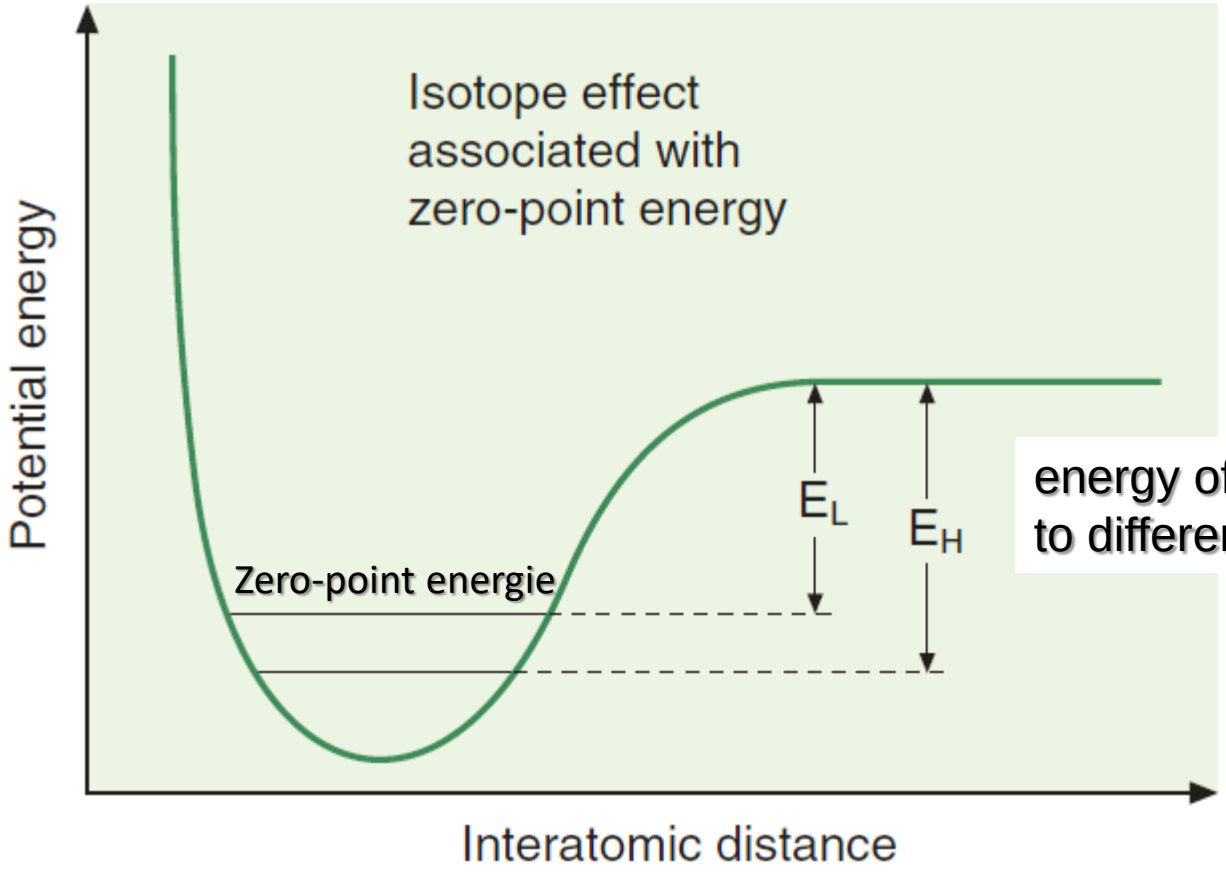

energy of molecule restricted to different levels, i.e. ½ hν

h = Planck's constant
ν = energy of vibration

Isotope fractionation processes

Isotope fractionation during chemical, physical and biological processes:

reversible chemical reaction at equilibrium state
A ←→ B

physical changes – phase transitions
water – vapor

biological and biochemical reactions
CO_2 into C_{org}

Isotope fractionation processes

1. **Isotope exchange reaction** (equilibrium isotope distribution)
reversible reaction that has reched an equilibrium,
A ←→ B
Examples: chemical equilibrium, phase equilibrium

2. **Kinetic processes** which depend primarily on differences in reaction rates of isotopic molecules
Non-reversible reaction, A → B
Examples: reaction products, diffusion

Isotopensignatur von Wasserdampf über einer Wasseroberfläche deutlich leichter, als eine Gleichgewichtsfraktionierung vorhersagen würde

Isotope fractionation processes

1. isotope exchange reactions (equilibrium isotope distribution)

$$aA_1 + bB_2 = aA_2 + bB_1$$

$$K = \frac{\left(\frac{A_2}{A_1}\right)^a}{\left(\frac{B_2}{B_1}\right)^b}$$

K (equilibrium constant), although close to 1, is different to 1 (Urey 1947, Bigeleisen & Meyer 1947)

$$\alpha_{A-B} = \frac{R_A}{R_B}$$

$$\alpha = K^{1/n}$$

n = number of exchangeable atoms. Usually α = K (see next slide)

Isotope fractionation processes

1. isotope exchange reactions – example

$$H_2^{18}O + \frac{1}{3}CaC^{16}O_3 \Leftrightarrow H_2^{16}O + \frac{1}{3}CaC^{18}O_3$$

$$\alpha_{CaCo_3-H_2O} = \frac{\left(\frac{^{18}O}{^{16}O}\right)_{CaCo_3}}{\left(\frac{^{18}O}{^{16}O}\right)_{H_2O}} = 1.031 \text{ at } 25°C$$

$\varepsilon = \alpha - 1$

ε = isotope enrichment factor
ε x 1000 ~δ-value (see next slide)

Isotope fractionation processes

1. isotope exchange reactions - Delta-value (δ)

$$\delta = \left(\frac{\text{sample isotope ratio} - \text{standard isotope ratio}}{\text{standard isotope ratio}} \right) \times 10^3$$

δ is a relative deviation from a standard, expressed as the number of parts per mil.

Isotope ratios are expressed with the heavier isotope in the numerator, e.g.: $^{18}O/^{16}O$, D/H, $^{13}C/^{12}C$

Isotope fractionation processes

Table 1.3 Comparison between δ, α, and $10^3 \ln \alpha_{A-B}$

$^{\delta}A$	$^{\delta}B$	$^{\Delta}A\text{-}B$	$^{\alpha}A\text{-}B$	$103 \ln\alpha_{A-B}$
1.00	0	1.00	1.001	1.00
5.00	0	5.00	1.005	4.99
10.00	0	10.00	1.01	9.95
15.00	0	15.00	1.015	14.98
20.00	0	20.00	1.02	19.80
10.00	5.00	5.00	1.00498	4.96
20.00	15.00	5.00	1.00493	4.91
30.00	15.00	15.00	1.01478	14.67
30.00	20.00	10.00	1.00980	9.76
30.00	10.00	20.00	1.01980	19.61

$$\Delta_{AB} = \delta_A - \delta_B$$

$$\alpha_{A-B} = \frac{R_A}{R_B}$$

For the two compounds A and B, the δ-values and fractionation factor α are related by:

$$\delta_A - \delta_B = \Delta_{A-B} \approx 10^3 \ln \alpha_{A-B} \qquad (1.12)$$

Jochen Hoefs (Stable Isotopes)

Exercise 1

Oxygen has three stable isotopes, ^{16}O, ^{17}O, and ^{18}O, with average abundances of 99.756%, 0.039%, and 0.205%, respectively.

The $^{16}O/^{18}O$ ratio in a Jurassic limestone is 472.4335. In average sea water, this same ratio is $^{16}O/^{18}O = 486.594$.

If average sea water is taken as the standard, what is the δ of the limestone in question?

δ is always expressed relative to the heavy isotope.
Must invert the ratios stated in the question, giving 0.0021167 and 0.0020551, respectively

Applying the formula defining $\delta^{18}O$ gives $\delta^{18}O = +30$

Isotope variations of oxygen

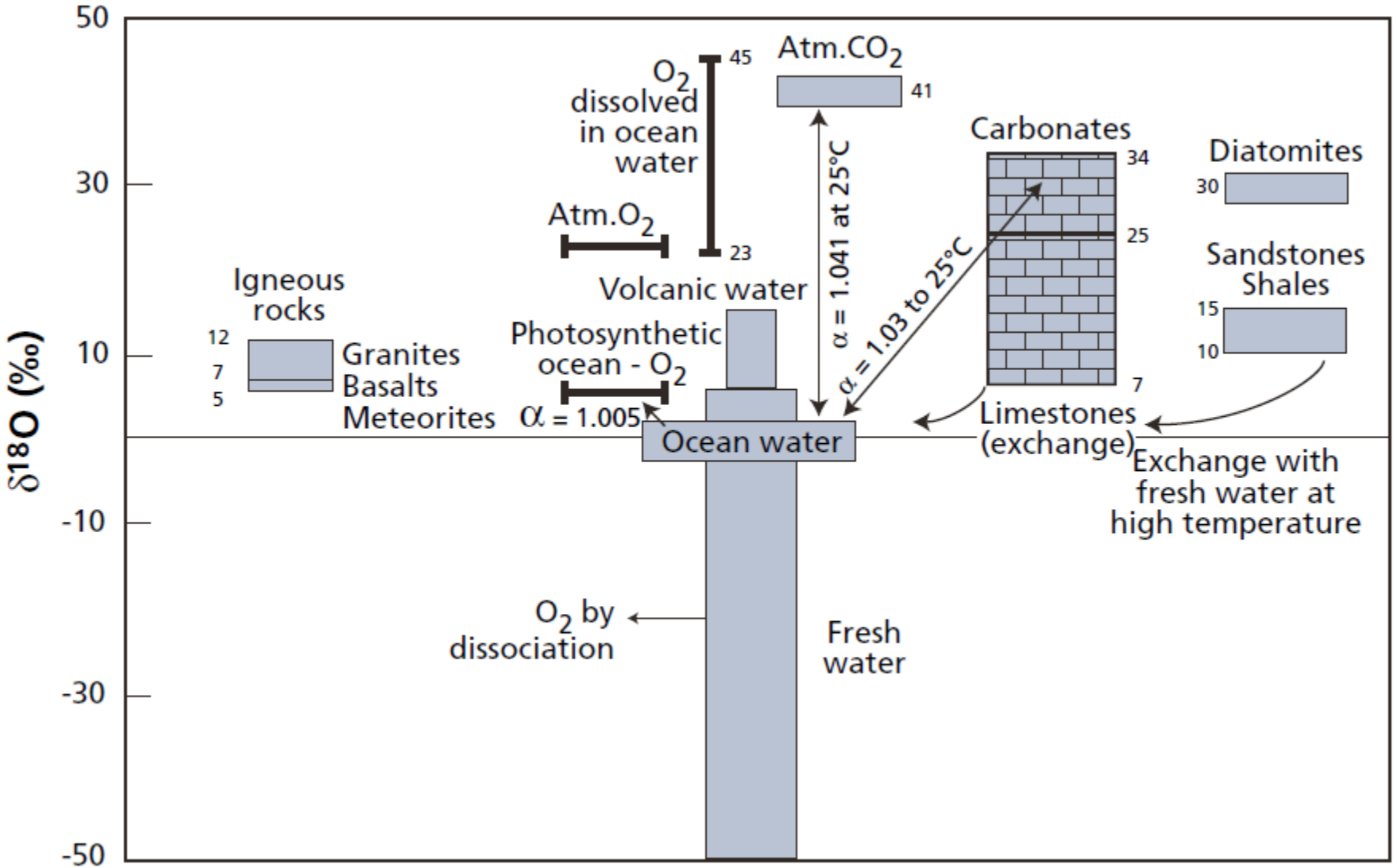

Claude Allègre (Isotope Geology)

Isotope variations – oxygen

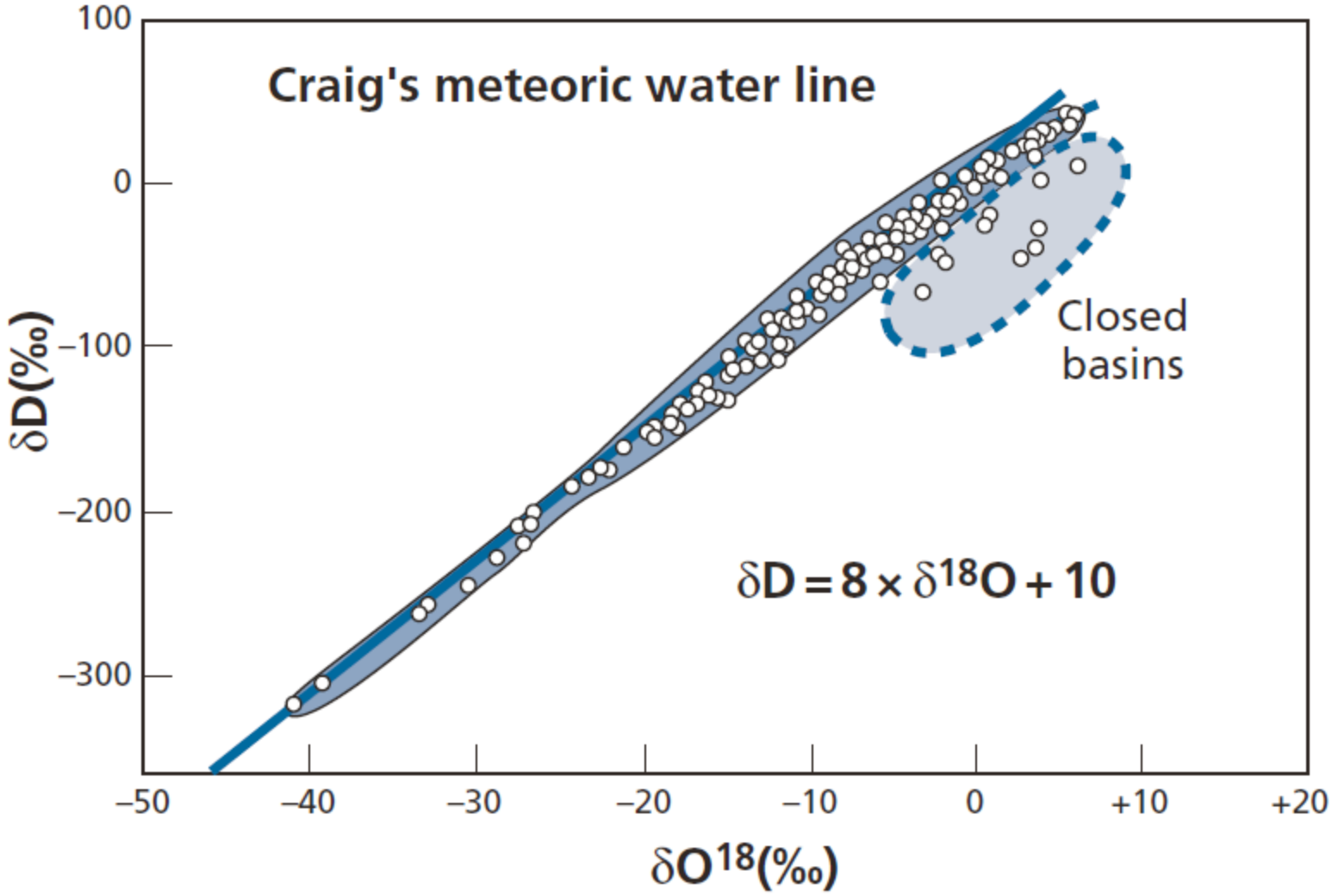

Claude Allègre (Isotope Geology)

Exercise 2

Naturally occurring stable isotopes of sulfur are ^{32}S, ^{33}S, ^{34}S, and ^{36}S. Their average abundances are 95.02%, 0.75%, 4.21%, and 0.017%, respectively. Generally, we are interested in the ratio of the two most abundant isotopes, ^{34}S and ^{32}S. The standard for sulfur is the sulfide of the Canyon Diablo meteorite with a $^{32}S/^{34}S$ value of 22.22.

$$\delta = \left(\frac{(^{34}S/^{32}S)_{sample}}{(^{34}S/^{32}S)_{standard}} - 1 \right) \times 10^3$$

We have a sample of sulfur from a natural sulfide with $^{32}S/^{34}S$ = 23.20. What is its $\delta^{34}S$?

Given that the standard has a $^{34}S/^{32}S$ ratio of 0.0450 and the sample a ratio of 0.0431, δ34S = -42.22 (negative!)
By definition, the standard has a value δ = 0

Exercise 3

Given that the $\delta^{18}O$ value of a limestone is +24 and that the limestone formed by precipitation from sea water, calculate the overall limestone–sea water fractionation factor α.

$$\delta = \left(\frac{\text{sample isotope ratio} - \text{standard isotope ratio}}{\text{standard isotope ratio}}\right) \times 10^3$$

$$\alpha_{A-B} = \frac{R_A}{R_B} = \frac{1 + \frac{\delta_A}{1000}}{1 + \frac{\delta_B}{1000}} \approx 1 + \frac{(\delta_A - \delta_B)}{1000}$$

following the approximation $(1 + \varepsilon) / (1 + \varepsilon') \sim 1 + (\varepsilon - \varepsilon')$

$\Delta_{limstone\text{-}H2O} = \delta CaCO_3 - \delta H_2O = 24 - 0$

$\alpha = 1.024$

Exercise 4

We measure the $\delta^{18}O$ of calcite and water with which we have tried to establish equilibrium. We find δ_{cal} = 18.9 and δ_{H2O} = -5 at 50 °C. What is the calcite–water partition coefficient? Calculate it without and with the approximation

$$(1 + e) / (1 + e') \sim 1 + (e - e')$$

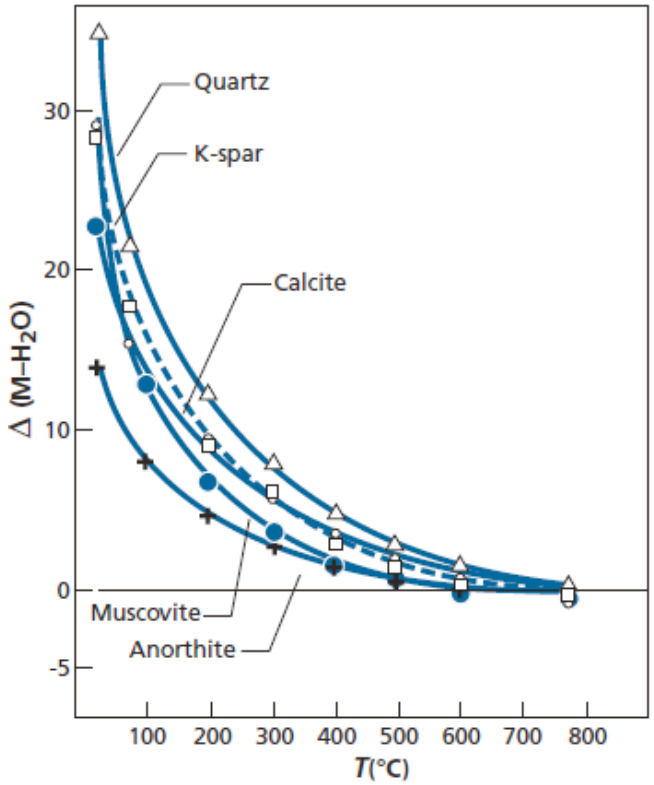

$$\alpha_{A-B} = \frac{R_A}{R_B} = \frac{1 + \frac{\delta_A}{1000}}{1 + \frac{\delta_B}{1000}} \approx 1 + \frac{(\delta_A - \delta_B)}{1000}$$

(1) Without approximation: $\alpha_{cal\text{-}H2O}$ = 1.02402
(2) With approximation: $\alpha_{cal\text{-}H2O}$ = 1.02390

Isotope variations during evaporation - condensation

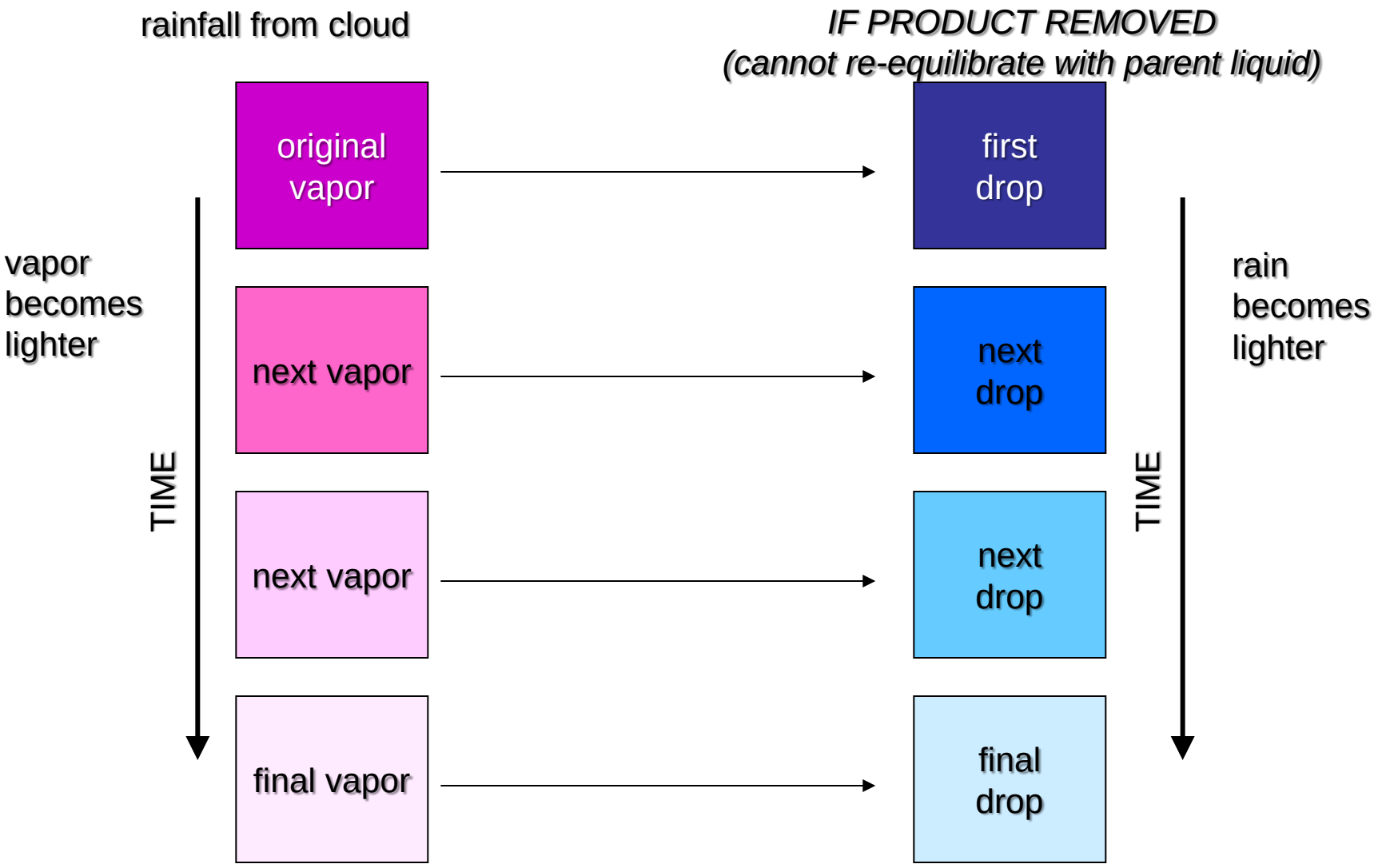

Evaporation-Condensation Processes

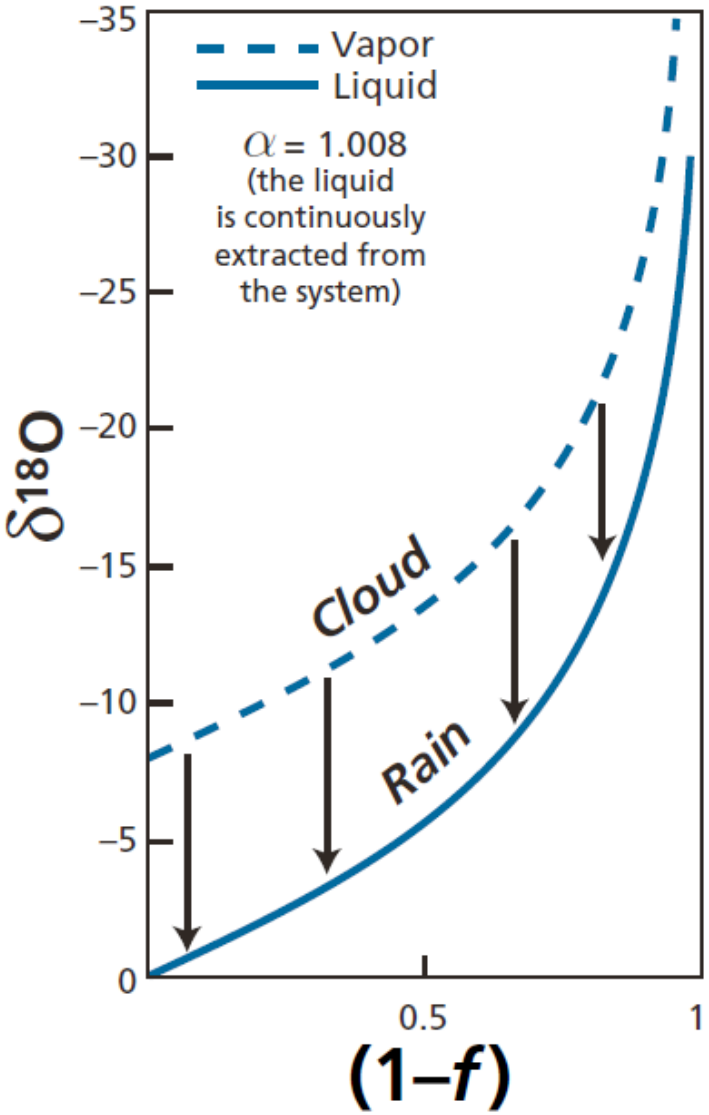

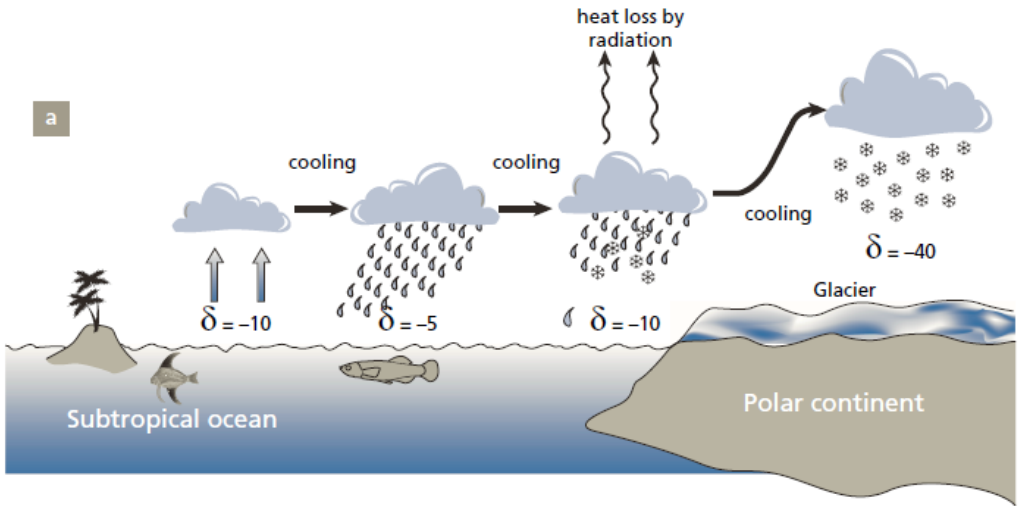

$$\frac{R_V}{R_{V_0}} = f^{\alpha-1}$$

Claude Allègre (Isotope Geology)

Evaporation-Condensation Processes

Temperature dependence of water isotope fractionation

$$\alpha = \frac{R_A}{R_B}$$

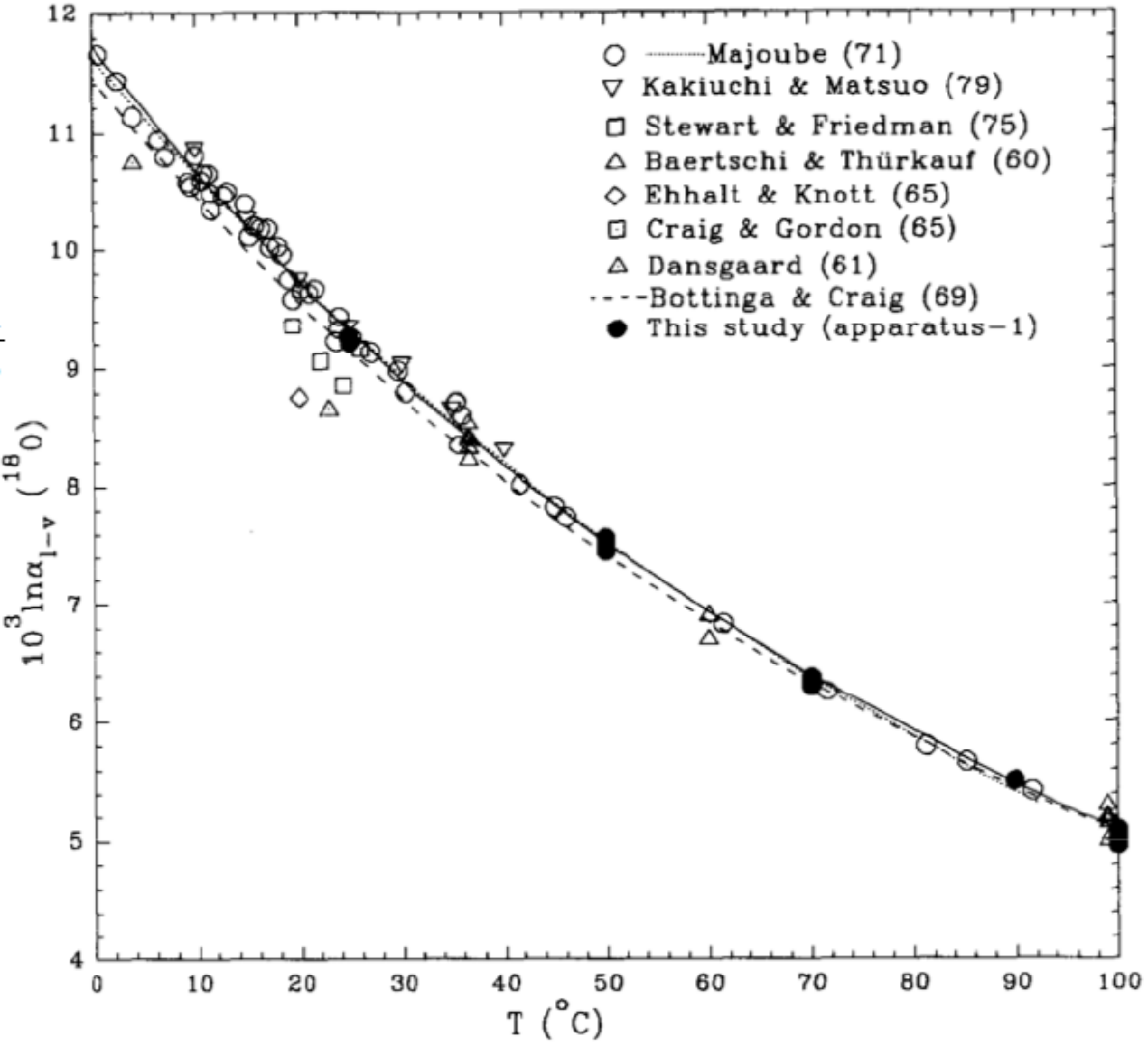

Anwendung der Isotopen-fraktionierung als Paläo-thermometer

Evaporation-Condensation Processes

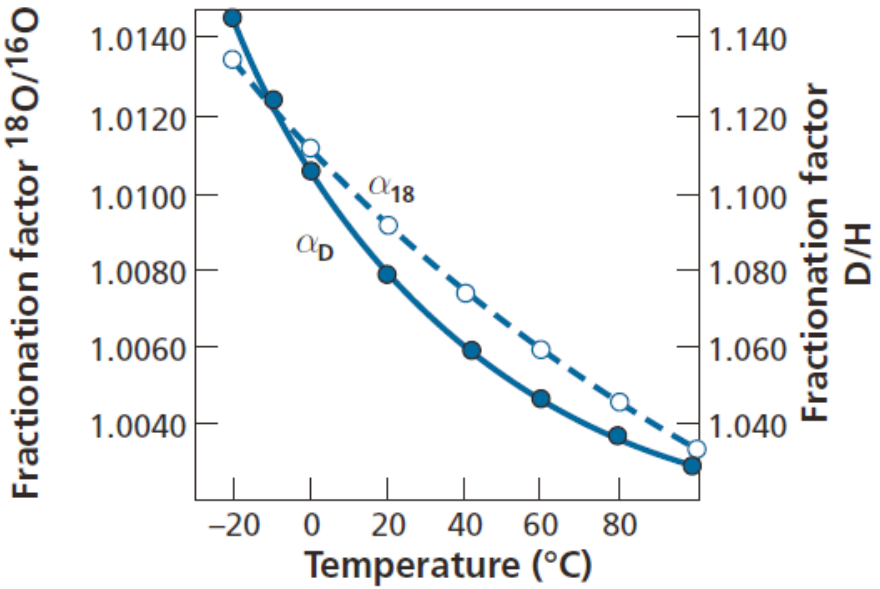

Claude Allègre (Isotope Geology)

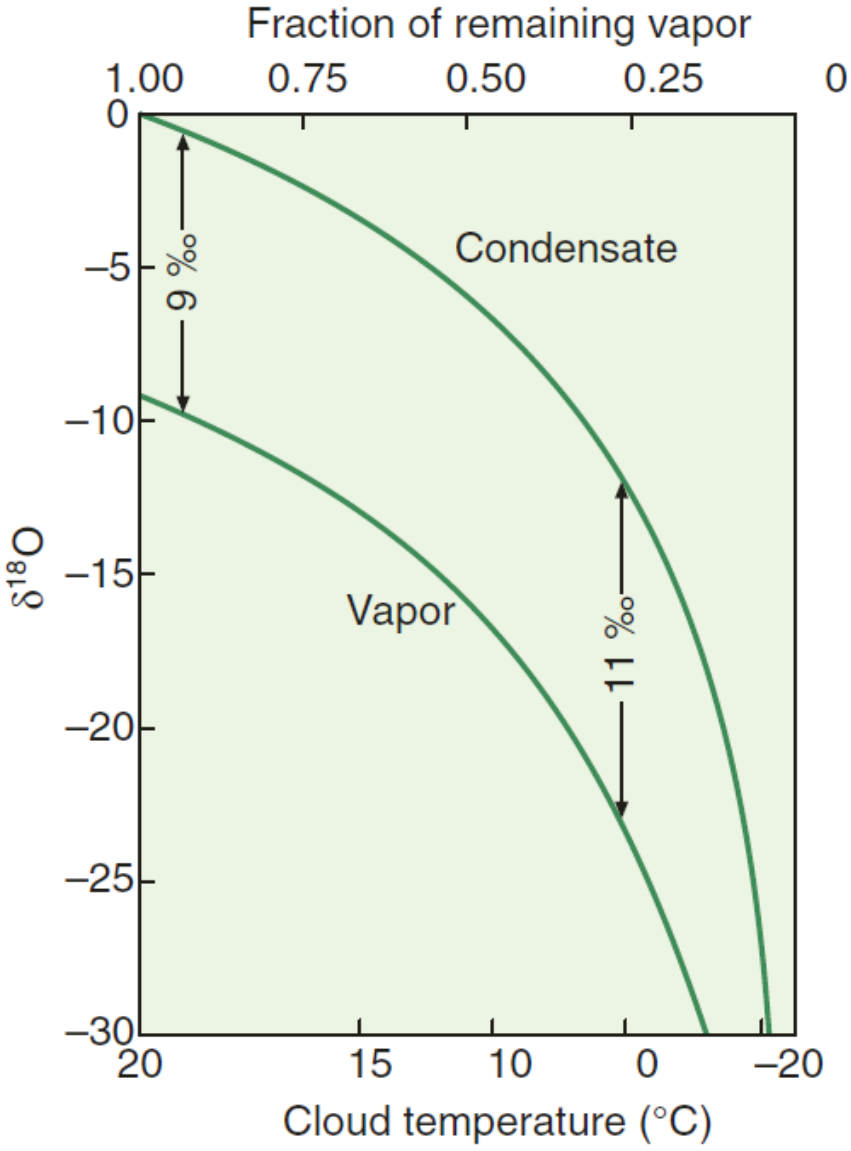

Jochen Hoefs (Stable Isotopes)

Isotope variations – oxygen

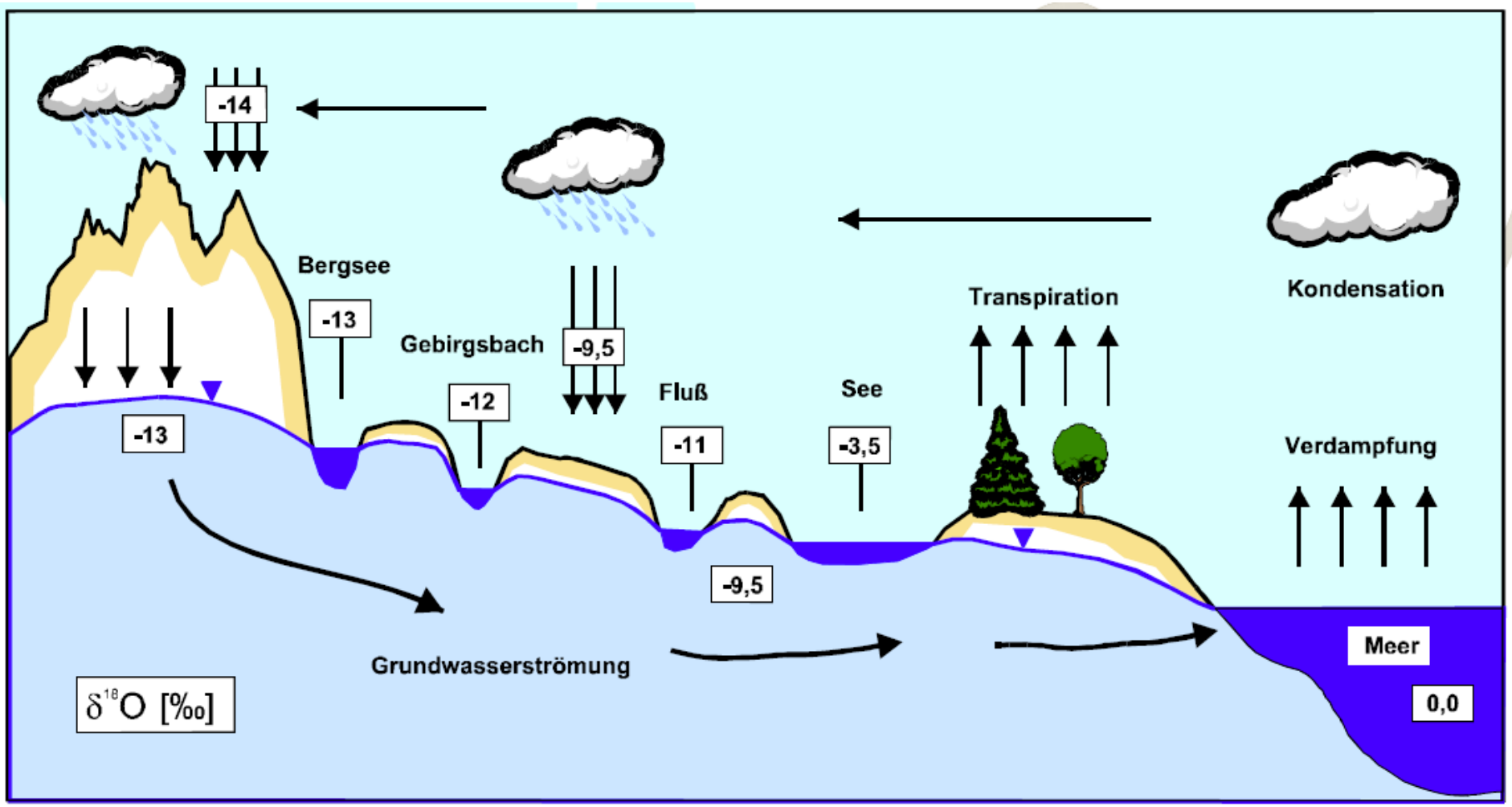

Quelle: Hydroisotop GmbH

Isotopenvariationen

Kontinentaleffekt

Abreicherung der Niederschläge an schwereren Isotopen über Landmassen

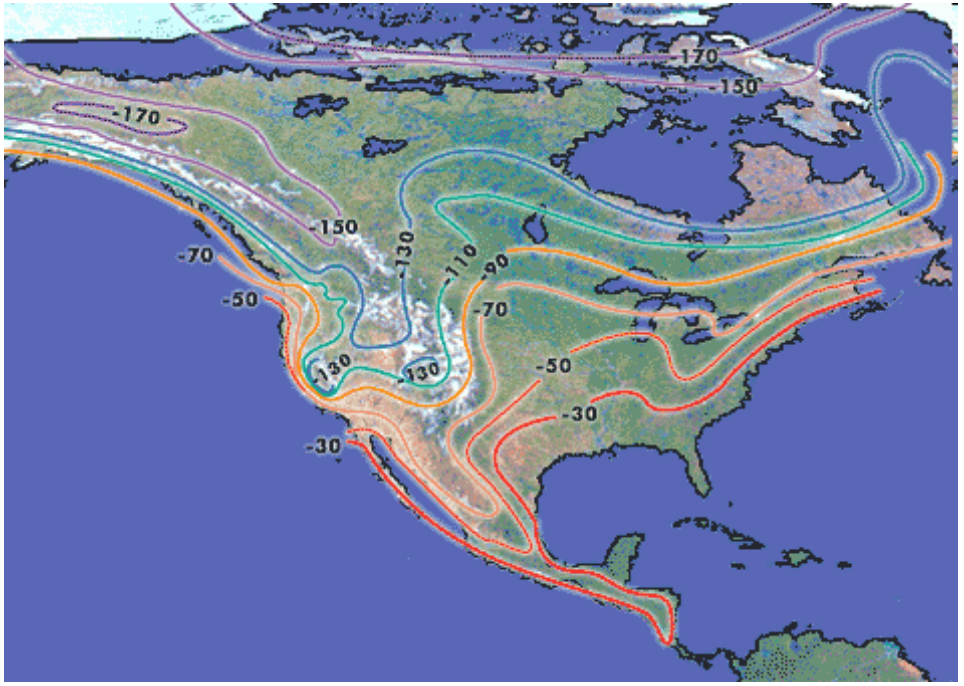

Dansgaard 1964, Craig und Gordon (1965)

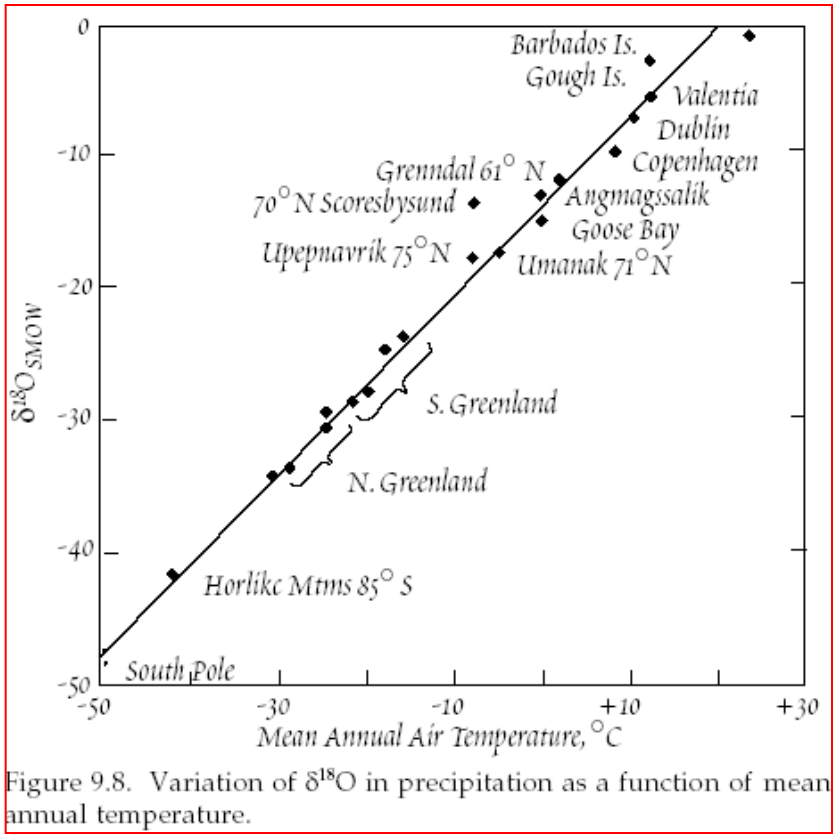

Figure 9.8. Variation of $\delta^{18}O$ in precipitation as a function of mean annual temperature.

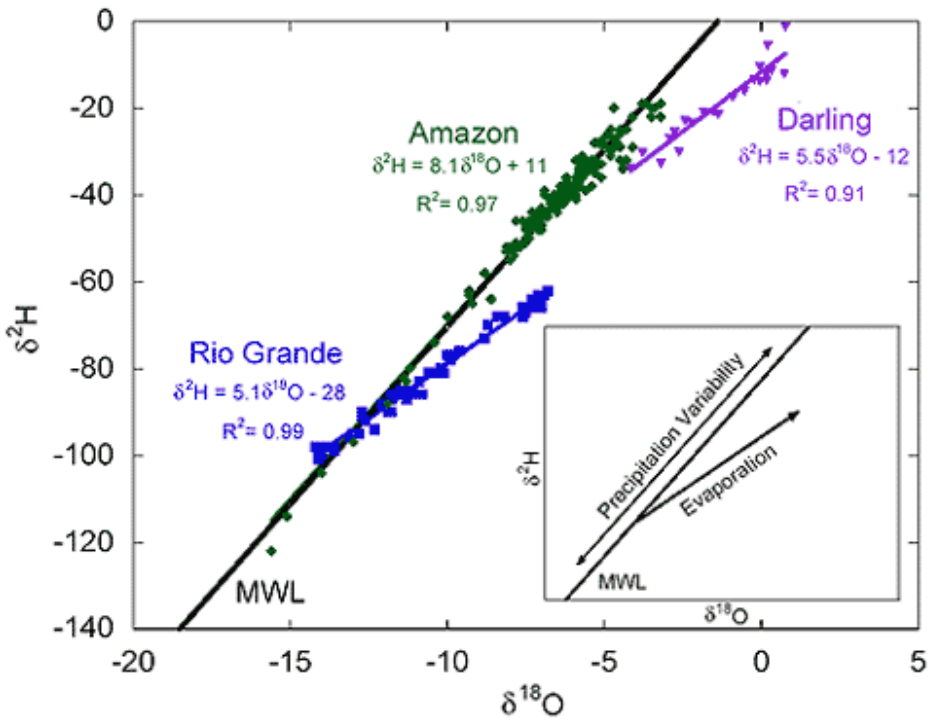

Isotope variations of oxygen in the surface oceans

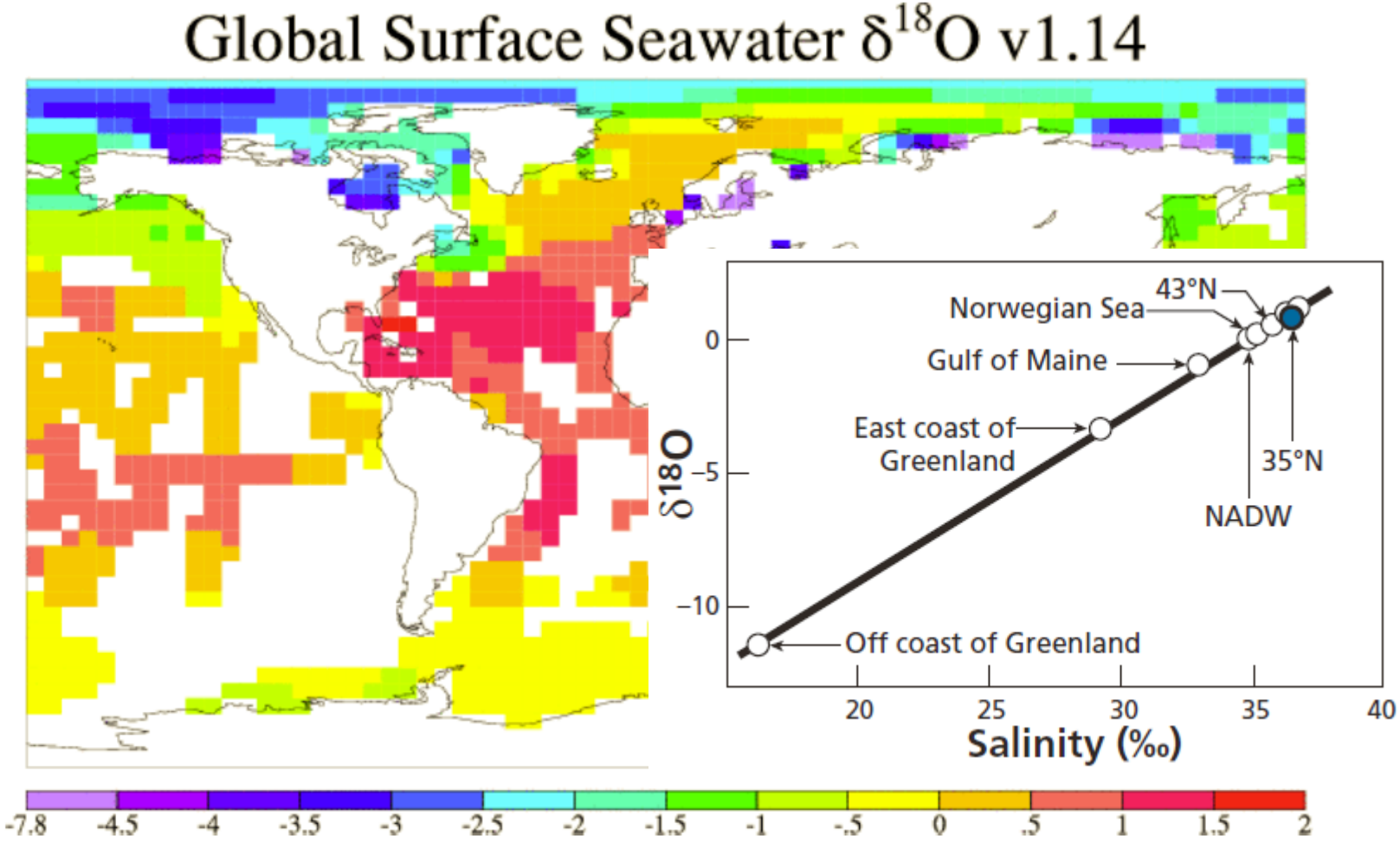

Figure 3. Example of output from the Schmidt et al (1999) global sea-water $\delta^{18}O$ database (extracted 1 February 2006). The image shows surface-water $\delta^{18}O$ integrated over the top 50 m on a 4° x 5° degree grid.

E.J. Rohling (2013)

Geothermal fluids

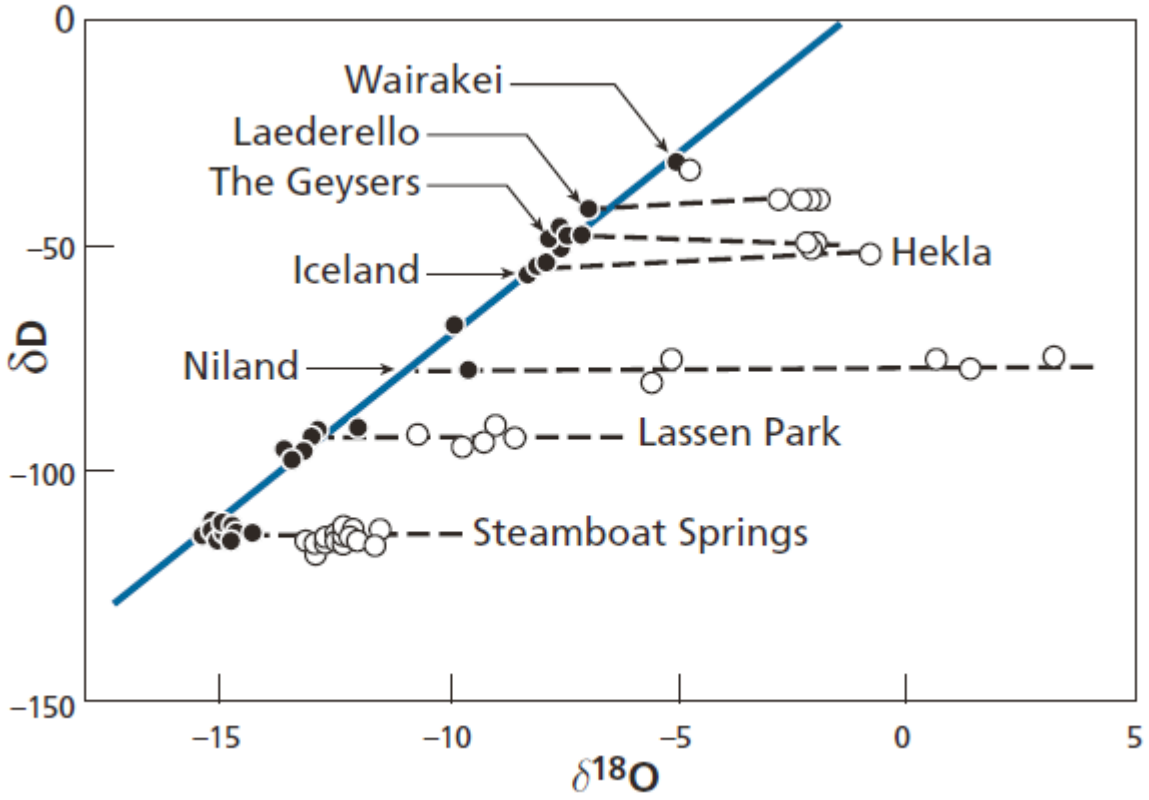

Correlation diagram for ($^{18}O/^{16}O$, D/H) in geothermal waters. They form horizontal lines cutting the meteoric straight line at the point corresponding to local rainwater. Water has exchanged its oxygen isotopically with the rock but the hydrogen of water does not change because it is an infinite hydrogen isotope reservoir compared with rocks that are poor in hydrogen

Exercise 5

Sea water has a $\delta^{18}O$ value of 0. Liquid–vapor fractionation at equilibrium at 20 °C is $\alpha = 1.0098$. What is the composition of the **water vapor** evaporating if it is in equilibrium with the water?

If the isotope composition of the infinite reservoir is R_0, the‘‘large’’ reservoir (e.g. sea water) imposes its isotope composition through the fractionation factor:

$R = \alpha R_0$ and $\delta = \delta_0 + (\alpha - 1) \times 1000$

The fractionation factor $(^{18}O/^{16}O)_{vapor} / (^{18}O/^{16}O)_{liquid} = 1/\alpha = 0.99030$
Therefore $(\alpha - 1) = -0.0097$, and
$\delta^{18}O = -9.7$ ‰ (per mil, parts per thousand)

Isotope fractionation processes

2. kinetic processes (depend primarily on differences in reaction rates of isotopic molecules)

associated with incomplete and unidirectional processes

evaporation,
dissociation reactions,
biologically mediated reactions,
diffusion

Rayleigh distillation process

Changes in the instantaneous isotopic composition of a reservoir (δR) and an extract (δE) during a Rayleigh distillation process as a function of the partition coefficient α (1.01 & 0.99 resp.)

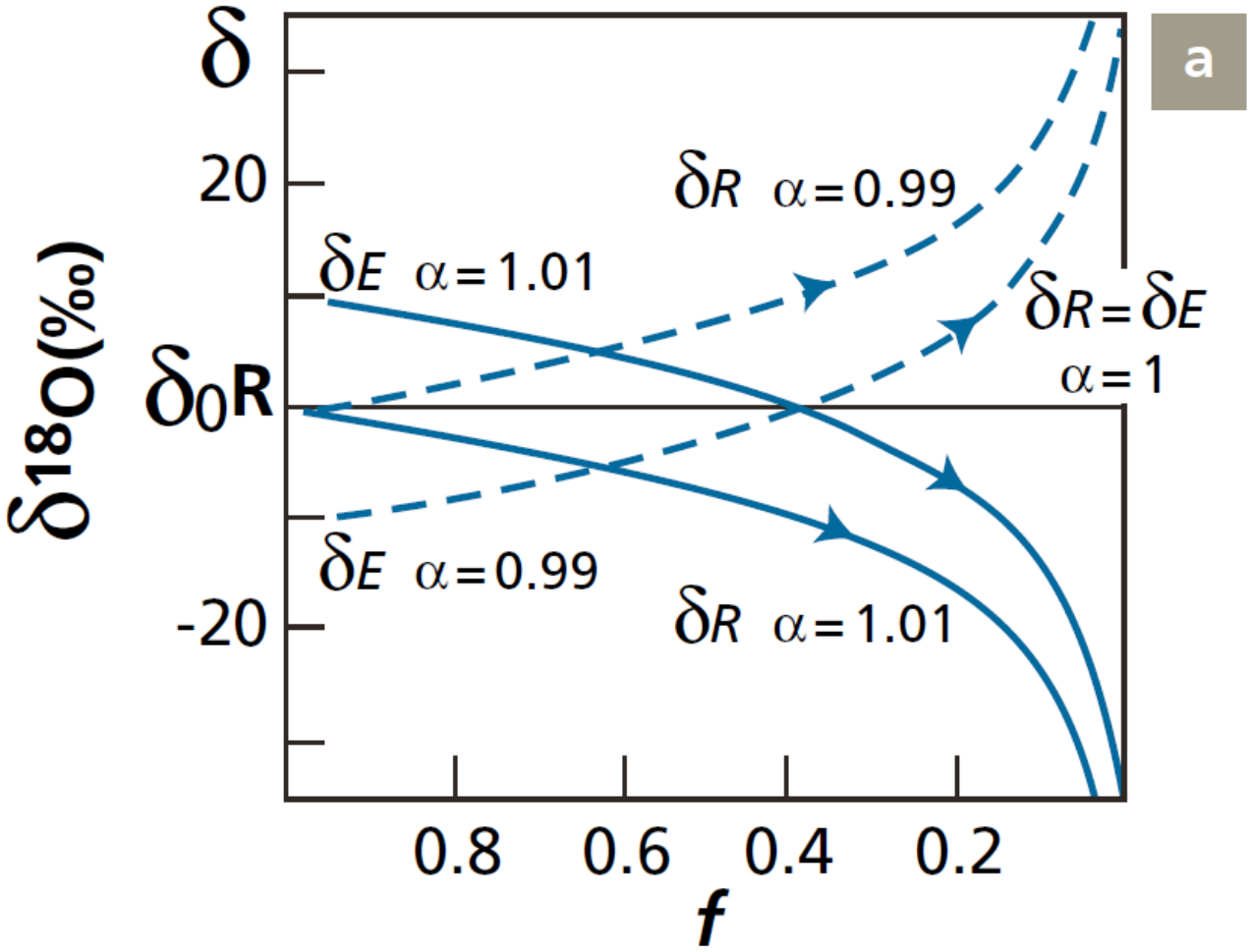

Exercise 6

Let us consider bacterial reduction $SO_4^{2-} \rightarrow S^{2-}$ by Desulfovibrio desulfuricans. The kinetic fractionation factor $^{34}S/^{32}S$ between sulfate and sulfide at 25 °C is 1.025. Let us suppose that bacterial reduction occurred in oceanic sediment that was continually supplied with sulfate ions. The sulfate stock can therefore be considered infinite.

What is the composition of the S^{2-} on the ocean floor if the $\delta^{34}S$ of the sulfate is = +24?

Applying the equation $\Delta_{AB} = 10^3 \ln\alpha$ gives $\Delta_{AB} = +24.7$
$\delta_{sulfate} - \delta_{sulfide} = +24.7$
hence it can be deduced that
$\delta_{sulfide} = -0.7$

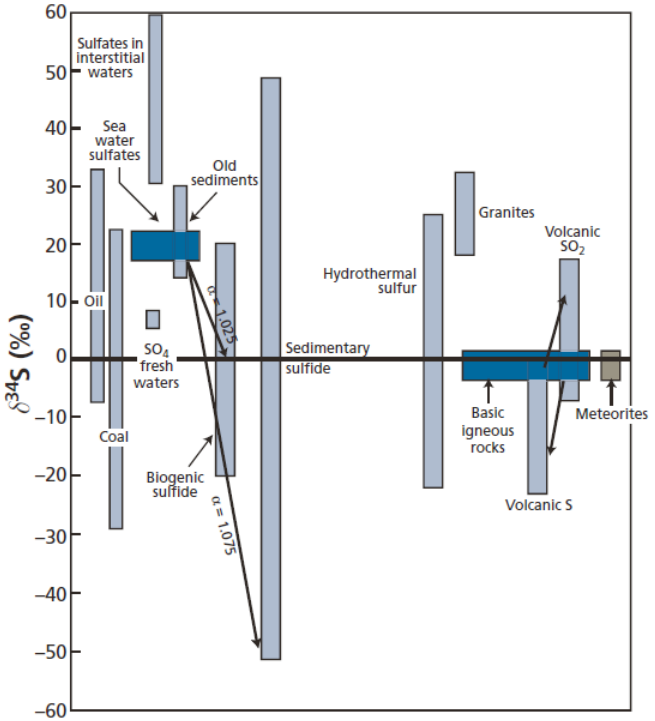

$$\delta_A - \delta_B = \Delta_{A-B} \approx 10^3 \ln \alpha_{A-B}$$

Claude Allègre (Isotope Geology)

Sulfur isotopes in sulfur-bearing deposits

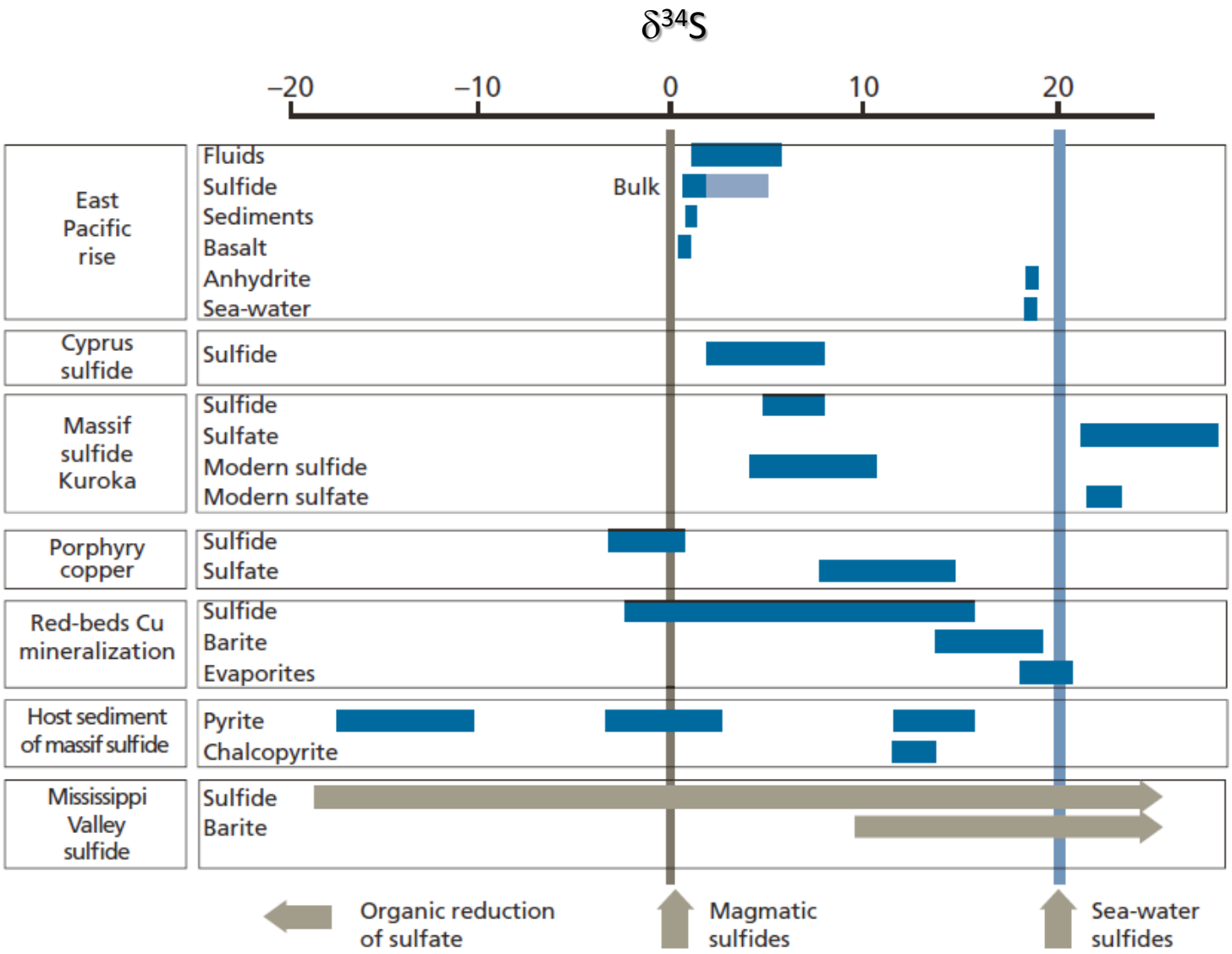

Isotope fractionation processes

Mass dependent effects

diffusion,
metabolism,
temperature dependent equilibrium processes

Mass independent effects (MIF)

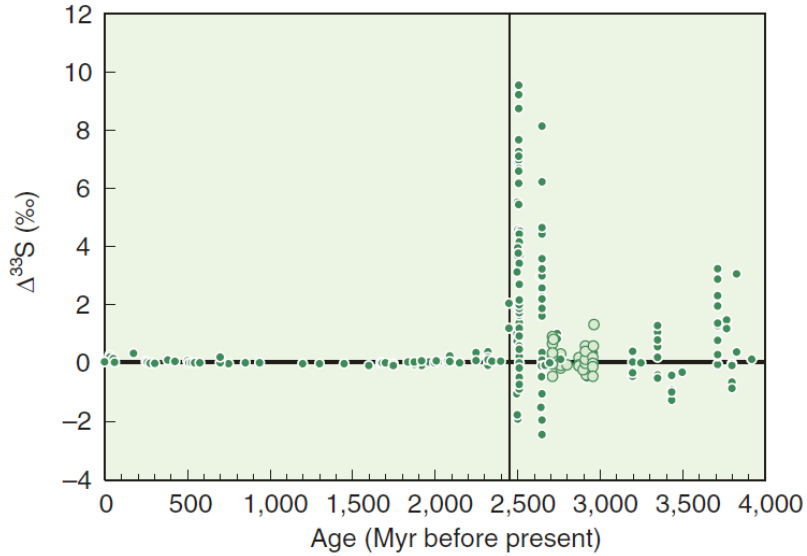

Fig. 2.24 Compilation of $\Delta^{33}S$ versus age for rock samples. Note large $\Delta^{33}S$ before 2.45 Ga, indicated by *vertical line*, small but measurable $\Delta^{33}S$ after 2.45 Ga (Farquahar et al. 2007) (Fig. 3.29, 6th edition, p. 167)

Jochen Hoefs (Stable Isotopes)

Mass independent fractionation (MIF)

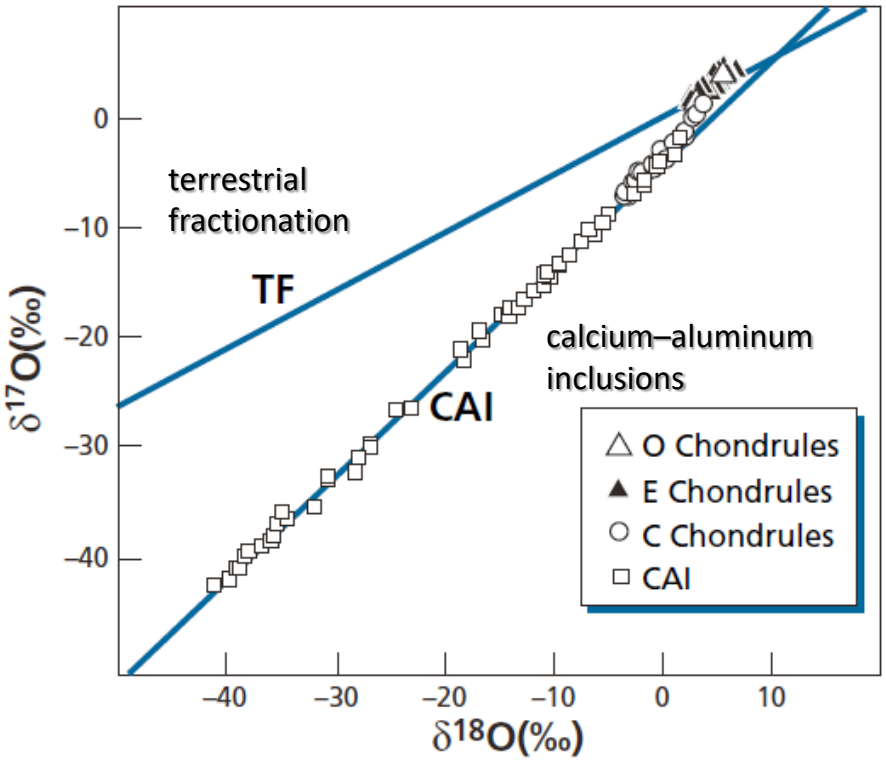

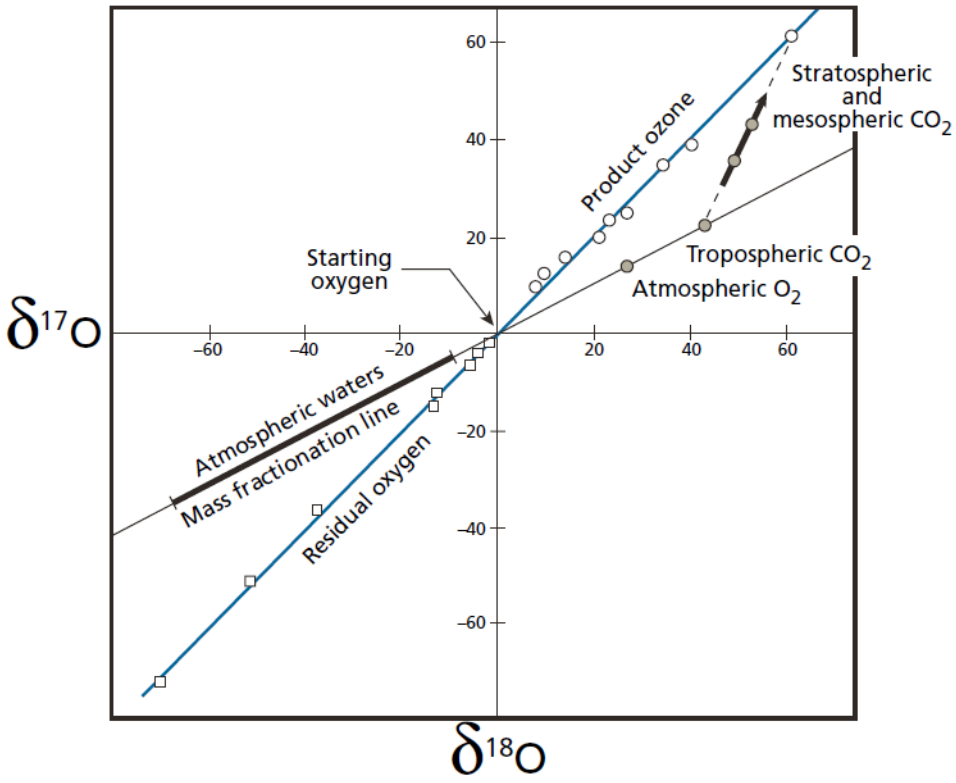

Claude Allègre (Isotope Geology)

Isotopic exchange

$$\frac{(^{18}O/^{16}O)_{AO}}{(^{18}O/^{16}O)_{BO}} = K(T)$$

Three types of water with different compositions brought into contact with quartz at 500°C

Curves show speed of equilibration by water–quartz exchange

Quartz with $\delta^{18}O = 10$

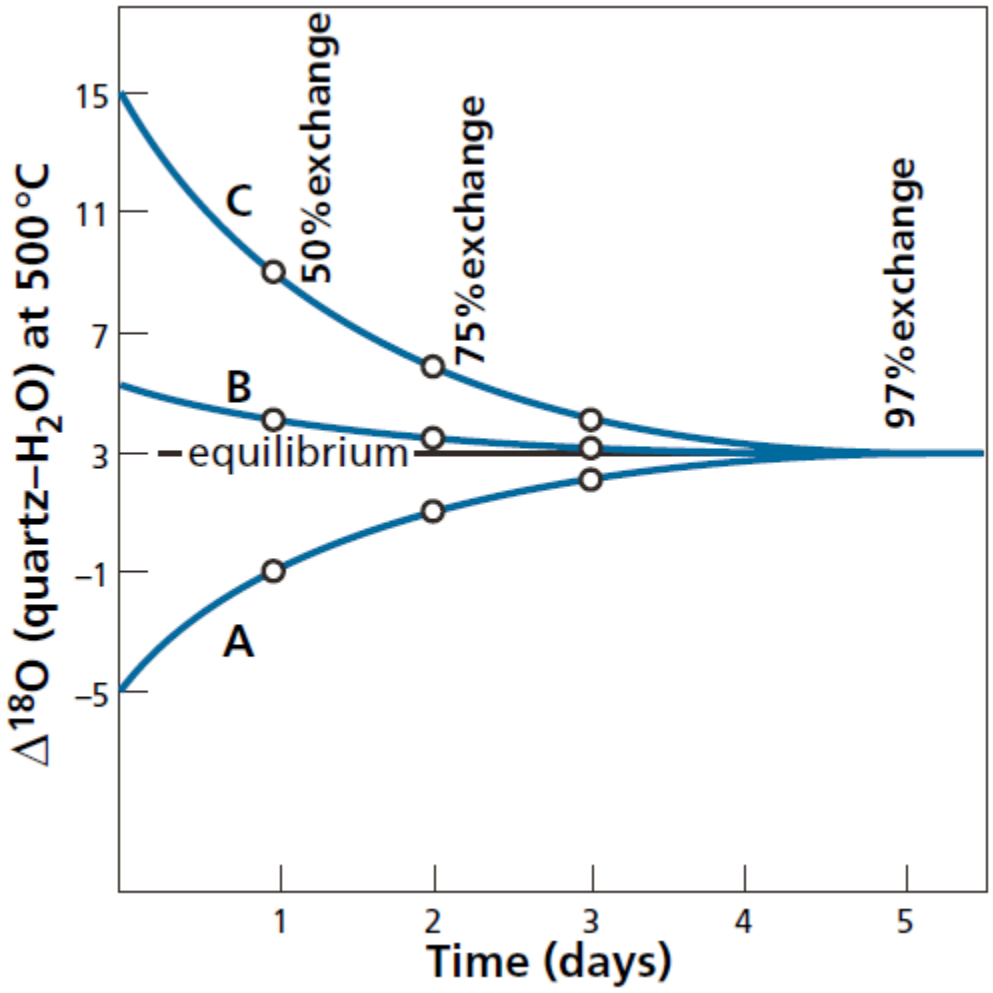

Paleothermometer - Carbonate Thermometer

$$T\,^{\circ}\mathrm{C} = 16.5 - 4.3\left(\delta^{18}_{CO_3} - \delta^{18}_{H_2O}\right) + 0.13\left(\delta^{18}_{CO_3} - \delta^{18}_{H_2O}\right)^2$$

$$\delta^{18}_{CO_3} = \left[\frac{\left(^{18}O/^{16}O\right)_{CO_2,\,carbonate\,X} - \left(^{18}O/^{16}O\right)_{CO_2,\,standard}}{\left(^{18}O/^{16}O\right)_{CO_2,\,standard}}\right] \cdot 10^3$$

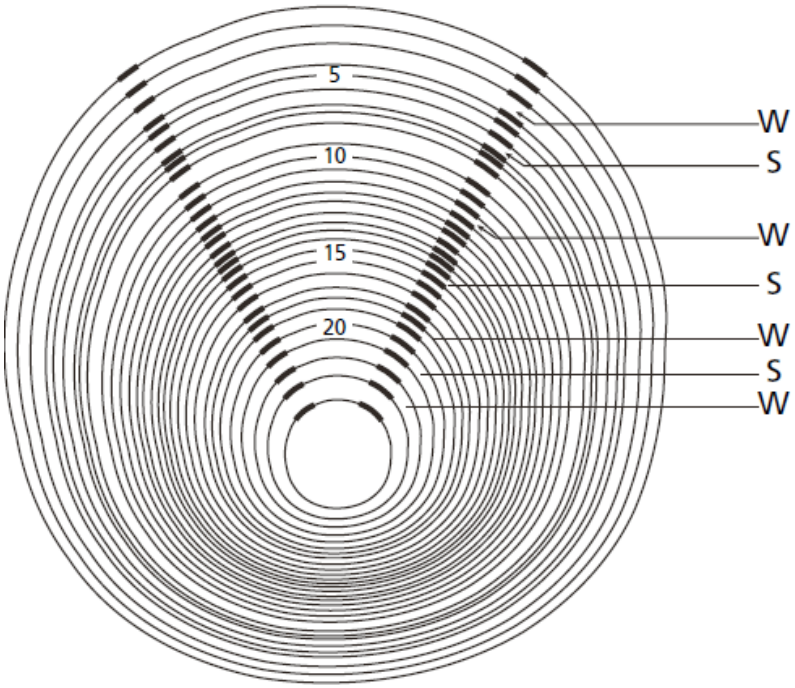

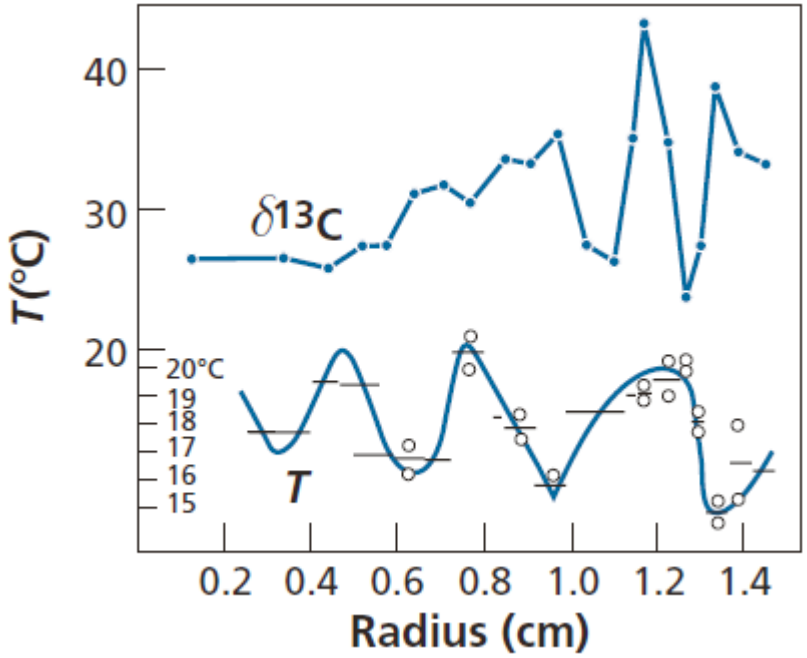

Claude Allègre (Isotope Geology)

Paleothermometer

Table 7.1 Isotope fractionation for mineral–water pairs

Mineral	Temperature (°C)	A	B
Calcite (CO_3Ca)	0–500	2.78	− 2.89
Dolomite	300–500	3.20	− 1.5
Quartz	200–500	3.38	− 2.90
Quartz	500–800	4.10	− 3.7
Alkali feldspar	350–800	3.13	− 3.7
Plagioclase	500–800	3.13	− 3.7
Anorthite	500–800	2.09	− 3.7
Muscovite	500–800	1.9	− 3.10
Magnetite	(reversed slope) 0–500	− 1.47	− 3.70

for two minerals in equilibrium:

$$\Delta_{m_1 m_2} = \delta_{m_1} - \delta_{m_2} \approx A\left(10^6\, T^{-2}\right) + B = 1000 \ln \alpha$$

Table 7.2 Results of ^{18}O isotope thermometry based on $^{18}O/^{16}O$ fractionation of mineral pairs

Pair	A	B
Quartz–albite	0.97	0
Quartz–anorthite	2.01	0
Quartz–diopside	2.08	0
Quartz–magnetite	5.57	0
Quartz–muscovite	2.20	− 0.6
Diopside–magnetite	5.57	0

Claude Allègre (Isotope Geology)

Paleothermometer

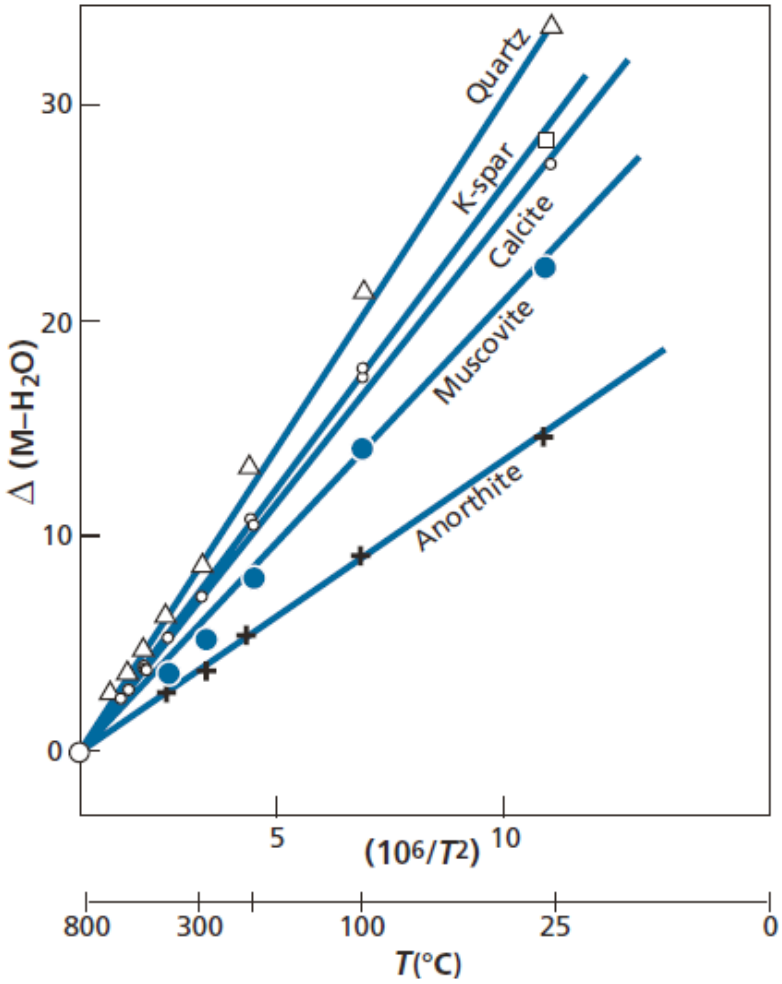

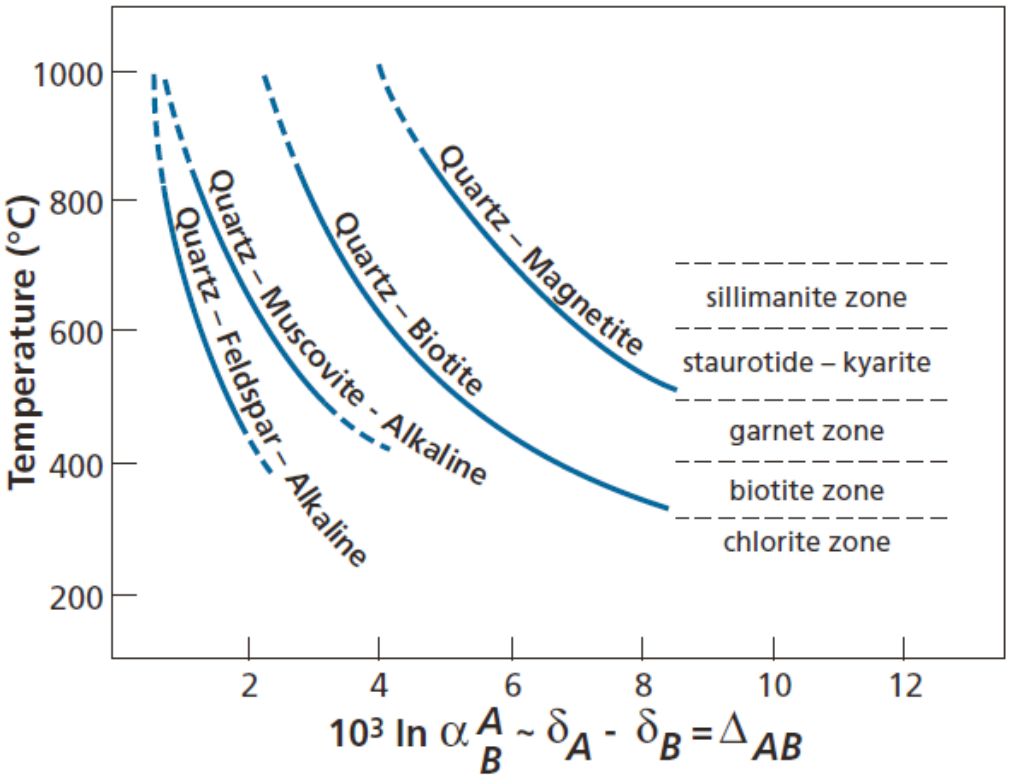

Claude Allègre (Isotope Geology)

Exercise 7

What is the $\delta^{18}O$ composition of a muscovite in quilibrium with water at 600 °C whose $\delta = -10$?

General equation:

$\Delta = A \times (10^6 \times 1/T^2) + B$

Applying the equation:

$\Delta = 1.9\ (10^6 \times 1/873^2) - 3.1 = -0.6$

where $\Delta = \delta_{musc} - \delta_{water}$

$-0.6 = \delta_{musc} - (-10)$

from this we obtain $\delta_{musc} = -10.6$

Exercise 8

The δ18O values of the minerals of a metamorphic rock are: quartz +14.8, magnetite +5.

Calculate the equilibrium temperature of quartz–magnetite.

General formula: $\Delta_{quartz-mineral} - B = A \times 10^6/T^2$

Table 7.2 Results of ^{18}O isotope thermometry based on $^{18}O/^{16}O$ fractionation of mineral pairs

Pair	*A*	*B*
Quartz–albite	0.97	0
Quartz–anorthite	2.01	0
Quartz–diopside	2.08	0
Quartz–magnetite	5.57	0
Quartz–muscovite	2.20	−0.6
Diopside–magnetite	5.57	0

481 °C

Low-temperature paleothermometry

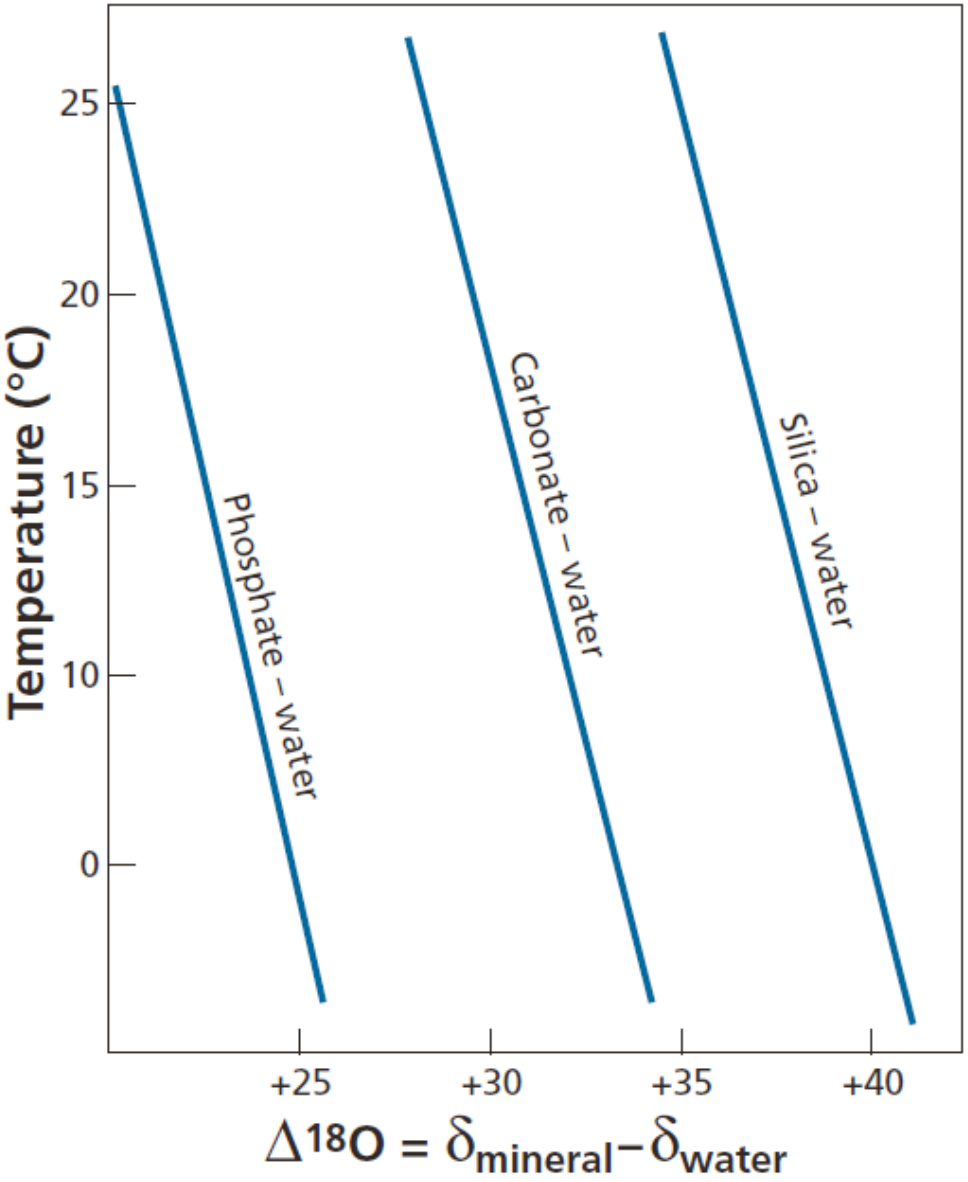

Isotopologues – clumbed isotope thermometry

Table 1.4 Stochastic abundances of CO_2 isotopologues (Eiler 2007)

Mass	Isotopologue	Relative abundance
44	$^{12}C^{16}O_2$	98.40 %
45	$^{13}C^{16}O_2$	1.11 %
	$^{12}C^{17}O^{16}O$	748 ppm
46	$^{12}C^{18}O^{16}O$	0.040 %
	$^{13}C^{17}O^{16}O$	8.4 ppm
	$^{12}C^{17}O_2$	0.142 ppm
47	$^{13}C^{18}O^{16}O$	44.4 ppm
	$^{12}C^{17}O^{18}O$	1.50 ppm
	$^{13}C^{17}O_2$	1.60 ppb
48	$^{12}C^{18}O_2$	3.96 ppm
	$^{13}C^{17}O^{18}O$	16.8 ppb
49	$^{13}C^{18}O_2$	44.5 ppb

$$^{13}C^{16}O_3^{2-} + {}^{12}C^{18}O^{16}O_2^{2-} \Leftrightarrow {}^{13}C^{18}O^{16}O_2^{2-} + {}^{12}C^{16}O^{2-}.$$

(61) (62) (63) (60).

Isotopologues – clumbed isotope thermometry

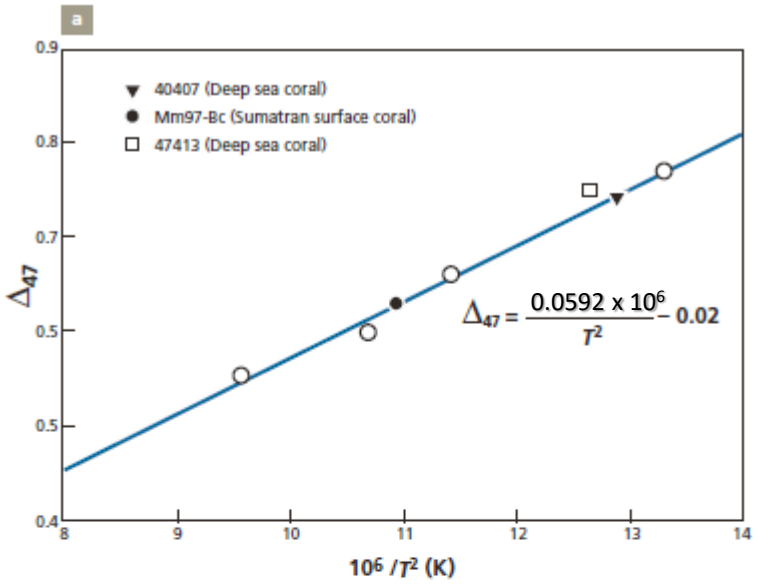

$$\Delta_{47} = \left[(47/44)_{\text{sample}} - (47/44)_{\text{reference}} \right] \times 10^3$$

$$\Delta_{47} = 0.0592 \cdot 10^6 T^{-2} - 0.02$$

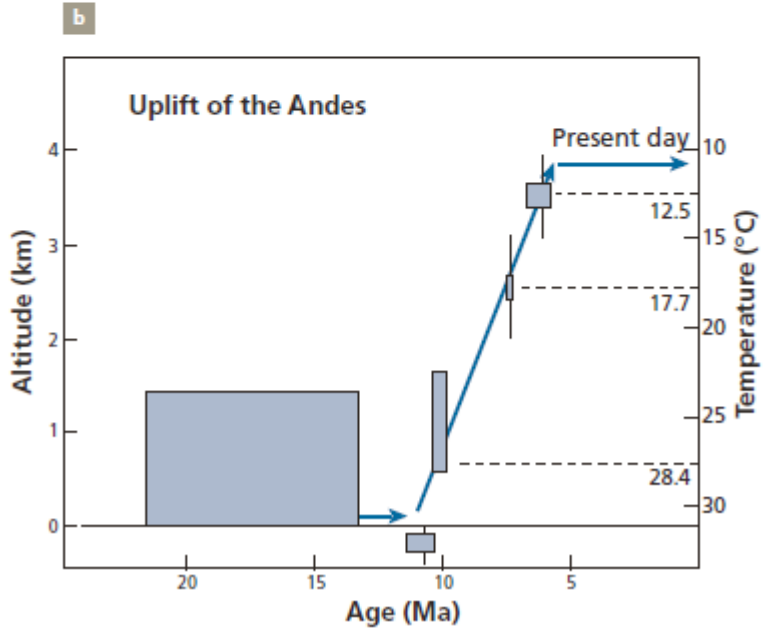

Claude Allègre (Isotope Geology)

Isotopic variations of oxygen in rocks

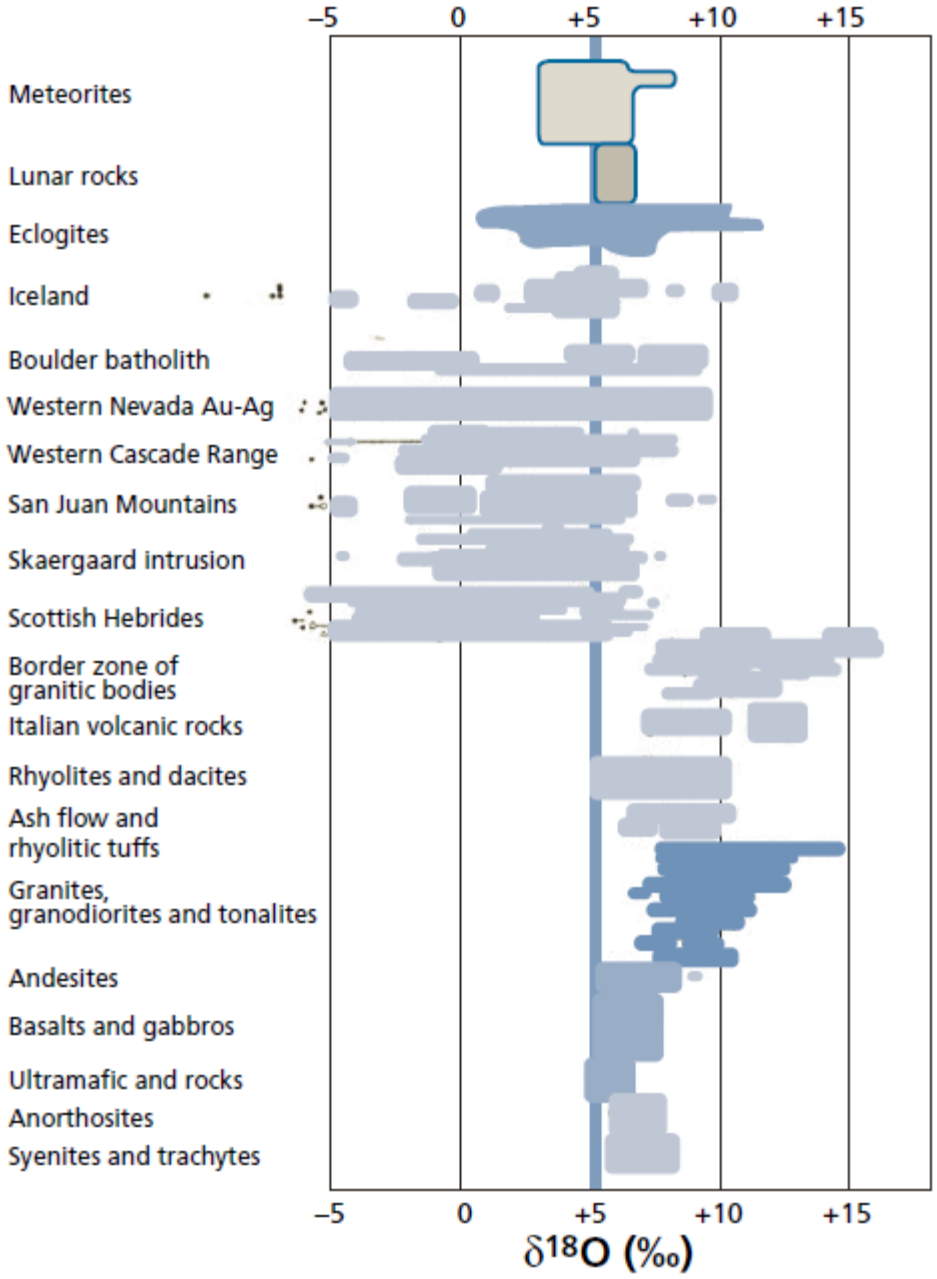

Claude Allègre (Isotope Geology)

The diet of early humans

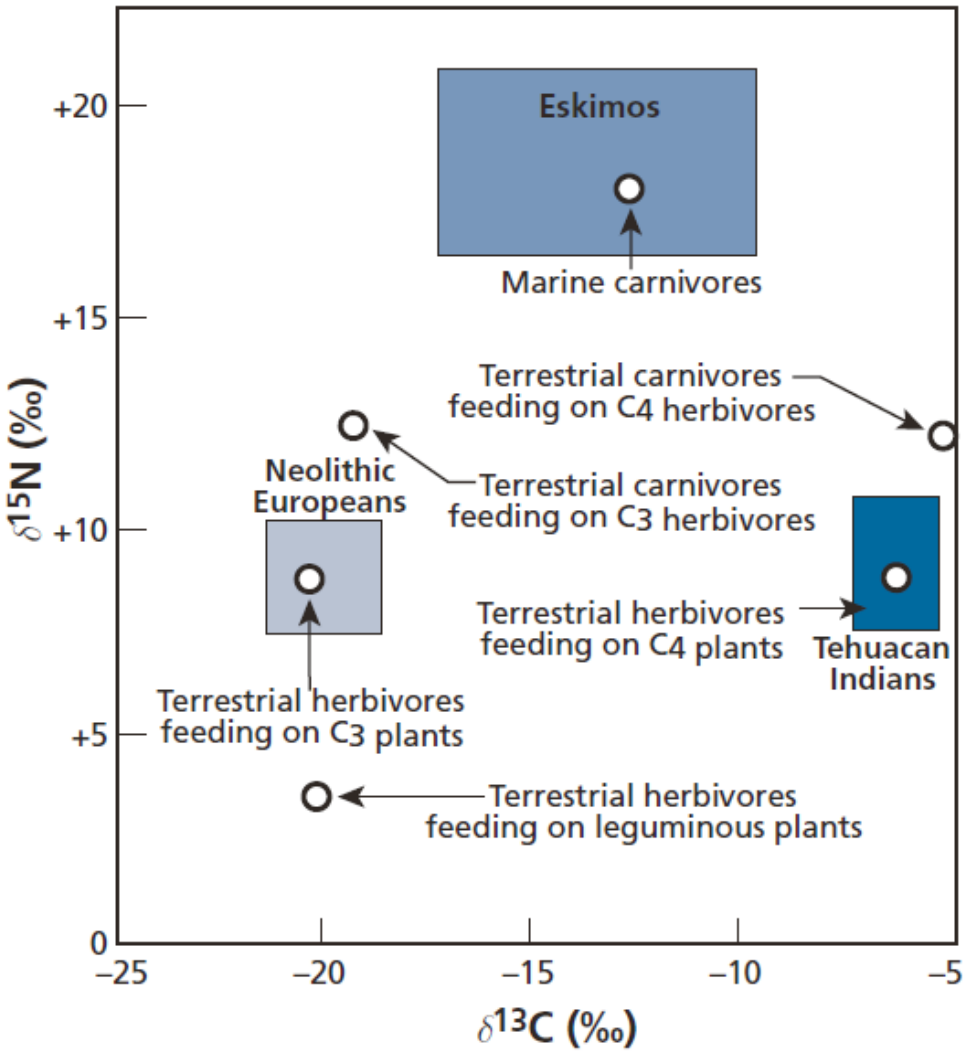

Isotopic variations of oxygen, strontium and neodymium

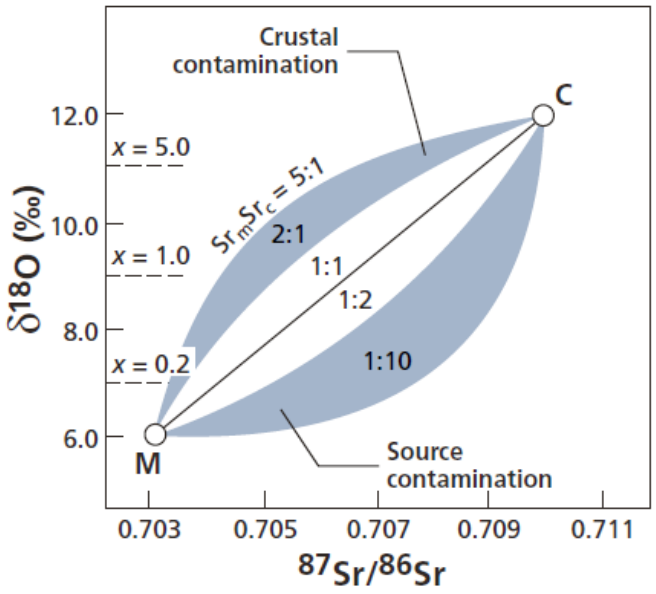

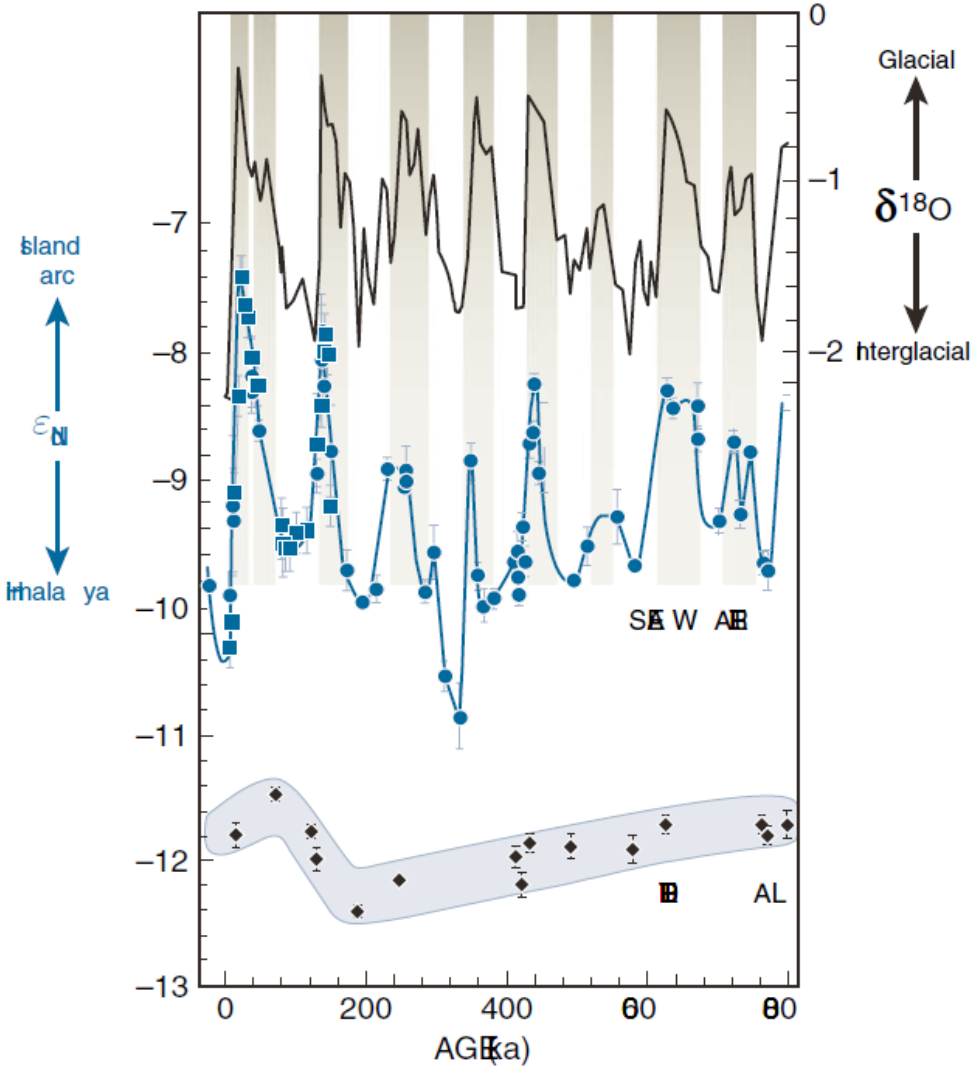

Claude Allègre (Isotope Geology)